DECLARATION OF JUNE ANN MUNFORD

1. My name is June Ann Munford. I am over the age of 18, have personal knowledge of the facts set forth herein, and am competent to testify to the same.

2. I earned a Master of Library and Information Science (MLIS) from the University of Wisconsin-Milwaukee in 2009. I have over ten years of experience in the library/information science field. Beginning in 2004, I have served in various positions in the public library sector including Assistant Librarian, Youth Services Librarian and Library Director. I have attached my Curriculum Vitae as Appendix CV.

3. During my career in the library profession, I have been responsible for materials acquisition for multiple libraries. In that position, I have cataloged, purchased and processed incoming library works. That includes purchasing materials directly from vendors, recording publishing data from the material in question, creating detailed material records for library catalogs and physically preparing that material for circulation. In addition to my experience in acquisitions, I was also responsible for analyzing large collections of library materials, tailoring library records for optimal catalog

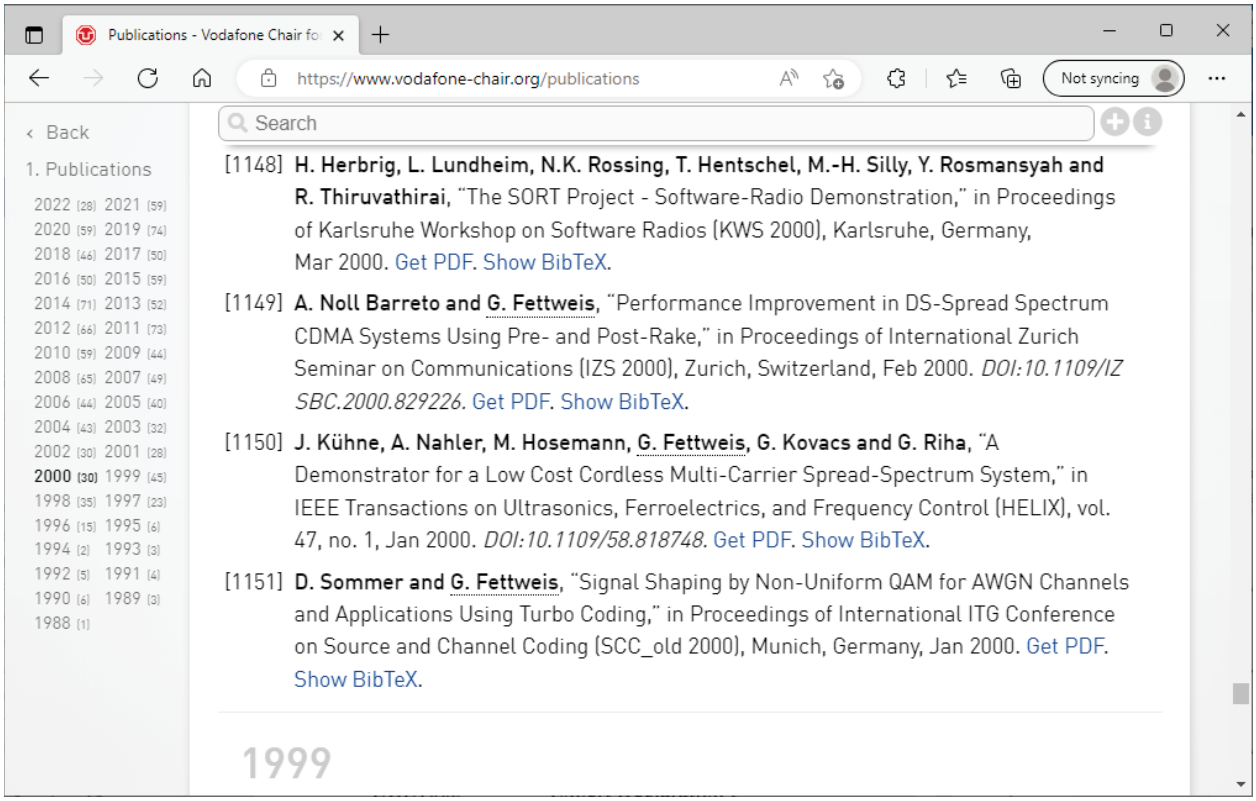
search performance and creating lending agreements between libraries during my time as a Library Director.

4. I am fully familiar with the catalog record creation process in the library sector. In preparing a material for public availability, a library catalog record describing that material would be created. These records are typically written in Machine Readable Catalog (herein referred to as "MARC") code and contain information such as a physical description of the material, metadata from the material's publisher, and date of library acquisition. In particular, the 008 field of the MARC record is reserved for denoting the date of creation of the library record itself. As this typically occurs during the process of preparing materials for public access, it is my experience that an item's MARC record indicates the date of an item's public availability.

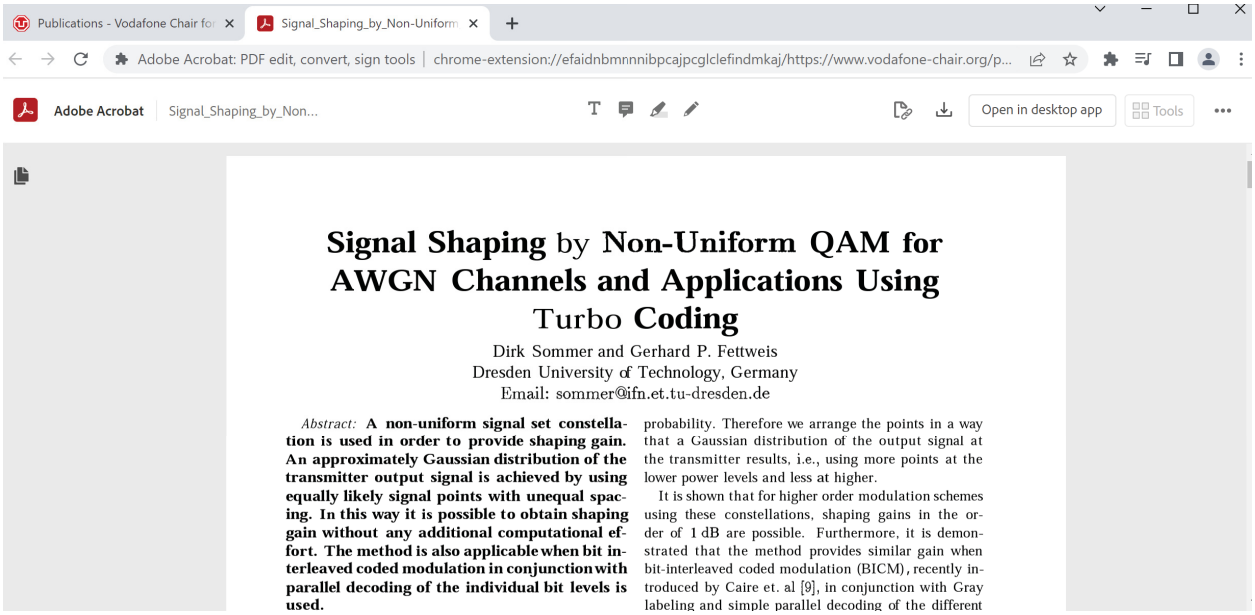
5. Typically, in creating a MARC record, a librarian would gather various bits of metadata such as book title, publisher and subject headings among others and assign each value to a relevant numerical field. For example, a book's physical description is tracked in field 300 while title/attribution is tracked in field 245. The 008 field of the MARC record is reserved for denoting the creation of the library record itself. As this is the only date reflecting the inclusion of said materials within the library's collection, it is my experience

that an item's 008 field accurately indicates the date of an item's public availability.

6. I have reviewed Exhibit LGE1006, "Signal Shaping by Non-Uniform QAM for AWGN Channels and Applications Using Turbo Coding" by Dirk Sommer and Gerhard P. Fettweis as published in *Proceedings of International ITG Conference on Source and Channel Coding, January 2000, pp. 81-86*. A copy of this article can be obtained easily on the Internet. For example, after searching for the article title and Professor Gerhard P. Fettweis's name in Google, I was able to access the list of publications of Professor Gerhard P. Fettweis on the vodafone-chair.org website (https://www.vodafone-chair.org/publications - as shown in the webpage snapshot below). As can be seen, item 1151 lists the same article, which was listed under the year 2000 section on the publications page. Upon clicking on the "Get PDF" link, I am directed to a web page (address https://www.vodafone-chair.org/pbls/legacy/d-sommer/Signal_Shaping_by_Non-Uniform_QAM_for_AWGN_Channels_and_Applications_Using_Turbo_Coding.pdf) that produces an identical copy to the article in LGE1006. I have included a copy of this article as Appendix SOMMER01.



Snapshot of webpage vodafone-chair.org/publications (with the year 2000 selected); last visited November 26, 2022



Snapshot of article produced on the web page (https://www.vodafone-chair.org/pbls/legacy/d-sommer/Signal_Shaping_by_Non-Uniform_QAM_for_AWGN_Channels_and_Applications_Using_Turbo_Coding.pdf) when the "Get PDF" link was selected in the page reproduced above; last visited November 26, 2022

7. Attached hereto are APPENDICES SOMMER02-SOMMER06 which are copies of publications of technical conference proceedings and journals from 2003-2007. Each of the publications in APPENDICES SOMMER02-SOMMER06 cite to the article in LGE1006. The authors of these publications are located in different parts of the world including Beijing, China, Pasadena, CA, Newcastle Upon Tyne, United Kingdom, and Tel Aviv, Israel. The variation in the authors, universities, dates, and locations

of these publications that all cite to the article in LGE1006 indicate to me that the article in LGE1006 was publically available at least as of 2003.

8. In addition to the technical publications, I also located numerous patent documents, such as U.S. Patent No. 9,036,694[1] invented by Zhou et al. in Beijing, China, U.S. Patent No. 10,003,436[2] invented by Tosato et al. in Tokyo, Japan, and U.S. Patent No. 7,978,777[3] invented by Barsoum et al. in Pasadena, CA, USA, each of which also cite to the article in LGE1006. Again, the variation in the inventors and their respective locations indicate to me that the article in LGE1006 was globally available to the public.

[1] U.S. Patent No. 9,036,694 is available at https://patentimages.storage.googleapis.com/bd/29/fa/08e5f9e430335a/US9036694.pdf

[2] U.S. Patent No. 10,003,436 is available at https://patentimages.storage.googleapis.com/98/52/0b/da95f4f525a6a9/US10003436.pdf

[3] U.S. Patent No. 7,978,777 is available at https://patentimages.storage.googleapis.com/2b/d2/c0/efec1b56e7907f/US7978777.pdf

9. I have reviewed Exhibit 1008, *DVB - The Family of International Standards for Digital Video Broadcasting* edited by Ulrich Reimers, 2nd Edition.

10. Attached hereto as Appendix REIMERS01 is a true and correct copy of the MARC record for *DVB - The Family of International Standards for Digital Video Broadcasting* as held by the University of Pittsburgh library. I secured this record myself from the library's public catalog. The MARC record contained within Appendix REIMERS01 accurately describes the title, author, publisher, and ISBN number of *DVB - The Family of International Standards for Digital Video Broadcasting.*

11. Attached hereto as REIMERS02 are selections from *DVB - The Family of International Standards for Digital Video Broadcasting* as held by the University of Pittsburgh's library. I secured these scans myself from the University of Pittsburgh library. In comparing Exhibit 1008 to Appendix REIMERS02, it is my determination that Exhibit 1008 is a true and correct copy of *DVB - The Family of International Standards for Digital Video Broadcasting* 2nd Edition.

12. The 008 field of the MARC record in Appendix REIMERS01 indicates the date of record creation. The 008 field of Appendix REIMERS01 indicates the University of Pittsburgh library first acquired this book as of July 3, 2003. Considering this information, it is my determination that *DVB - The Family of International Standards for Digital Video Broadcasting* was made available to the public shortly after its initial acquisition in July 2003.

13. I have reviewed Exhibit 1015, "Channel Coding with Multilevel/Phase Signals" by Gottfried Underboeck as published in *IEEE Transactions on Information Theory*, January 1982.

14. Attached hereto as Appendix UNDERBOECK01 is a true and correct copy of the MARC record for *IEEE Transactions on Information Theory* as held by the Penn State University library. I secured this record myself from the library's public catalog. The MARC record contained within Appendix UNDERBOECK01 accurately describes the title, author, publisher, and ISSN number of *IEEE Transactions on Information Theory.* The 'Availability' field of this record visible on page 4 indicates this collection includes the January 1982 edition of *IEEE Transactions on Information Theory* containing "Channel Coding with Multilevel/Phase Signals". In comparing Exhibit 1015 to Appendix UNDERBOECK01, it is my

determination that Exhibit 1015 is a true and correct copy of "Channel Coding with Multilevel/Phase Signals" by Gottfried Underboeck as published in *IEEE Transactions on Information Theory* January 1982.

15. The 008 field of the MARC record in Appendix UNDERBOECK01 indicates the date of record creation. The 008 field of Appendix UNDERBOECK01 indicates the Penn State library first acquired this journal as of May 14, 1982 and held the journal in perpetuity until 2006. Considering this information, it is my determination that *IEEE Transactions on Information Theory* January 1982 and therefore "Channel Coding with Multilevel/Phase Signals" was made available to the public shortly after its initial release in Winter 1982.

16. I have reviewed Exhibit 1016, "Signal Constellation Design Tool: A Case Study in User Interface Synthesis" by Gabriel Robins as published in *Proceedings of the 1989 International Conference on Computer Assisted Learning*.

17. Attached hereto as Appendix ROBINS01 is a true and correct copy of the MARC record for *Proceedings of the 1989 International Conference on Computer Assisted Learning* as held by the Penn State University library. I

secured this record myself from the library's public catalog. The MARC record contained within Appendix ROBINS01 accurately describes the title, author, publisher, and ISBN number of *Proceedings of the 1989 International Conference on Computer Assisted Learning.* In comparing Exhibit 1016 to Appendix ROBINS01, it is my determination that Exhibit 1016 is a true and correct copy of "Signal Constellation Design Tool: A Case Study in User Interface Synthesis" as published in *Proceedings of the 1989 International Conference on Computer Assisted Learning* by Gabriel Robins.

18. The 008 field of the MARC record in Appendix ROBINS01 indicates the date of record creation. The 008 field of Appendix ROBINS01 indicates the Penn State University library first acquired these proceedings as of July 24, 1989. Considering this information, it is my determination that *Proceedings of the 1989 International Conference on Computer Assisted Learning* and therefore "Signal Constellation Design Tool: A Case study in User Interface Synthesis" was made available to the public shortly after its initial acquisition in July 1989.

19. I have reviewed Exhibit EX1021, Digital Communications by J. G. Proakis, 4th Edition.

20. Attached hereto as Appendix PROAKIS01 is a true and correct copy of the MARC record for Digital Communications as held by the Penn State University library. I secured this record myself from the library's public catalog. The MARC record contained within Appendix PROAKIS01 accurately describes the title, author, publisher, and ISBN number of Digital Communications.

21. Attached hereto as Appendix PROAKIS02 are selections from Digital Communications by J.G. Proakis, 4th Edition. I secured these scans myself from the Penn State University library's collection. In comparing Exhibit EX1021 to Appendix PROAKIS02, it is my determination that Exhibit EX1021 is a true and correct copy of Digital Communications by J. G. Proakis, 4th Edition.

22. The 008 field of the MARC record in Appendix PROAKIS01 indicates the date of record creation. The 008 field of Appendix PROAKIS01 indicates that the Penn State University library first acquired this book as of November 16, 2000. Considering this information, it is my determination that Digital Communications was made available to the public shortly after its initial acquisition in Winter 2000.

23. I have reviewed Exhibit LGE1014, "Turbo-coded APSK Modulations Design for Satellite Broadband Communications" by R. De Gaudenzi, A. Guillen I Fabregas and A. Martinez as published in *International Journal of Satellite Communications and Networking*, July/August 2006.

24. Attached hereto as Appendix DEGAUDENZI01 is a true and correct copy of the MARC record for *International Journal of Satellite Communications and Networking* as held by the Penn State University library. I secured this record myself from the library's public catalog. The MARC record contained within Appendix DEGAUDENZI01 accurately describes the title, author, publisher, and ISSN number of *International Journal of Satellite Communications and Networking.* The 'Dates of Publication and/or Sequential Designation' field of this record visible on page 2 indicates this collection includes the July/August 2006 edition of *International Journal of Satellite Communications and Networking* containing "Turbo-coded APSK Modulations Design for Satellite Broadband Communications" by R. De Gaudenzi, A. Guillen I Fabregas and A. Martinez.

25. Attached hereto as Appendix DEGAUDENZI02 is a true and correct copy of "Turbo-coded APSK Modulations Design for Satellite Broadband Communications," as published in *International Journal of Satellite*

Communications and Networking. I secured this PDF copy myself from Penn State University's digital collection. In comparing Exhibit LGE1014 to Appendix DEGAUDENZI02, it is my determination that Exhibit LGE1014 is a true and correct copy of "Turbo-coded APSK Modulations Design for Satellite Broadband Communications" by R. De Gaudenzi, A. Guillen I Fabregas and A. Martinez as published in *International Journal of Satellite Communications and Networking* July/August 2006.

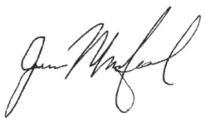
26. The 008 field of the MARC record in Appendix DEGAUDENZI01 indicates the date of record creation. The 008 field of Appendix DEGAUDENZI01 indicates the Penn State University library first acquired this journal as of October 21, 2002 and holds the journal in perpetuity since that date. Considering this information, it is my determination that *International Journal of Satellite Communications and Networking* July/August 2006 and therefore "Turbo-coded APSK Modulations Design for Satellite Broadband Communications" was made available to the public shortly after its initial release in Summer 2006.

27. I have been retained on behalf of the Petitioner to provide assistance in the above-illustrated matter in establishing the authenticity and public availability of the documents discussed in this declaration. I am being

compensated for my services in this matter at the rate of $100.00 per hour plus reasonable expenses. My statements are objective, and my compensation does not depend on the outcome of this matter.

28. I declare under penalty of perjury that the foregoing is true and correct. I hereby declare that all statements made herein of my own knowledge are true and that all statements made on information and belief are believed to be true; and further that these statements were made the knowledge that willful false statements and the like so made are punishable by fine or imprisonment, or both, under Section 1001 of Title 18 of the United States Code.

Dated: 11/28/2022



June Ann Munford

APPENDIX CV

J. Munford
Curriculum Vitae

Education

University of Wisconsin-Milwaukee - MS, Library & Information Science, 2009
Milwaukee, WI

- Coursework included cataloging, metadata, data analysis, library systems, management strategies and collection development.
- Specialized in library advocacy, cataloging and public administration.

Grand Valley State University - BA, English Language & Literature, 2008
Allendale, MI

- Coursework included linguistics, documentation and literary analysis.
- Minor in political science with a focus in local-level economics and government.

Professional Experience

Researcher / Expert Witness, October 2017 – present
Freelance ● Pittsburgh, Pennsylvania & Grand Rapids, Michigan

- Material authentication and public accessibility determination. Declarations of authenticity and/or public accessibility provided upon research completion. Experienced with appeals and deposition process.

- Research provided on topics of public library operations, material publication history, digital database services and legacy web resources.

- Past clients include Alston & Bird, Arnold & Porter, Baker Botts, Fish & Richardson, Erise IP, Irell & Manella, O'Melveny & Myers, Perkins-Coie, Pillsbury Winthrop Shaw Pittman and Slayden Grubert Beard.

Library Director, February 2013 - March 2015
Dowagiac District Library ● Dowagiac, Michigan

- Executive administrator of the Dowagiac District Library. Located in

Southwest Michigan, this library has a service area of 13,000, an annual operating budget of over $400,000 and total assets of approximately $1,300,000.

● Developed careful budgeting guidelines to produce a 15% surplus during the 2013-2014 & 2014-2015 fiscal years while being audited.

● Using this budget surplus, oversaw significant library investments including the purchase of property for a future building site, demolition of existing buildings and building renovation projects on the current facility.

● Led the organization and digitization of the library's archival records.

● Served as the public representative for the library, developing business relationships with local school, museum and tribal government entities.

● Developed an objective-based analysis system for measuring library services - including a full collection analysis of the library's 50,000+ circulating items and their records.

November 2010 - January 2013
Librarian & Branch Manager, Anchorage Public Library ● Anchorage, Alaska

● Headed the 2013 Anchorage Reads community reading campaign including event planning, staging public performances and creating marketing materials for mass distribution.

● Co-led the social media department of the library's marketing team, drafting social media guidelines, creating original content and instituting long-term planning via content calendars.

● Developed business relationships with The Boys & Girls Club, Anchorage School District and the US Army to establish summer reading programs for children.

June 2004 - September 2005, September 2006 - October 2013
Library Assistant, Hart Area Public Library
Hart, MI

● Responsible for verifying imported MARC records and original MARC

cataloging for the local-level collection as well as the Michigan Electronic Library.

● Handled OCLC Worldcat interlibrary loan requests & fulfillment via ongoing communication with lending libraries.

Professional Involvement

Alaska Library Association - Anchorage Chapter
- Treasurer, 2012

Library Of Michigan
- Level VII Certification, 2008
- Level II Certification, 2013

Michigan Library Association Annual Conference 2014
- New Directors Conference Panel Member

Southwest Michigan Library Cooperative
- Represented the Dowagiac District Library, 2013-2015

Professional Development

Library Of Michigan Beginning Workshop, May 2008
Petoskey, MI
- Received training in cataloging, local history, collection management, children's literacy and reference service.

Public Library Association Intensive Library Management Training, October 2011
Nashville, TN
- Attended a five-day workshop focused on strategic planning, staff management, statistical analysis, collections and cataloging theory.

Alaska Library Association Annual Conference 2012 - Fairbanks, February 2012
Fairbanks, AK
- Attended seminars on EBSCO advanced search methods, budgeting, cataloging, database usage and marketing.

Depositions

2019 ● Fish & Richardson
IPR Petitions of 865 Patent, Apple v. Qualcomm (IPR2018-001281 / 39521-00421IP & IPR2018-01282 / 39521-00421IP2)

2019 ● Erise IP
Implicit, LLC v. Netscout Systems, Inc (Civil Action No. 2:18-cv-53-JRG)

2019 ● Perkins-Coie
Adobe Inc. v. RAH Color Technologies LLC (Cases IPR2019-00627, IPR2019-00628, IPR2019-00629 and IPR2019-00646)

2020 ● O'Melveny & Myers
Maxell, Ltd. v. Apple Inc. (Case 5:19-cv-00036-RWS)

2021 ● Pillsbury Winthrop Shaw Pittman LLP
Intel v. SRC (Case IPR2020-1449)

Limited Case History & Potential Conflicts

Alston & Bird
- Nokia (v. Neptune Subsea, Xtera)

Arnold & Porter
- Ivantis (v. Glaukos)

Erise I.P.
- Apple
  - v. Future Link Systems (IPRs 6317804, 6622108, 6807505, and 7917680)
  - v. INVT
  - v. Navblazer LLC (Case No. IPR2020-01253)

v. Qualcomm (IPR2018-001281, 39521-00421IP, IPR2018-01282, 39521-00421IP2)

v. Quest Nettech Corp, Wynn Technologies (Case No. IPR2019-00XXX, RE. Patent Re38137)

- Fanduel (v CGT)

- Garmin (v. Phillips North America LLC, Case No. 2:19-cv-6301-AB-KS Central District of California)

- Netscout

  v. Longhorn HD LLC)

  v. Implicit, LLC (Civil Action No. 2:18-cv-53-JRG)

- Sony Interactive Entertainment LLC

  v. Bot M8 LLC

  v. Infernal Technology LLC

- Unified Patents (v GE Video Compression, Civil Action No. 2:19-cv-248)

Fish & Richardson

- Apple

  v. LBS Innovations

  v. Masimo (IPR 50095-0012IP1, 50095-0012IP2, 50095-0013IP1, 50095-0013IP2, 50095-0006IP1)

  v. Neonode

  v. Qualcomm (IPR2018-001281, 39521-00421IP, IPR2018-01282, 39521-00421IP2)

- Dish Network

  v. Realtime Adaptive Streaming, Case No 1:17-CV-02097-RBJ)

v. TQ Delta LLC

- Huawei (IPR 76933211)
- Kianxis
- LG Electronics (v. Bell Northern Research LLC, Case No. 3:18-cv-2864-CAB-BLM)
- Metaswitch
- MLC Intellectual Property (v. MicronTech, Case No. 3:14-cv-03657-SI)
- Realtek Semiconductor
- Quectel
- Samsung (v. Bell Northern Research, Civil Action No. 2:19-cv-00286-JRG)
- Texas Instruments

Irell & Manella

- Curium

O'Melveny & Myers

- Apple (v. Maxell, Case 5:19-cv-00036-RWS)

Perkins-Coie

- TCL Industries (v. Koninklijke Philips NV, PTAB Case Nos. IPR2021-00495, IPR2021-00496, and IPR2021-00497)

Pillsbury Winthrop Shaw Pittman

- Intel (v. FG SRC LLC, Case No. 6:20-cv-00315 W.D. Tex)

APPENDIX SOMMER01

Signal Shaping by Non-Uniform QAM for AWGN Channels and Applications Using Turbo Coding

Dirk Sommer and Gerhard P. Fettweis
Dresden University of Technology, Germany
Email: sommer@ifn.et.tu-dresden.de

Abstract: **A non-uniform signal set constellation is used in order to provide shaping gain. An approximately Gaussian distribution of the transmitter output signal is achieved by using equally likely signal points with unequal spacing. In this way it is possible to obtain shaping gain without any additional computational effort. The method is also applicable when bit interleaved coded modulation in conjunction with parallel decoding of the individual bit levels is used.**

Keywords **- Channel capacity, entropy, quadrature amplitude modulation, error correction coding.**

I. Introduction

From information theory it is known that, in addition to coding gain, shaping gain can be obtained if the amplitude of the transmitter output follows a Gaussian distribution.

In most cases, a uniform QAM constellation together with different probabilities for each signal point is used to provide shaping gain. The idea has been investigated in [1]. Other examples are trellis shaping [2], the use of prefix codes [3], or similar, subdivision of the signal constellation into variable-size regions [4]. Recently, shaping also has been used in conjunction with multilevel coding/multistage decoding [5]. While trellis shaping requires an additional Viterbi-algorithm at the transmitter but maintains a fixed data rate, the approaches in [3; 4] are conceptually simpler but possibly impractical since the non-constant data rate may involve buffer over- or underrun. Also, resynchronisation has to be carried out frequently in this case to avoid catastrophic error propagation.

Non-uniform (NU) signal point constellations have a long tradition, e.g., in order to create a signal set for hierarchical (rate adaptive) transmission [6; 7], sometimes also called multiresolution modulation. An approach to use an asymmetric coded-modulation scheme in order to optimize trellis coding has been presented in [8].

In this paper we make use of a non-uniform signal point constellation in order to obtain shaping gain. Contrary to other approaches to signal shaping, each signal point is assumed to be chosen with the same probability. Therefore we arrange the points in a way that a Gaussian distribution of the output signal at the transmitter results, i.e., using more points at the lower power levels and less at higher.

It is shown that for higher order modulation schemes using these constellations, shaping gains in the order of 1 dB are possible. Furthermore, it is demonstrated that the method provides similar gain when bit-interleaved coded modulation (BICM), recently introduced by Caire et. al [9], in conjunction with Gray labeling and simple parallel decoding of the different bit levels is used. Finally, some examples using turbo coding over the AWGN channel are given in order to verify that the principle works when used with common coding schemes.

In the following, all considerations regarding the channel capacity are made with respect to amplitude shift keying (ASK). This can of course simply be extended to QAM by adding a second dimension.

The transmission model is depicted in Fig. 1. The info bits d_k are first coded and bitwise interleaved. Then m interleaved coded bits $x_0, x_1, \ldots, x_{m-1}$ are mapped onto a symbol $a_j \in \boldsymbol{A}$ of the signal space using uniform or non-uniform ASK with Gray labeling. The symbol a_j passes a memoryless white Gaussian noise channel, and y is received.

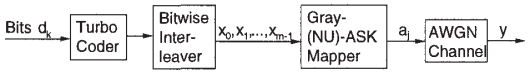


Figure 1. Transmission model

II. Shaping principle

A. *Signal set constellation*

In order to find a signal set with the desired properties, an empirical approach can be made as follows. Each point of the signal constellation is assumed to be chosen with the same probability, and we want the output of the transmitter to give an approximately Gaussian distribution. Therefore, using N-ASK, $N = 2^m$, we split the Gaussian cumulative distribution function (CDF) into N sections of *equal probability,* i.e., the *ordinate* of the CDF is partitioned into N equal parts. Since each signal point shall represent exactly one of the sections, each signal point (placed on the abscissa)

will be chosen such that the corresponding *probability* is exactly in the middle of a section.

In other words, the points u_j on the abscissa of the Gaussian PDF $f_u(u) = \frac{1}{\sqrt{2\pi}} e^{-\frac{u^2}{2}}$ (to be approximated) will be chosen such that

$$\int_{-\infty}^{u_j} \frac{1}{\sqrt{2\pi}} e^{-\frac{u^2}{2}} du = p_j \qquad (1)$$

for $p_j \in \{\frac{1}{2N}, \frac{3}{2N}, ..., \frac{2N-1}{2N}\}$. Fig. 2(a) illuminates the procedure. Finally the u_j are normalized by a factor h, $a_j = hu_j$, such that the average power of the transmitted signal is one

$$\frac{1}{N} \sum_{j=0}^{N-1} a_j^2 = 1 \qquad (2)$$

Alternatively, it has been tried to find the points u_i by calculating the mean of each probability section, i.e., $u_i = N \int_{u_a}^{u_b} u f_u(u) du$, where u_a and u_b are the limits of the current section, but the results did not change significantly.

Fig. 2(b) illustrates how the Gaussian CDF is approximated. The corresponding PDF consists of δ-functions of height $1/N$ at locations u_i. Signal points values for various ASK constellations are listed in the Appendix.

B. Peak-to-average power ratio expansion

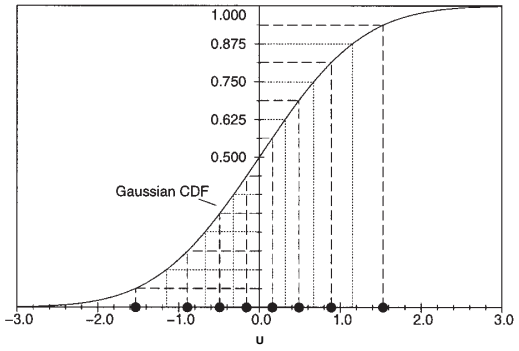
4-ASK	0.1 dB
8-ASK	0.7 dB
16-ASK	1.5 dB
32-ASK	2.3 dB
64-ASK	3.1 dB
128-ASK	3.8 dB

Table 1. PAPR expansion (NU-ASK **vs.** uniform ASK)

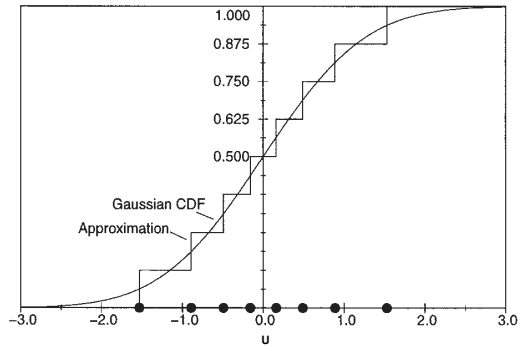
One of the drawbacks of the presented shaping principle is the expansion of the peak-to-average power ratio (PAPR) compared to uniform ASK. If for some reason not the average but the maximum transmission power is limited it might be better to dispense with that sort of signal shaping and exploit the higher signal to noise ratio of a uniformly distributed signal set instead, or to use other methods. Table 1 lists the PAPR expansion for the different modulation schemes. In all cases the PAPR expansion exceeds the shaping gain (see sec. III.C) so the kind of shaping presented here is generally not useful when the power constraint is only on the maximum power.

III. Capacity for Gaussian NU-ASK

In the following, the capacity of the non-uniform signal constellation is calculated under the assumption of equal probability for each signal point. Two cases are distinguished.



(a) Signal points u, for 8-NU-ASK



(b) **Approx.** of the Gaussian CDF by 8-NU-ASK

Figure 2. Signal set constellation

A. Signal set capacity

First, the capacity of the signal set that can principly be reached at a certain SNR is calculated, i.e., when all information contained in received signal y is exploited. This could possibly be done using multi-level-coding (MLC) / multi-stage-decoding (MSD) as proposed in [10; 5], or by BICM with additional feedback decoding (AFD) as presented in section IV (see also Fig. 4(b)). This capacity will be referred to as C_{SS} (signal set capacity). Under the assumption of equally likely source signals, C_{SS} can be calculated as follows [11]

$$C_{SS} = \mathrm{I}(\mathbf{X}, Y) = \mathrm{H}(Y) - \mathrm{H}(Y|\mathbf{X}) \qquad (3)$$

where the random variable $\mathbf{X} = (X_0, X_1, X_2, ..., X_{m-1})$ represents the bits of the 2^m-ASK constellation, I(.., ..) denotes the mutual information between two random variables, and H(..) the entropy.

B. Parallel decoding capacity

Second, each bit-level is considered separately, i.e., the assumption is made that each bit level is decoded without prior knowledge of the decoding results of some other bit levels. The corresponding decoding scenario is depicted in Fig. 4(a). From the received signal y, a metric is calculated for each bit. Subsequent decoding is performed without the attempt to improve that metric using the decoding results. Caire et. al noticed [9] that in this case the capacity strongly depends on the labeling scheme and conjectured that Gray labeling maximizes the capacity. Therefore no other labeling schemes will be considered in the sequel. As remarked in [10] this is equivalent to the capacity when MLC is used with parallel independent decoding of the different bit levels. Adopting the term of [10] the capacity will be referred to as C_{PD} (parallel decoding of individual levels).

C_{PD} can be calculated as

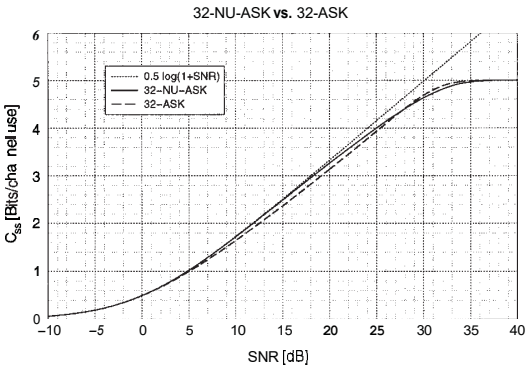
$$C_{PD} = \sum_{i=0}^{m-1} \mathrm{I}(X_i, Y) \qquad (4)$$

$$= \sum_{i=0}^{m-1} \left[\mathrm{H}(Y) - \sum_{k=0}^{1} \mathrm{H}(Y|x_i = k)\Pr(x_i = k) \right]$$

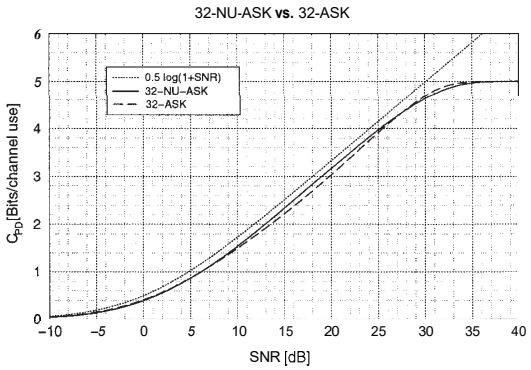
which means that different from (3) one has to sum up the mutual information between Y and the individual bits X_i while averaging the conditional entropy $H(Y|x_i = k)$ over the possibilities $x_i = k$, $k \in \{0, 1\}$. In the sequel, we use the term PD for BICM, too, in order to distinguish from BICM with AFD, although the bit levels are not really decoded in parallel.

C. Shaping gain results

The shaping gain is usually defined as the reduction in average power of the signal set at afixed data rate [2] compared to a rectangular (hypercube) constellation. With the approach taken here this definition is not applicable since there would be no shaping gain at all. Consequently, we need a different definition and use the term *shaping gain* for the *gain in SNR of a NU-ASK compared to* a *uniform ASK at a certain capacity.* In order to determine the shaping gain, (3) and (4) have been evaluated for the constellations presented in section II.A. Fig. 3(a) and Fig. 3(b) give an example of the capacity of the 32-NU-ASK constellation for C_{SS} and C_{PD}, respectively. As can be seen from Fig. 3(a), C_{SS} is very close to the optimum if less than ≈ 3 [bits/ channel use] are transmitted. In both cases the highest gain occurs at about 2.5 [bits/channel use], i.e., if a code rate of R $\approx$ 0.5 is used. Evaluating other NU-ASK constellations confirms that this generally seems to be the case. With turbo codes a powerful class of codes operating at this rate exists that can exploit this gain. However, contrary to common coded modulation or multilevel'coding schemes, the number of bits of the signal set has to be doubled instead being expanded by only 1 bit, since there is no shaping gain at code rates close to 1. This is a further drawback if the PAPR is of some importance.



(a) Signal set capacity



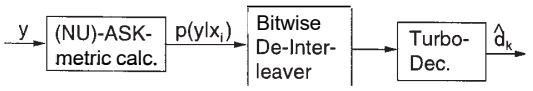
(b) Parallel decoding capacity

Figure 3. Capacities for NU-ASK vs. ASK

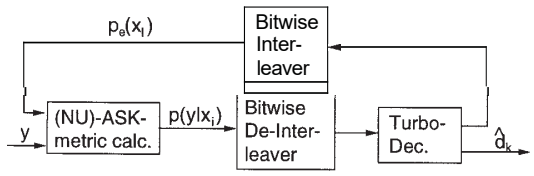
Gain (dB)	C_{SS}	C_{PD}
4-ASK	0.07	0.01
8-ASK	0.32	0.15
16-ASK	0.59	0.50
32-ASK	0.82	0.81
128-ASK	1.14	1.18

Table 2. Shaping gain at $R = 0.5$

Table 2 lists the capacity gains of C_{SS} and C_{PD} at R = 0.5. Clearly, the use of NU-ASK for shaping offers advantages only for higher order modulation schemes. However, it can provide shaping gains up to $\approx$ 1 dB independent of whether BICM with PD or a coding/modulation scheme exploiting C_{SS} is used.



(a) BICM with PD



(b) BICM with AFD

Figure 4. Decoder structure

IV. Applications using turbo codes

Turbo codes, first introduced in [12], are known as a class of powerful codes that can approach the channel capacity relatively close. The BCJR-algorithm [13] used for turbo decoding requires $\Pr(y|x_i = k)$ for the branch metrics. When all signal points $a_j \in A$ are assumed to be equally likely, $\Pr(y|x_i = k)$ can be simply determined by summing up the transition probabilities over all signal points a_j with $x_i = k, k \in \{0, 1\}$, for each bit of the ASK symbol,

$$\Pr(y|x_i = k) = c_1 \sum_{a_j : x_i = k} \mathrm{e}^{-\frac{(y-a_j)^2}{2\sigma^2}} \qquad (5)$$

where σ^2 is the (one dimensional) noise variance, assumed to be known at the receiver. If a-priori information of the bits x_i is provided, then $\Pr(y|x_i = k)$ can be calculated as

$$\Pr(y|x_i = k) = c_2 \sum_{a_j : x_i = k} \left(\mathrm{e}^{-\frac{(y-a_j)^2}{2\sigma^2}} \prod_{\substack{l=0 \\ l \neq i}}^{m-1} \Pr(x_l) \right) \qquad (6)$$

which means that additionally, the probability of the current signal point a_j is taken into account, not using the input probability of the bit, for which the output soft value has to be determined. The expression in eq. (6) is a variant of the method presented in [14] for GSM speech frame decoding, and has also recently been used in [15] for feedback demodulation of BICM. Constant factors (c_1, c_2) in (5) and (6) can be neglected since they cancel out when likelihood ratios $\Pr(y|x_i = 0)/\Pr(y|x_i = 1)$ are computed for subsequent decoding.

In the following, the theoretical results have been tested using turbo codes over the AWGN channel. Two cases have been considered. First, BICM with simple subsequent turbo decoding was used, see Fig. 4(a). In this case, the maximum transmission rate is bounded by C_{PD}.

Second, the extrinsic soft values of the turbo decoder for info and parity bits were fed back into the metric calculator in order to serve as a-priori information according to (6), see Fig. 4(b), (AFD, additional feedback decoding). The corresponding capacity is C_{SS}. The soft values were calculated according to the method presented in [16].

The interleaver length was $\approx$ 8000 bits (slightly adapted to give a multiple of the actual QAM constellation size) for the turbo coding and twice that much (one complete coded burst) between coding and modulation. Both interleavers performed random permutation of the bits/soft values. The turbo code was the one presented in [12], i.e., a 16-state code with polynomials 21 and 37 (octal representation) and every second parity bit punctured.

V. Coding results

Fig. 5(a) and Fig. 5(b) compare turbo coding results for the AWGN channel using different modulation orders without and with AFD, respectively.

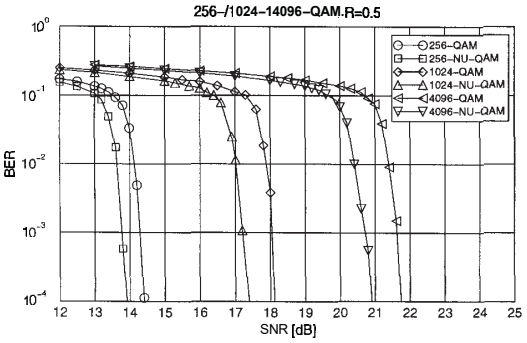
As can be seen, the difference between QAM and NU-&AM matches the shaping gain results of table 2 relatively close at BER=10^{-4} independent of whether AFD was used or not. Lower BER have not been considered since the typical turbo code error floor starts already in that region. If additional feedback for the metric calculation is provided, the results improve by about $0.5 - 1$ dB. The necessary SNR for 16-/32-/64-ASK with C_{SS}(NU-ASK),C_{SS}(ASK), C_{PD}(NU-ASK), and C_{PD}(ASK), respectively, are listed in table **3.** The

SNR (dB)	C_{SS}(NU-ASK)	C_{SS}(ASK)
16-ASK (256-&AM)	11.94	12.53
32-ASK (1024-QAM)	15.05	15.87
64-ASK (4096-QAM)	18.10	19.10
	C_{PD}(NU-ASK)	C_{PD}(ASK)
16-ASK (256-&AM)	12.75	13.25
32-ASK (1024-QAM)	15.96	16.77

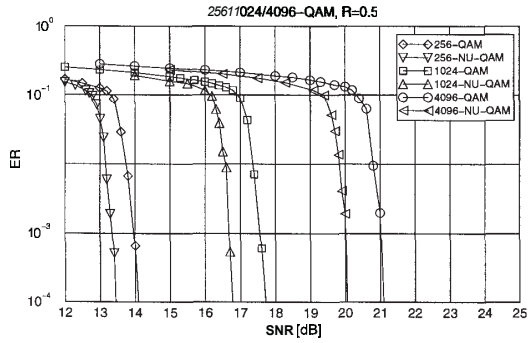
Table 3. Capacity at $R = 0.5$

SNR necessary to reach BER=10^{-4} are in all cases within $1 - 2$ dB from the capacity result.

For all simulation, 12 iterations of inner turbo decoding have been used. With AFD, 5 outer iterations have been made additionally resulting in a total of 60 iterations. This is impractical, however, the number could be dramatically lowered, if some suitable criterion on when to stop an inner (turbo code) iteration was applied. Simulations show that for the first outer iterations only a few inner iterations are necessary.



(a) With PD (without AFD)



(b) With AFD

Figure 5. Comparison between **NU-$AM** and uniform QAM for BICM

VI. Conclusions

A simple method to obtain shaping gain for higher order ASK modulation on AWGN channels was presented.

Using non-uniform ASK in conjunction with BICM, shaping gains in the order of the theoretically predicted capacity gains can be achieved with a real coding system, independent of whether parallel decoding (no AFD) or additional feedback decoding is used. Improvements due to AFD are within 0.5 - 1 dB.

Compared to other shaping methods, the achieved gain is lower, and even for higher order modulation scheme it does not seem approach the ultimate gain of 1.53 dB. Also, the fact that shaping gain is exhibited only when the constellations are used with code rates R = 0.5 might lead to a higher decoding effort in comparison to higher rate coding schemes. Furthermore, the enlarged signal point constellation, entailing a considerably higher peak-to-average power ratio, can be prohibitive in some applications.

The main Advantage is the simplicity of the method. Compared to uniform ASK with R = 0.5, shaping by NU-ASK does not entail any additional computational effort. Only the lookup tables for signal transmission and metric calculation have to be replaced, so signal shaping with gains up to about 1 dB has been demonstrated without changing the coder/decoder structure.

VII. Appendix

Signal point constellations for NU-ASK

4-NU-ASK

f0.377525	41.362892

8-NU-ASK

f0.170563	±0.529790	f0.961643	f1.662971

16-NU-ASK

f0.081626	±0.246854	f0.418533	±0.602594
f0.807881	f1.050833	51.371404	±1.938154

f0.039934	50.120107	f0.200994	f0.283207
f0.367358	f0.453957	f0.544127	f0.638580
f0.739052	f0.847173	±0.965699	f1.099117
f1.254465	f1.446126	f 1.709493	f2.196958

64-NU-ASK

±0.019745	f0.059337	410.099030	±0.138925
±0.178920	±0.219320	±0.259922	±0.301130
±0.342742	±0.384959	±0.427783	±0.471516
±0.516057	±0.561708	±0.608471	±0.656648
±0.706238	±0.757748	±0.811177	±0.867029
±0.925710	±0.987623	±1.053575	±1.124275
f1.201035	f1.285369	f1.379905	f1.488176
f1.617051	f1.779256	f2.007313	f2.441711

128-NU-ASK

±0.00984409	f0.0295222	f0.0492204	f0.0689388
±0.0886772	±0.108456	±0.128275	±0.148144
±0.168073	±0.188063	±0.208133	±0.228283
±0.248524	±0.268866	±0.289328	±0.3099
±0.330604	±0.351458	±0.372452	±0.393618
±0.414954	±0.436492	±0.45822	±0.480169
±0.50235	±0.524772	±0.547465	±0.57044
±0.593716	±0.617313	±0.641253	±0.665564
±0.690277	±0.715413	±0.741	±0.76708
±0.793683	±0.820858	±0.848647	±0.877099
±0.906274	±0.936234	±0.967047	±0.998796
±1.03158	±1.0655	±1.10067	±1.13725
±1.1754	±1.21533	±1.25726	±1.30152
±1.34844	±1.39851	±1.45232	±1.51064
±1.57454	±1.64553	±1.72583	±1.81897
±1.93098	±2.07387	±2.27758	±2.6734

References

[1] A. R. Calderbank, L. H. Ozarow, "Nonequiprobable Signaling on the Gaussian Channel", *IEEE Transactions on Information Theory,* vol. *36,* pp. 726–740, July 1990.

[2] G. D. Forney, "Trellis Shaping", *IEEE Transactions on Information Theory,* vol. 38, pp. 281–300, Mar. 1992.

[3] F. R. Kschischang, S. Pasupathy, "Optimal Nonuniform Signaling for Gaussian Channels", *IEEE Transactions on Information Theory,* vol. 39, pp. 913–929, May 1993.
[4] J. N. Livingston, "Shaping Using Variable-Size Regions", *IEEE Transactions on Information Theory,* vol. 38, pp. 1347–1353, July 1992.
[5] R. Fischer, J. Huber, U. Wachsmann,, "On the Combination of Multilevel Coding and Signal Shaping", *ITG Fachtagung für Codierung, Quelle, Kanal und Ubertragung,* (Aachen), pp. 273–278, Mar. 1998.
[6] K. Fazel, M. J. Ruf, "Combined Multilevel Coding and Multiresolution modulation", *ICC'93,* (Geneva), pp. 1081–1085, Sept. 1993.
[7] T. Todtmann, "Optimierung von Signalraumaufteilungen fur eine hierarchische Ubertragung (in German)", *ITG Fachtagung fur Codierung, Quelle, Kanal und Ubertragung,* (Aachen), Mar. 1998.
[8] D. Divsalar, M. K. Simon, "Trellis Coding with Asymmetric Modulations", *IEEE Transactions on Communications,* vol. 35, pp. 130–147, Feb. 1987.
[9] G. Caire, G. Taricco, E. Biglieri, "Bit-Interleaved Coded Modulation", *IEEE Transactions on Information Theory,* vol. 44, pp. 927–946, May 1998.
[10] J. Huber, U. Wachsmann, R. Fischer, "Coded Modulation by Multilevel-Codes: Overview and State of the Art", *ITG Fachtagung für Codierung, Quelle, Kanal und Ubertragung,* (Aachen), pp. 255–265, Mar. 1998.
[11] R. B. Ash, *Information theory.* John Wiley & Sons, 1965.
[12] C. Berrou, **A.** Glavieux, P. Thitimajshima, "Near Shannon Limit Error-Correcting Coding and Decoding: Turbo-Codes", *ICC'93,* (Geneva), pp. 1064–1070, May 1993.
[13] L. R. Bahl, J. Cocke, F. Jelinek, J. Raviv, "Optimal Decoding of Linear Codes for Minimizing Symbol Error Rate", *IEEE Transactions on Information Theory,* pp. 284–287, Mar. 1974.
[14] T. Hindelang, A. Ruscitto, "Kanaldecodierung mit Apriori-Wissen bei nicht binaren Quellensymbolen (in German)", *ITG Fachtagung fur Codierung, Quelle, Kanal und Ubertragung,* (Aachen), pp. 163–167, Mar. 1998.
[15] X. Li, J. A. Ritcey, "Bit-Interleaved Coded Modulation with Iterative Decoding", *ICC'99,* (Vancouver), pp. 858–863, June 1999.
[16] S. Benedetto, D. Divsalar, G. Montorsi, F. Pollara, "A Soft-Input Soft-Output APP Module for Iterative Decoding of Concatenated Codes", *IEEE Communications Letters,* vol. 1, pp. 22–24, Jan. 1997.

APPENDIX SOMMER02

Transactions Letters

Constellation Shaping for Pragmatic Turbo-Coded Modulation With High Spectral Efficiency

Dan Raphaeli, *Senior Member, IEEE,* and Assaf Gurevitz

***Abstract*—We propose a new turbo-encoding scheme for high spectral efficiency with performance close to the Gaussian channel capacity. The scheme combines nonuniform signaling on a Gaussian channel with pragmatic turbo-coded modulation (TCM) for simple and flexible implementation. A variable-rate turbo code is followed by a Huffmann code mapping onto nonequiprobable points in a quadrature amplitude modulation constellation. The rate of the turbo code is matched to the Huffmann code by variable puncturing, such that both the input bit rate and the output symbol rate are constant. It is shown that the new scheme provides shaping gains of 0.6 and 0.9 dB, at rates 2 and 3 b/dimension, respectively, compared with the equiprobable pragmatic TCM, and reach about 1 dB from the continuous input Gaussian channel capacity.**

***Index Terms*—high spectral efficiency modulation, signal shaping, turbo codes.**

I. Introduction

THE idea behind constellation shaping is that signals with large norm are used less frequently than signals with small norm, thus improving the overall gain by adding shaping gain to their original coding gain [1]. The nonuniform signaling reduces the entropy of the transmitter output, and hence, the average bit rate. However, if points with small energy are chosen more often than points with large one, energy savings may compensate for this loss in bit rate. Theoretically, constellation points would be selected according to a continuous Gaussian distribution at every dimension, and thus achieve the maximum shaping gain. Practically, in finite constellations, a smaller gain can be achieved.

For Gaussian channels, turbo-coded modulation (TCM) techniques can be broadly classified into binary schemes and turbo trellis-coded modulation (TTCM) [2]. The first group can be further divided into "pragmatic" schemes with a single component binary turbo code, and multilevel binary turbo codes [3]. The pragmatic approach for a bandwidth-efficient turbo-coding scheme has been presented in [4]. This approach is simple and versatile, and is much less complex to design and to implement than TTCM. It uses only one turbo decoder, and by modifying its puncturing function and modulation signal constellation, it can obtain a large family of TCM schemes. It is possible to include shaping in the framework of multilevel codes [3]. The multilevel approach may be less attractive than the pragmatic approach due to its increased complexity, delay (from the multistage decoding), and sophisticated design rules. The shaping that was applied to multilevel codes is multidimensional trellis-shaping code, which is much more complex than the method proposed here. The performance obtained in the multilevel approach is similar (within 0.1 dB) to our results. TTCM was shown to obtain the highest performance in the coding of equiprobable quadrature amplitude modulation (QAM). Fragouli and Wesel [5] have shown that by careful code selection and interleaver design, it is possible to reach a signal-to-noise ratio (SNR) of 0.5–0.6 dB from the (constrained) capacity. Moreover, by combining nonuniform constellations [6] with the symbol-interleaved encoder, they achieved a shaping gain of approximately 0.2 dB [7].

Many authors suggested various forms of shaping within the framework of TCM, like the trellis shaping of Forney [8]. Another approach to achieve shaping was already proposed in the 1960s by Gallager [9]. He showed that optimal coding for the Gaussian channel can be made by grouping bits from a binary code, where the larger group is assigned to the less probable points in the constellation, and smaller to the more frequent. Obviously, such a method leads to a variable-rate input to the channel. A more detailed analysis of the method and close to optimal variable-rate code was suggested in [10], which showed that a close-to-optimal solution is the Huffmann prefix code. The variable-rate scheme of [10] is simple to encode, but requires *variable-rate input*, which results in system problems such as buffering and resynchronization.

In this letter, we propose a practical method that uses this idea while overcoming the variable-rate input disadvantage. We combine the powerful but simple pragmatic turbo-code principle with this shaping method and supply a practical decoding scheme with good results. The matching is done by dynamic puncturing of a low-rate turbo code to match the symbol-dependent rate of the prefix code. For further improvement, we also apply a feedback to the log-likelihood ratio (LLR) calculation block, as suggested in [11]. We consider one-dimensional (1-D) pulse-amplitude modulation (PAM) constellations that are equivalent, on an additive white Gaussian

Paper approved by R. D. Wesel, the Editor for Coding and Communication Theory of the IEEE Communications Society. Manuscript received March 11, 2002; revised November 3, 2002 and September 5, 2003. This paper was presented in part at the IEEE Conference on Communications, Anchorage, AK, May 2003.

The authors are with the Department of Electrical Engineering—Systems, Faculty of Engineering, Tel-Aviv University, Tel-Aviv 66978, Israel (e-mail: danr@eng.tau.ac.il).

Digital Object Identifier 10.1109/TCOMM.2004.823564

0090-6778/04$20.00 © 2004 IEEE

noise (AWGN) channel, to square QAM constellations of twice the symbol rate.

Our method can be applied to any binary turbo or turbo-like code, including parallel concatenation, serial concatenation, and low-density parity-check (LDPC) codes.

II. Signal Shaping in a Finite Constellation

It is well known that the maximum theoretical shaping gain, or the maximum reduction in average transmit power for constellations of rates R bits/dimension (dim) $\rightarrow \infty$ is given by $G_{s,\max} = 10\log_{10}(\pi e/6) = 1.53$ dB.

In practice, when using signal sets with finite transmission rates, this gain can never be achieved. Therefore, in order to calculate the real gain that can be achieved when using small signal sets, we turn to the calculation of the *capacity gain* [3], which is the optimization of the mutual information of the AWGN channel with discrete inputs. Consider an AWGN channel having discrete inputs $\mathbf{c}$ taking on the values $\{c_j\}$ for $j = 0, \ldots, J-1$, with probabilities $\mathrm{P_r}(\mathbf{c}) = \{\mathrm{P_r}(c_0), \mathrm{P_r}(c_1), \ldots, \mathrm{P_r}(c_{J-1})\}$.

The capacity of the discrete input AWGN channel is given by the maximum of the mutual information

$$\begin{aligned} C &= \max_{\mathrm{P_r}(\mathbf{c})} I(\mathbf{c}; Y) \\ &= \max_{\mathrm{P_r}(\mathbf{c})} \sum_{j=0}^{J-1} \mathrm{P_r}(c_j) \int_{-\infty}^{\infty} Q(Y \mid c_j) \\ &\quad \times \log \frac{Q(Y \mid c_i)}{\sum_{i=0}^{J-1} \mathrm{P_r}(c_i) Q(Y \mid c_i)}\, dY. \end{aligned} \tag{1}$$

The SNR is given by $(S/N) = (P/\sigma^2)$, where P is the average input signal power

$$P = \sum_{j=0}^{J-1} \mathrm{P_r}(c_j) \cdot c_j^2 \tag{2}$$

and σ^2 is the noise variance. Optimizing the mutual information with respect to the input probabilities $\mathrm{P_r}(\mathbf{c})$ will give the lowest required SNR when transmitting at various rates $R = C$ bits/dim. We consider the maximum SNR reduction, compared to the equiprobable transmission, as the desired capacity gain. In [12], the authors proposed a numerical method that optimizes the mutual information for a power-constrained finite constellation. We found out that the *Maxwell–Boltzmann* (MB) distribution suggested by [10] provides a very good approximation to the optimal solution, and is obtained by the distribution

$$\mathrm{P_r}(c_j) = K(\lambda) \cdot e^{-\lambda |c_j|^2}, \quad \lambda \geq 0 \tag{3}$$

where

$$K(\lambda) = \left(\sum_{c_j} e^{-\lambda |c_j|^2} \right)^{-1} \tag{4}$$

is the distribution normalization factor. This distribution maximizes the entropy of a finite constellation $H(\mathbf{c})$ under an energy constraint [3], [10], but does not necessarily optimize the mutual information. The parameter λ governs the tradeoff between the average power P of signal points and the entropy $H(\mathbf{c})$. For $\lambda = 0$, the uniform distribution arises, while increasing λ results in more concentrated distributions close to the origin. By selecting λ properly, the minimum average energy can be achieved for a given transmission rate, and consequently, the minimum SNR in the calculation of (1). The idea is best explained using an example.

Example 1: Consider the transmission of $R = 2.0$ b/dim using a 16-PAM signal constellation. In this constellation, the signal set $\mathbf{c}$ consists of the 1-D signals $\{-15, -13, -11, \ldots, -1, 1, 3, 5, \ldots, 13, 15\}$. We first assume uniform distribution for each constellation point of $\mathrm{P_r}(c_j) = 1/16$, which gives an average input signal power $P = 85$. Applying (1) for a rate-$R = 2.0$ b/dim, we get $\sigma^2 = 4.74$, which gives an SNR $S/N = 17.9$. We now apply the MB distribution (3) and (4) to the constellation. If we apply a discrete Gaussian distribution (3) with an optimized value of $\lambda_{\mathrm{opt}} = 1/9$ to the constellation points $\mathbf{c}$ and use (1) again, we get the average power $P = 16.975$ and a minimum SNR $S/N = 15.0$. Therefore, the capacity gain that we achieve here is

$$10\log_{10}\left(\frac{17.9}{15.0}\right) = 0.768 \text{ dB}. \tag{5}$$

Similarly, using the same procedure for rate-$R = 3.0$ b/dim with an optimal discrete distribution of the 16-PAM constellation with $\lambda_{\mathrm{opt}} = 0.047$, we achieve a capacity gain

$$10\log_{10}\left(\frac{82.6}{64.5}\right) = 1.074 \text{ dB}. \tag{6}$$

The losses in (5) and (6), with respect to the gains achieved by the ideal continuous AWGN channel at similar rates, are 0.001 and 0.106 dB, respectively.

III. Combining Shaping and the Pragmatic Binary TCM

A. Construction of a Binary Distribution

We apply the theoretical considerations of the previous section to practical schemes. For practical reasons, the probabilities of the constellation points from the MB distribution (3) are rounded to the closest 2^{-k}. The results for a 16-ary PAM constellation is (the result holds for both $\mathrm{R} = 2.0$ b/symbol and $\mathrm{R} = 3.0$ b/symbol)

$$\begin{aligned} P_r(c = \pm 1, \pm 3) &= 2^{-3} \\ P_r(c = \pm 5, \pm 7, \pm 9) &= 2^{-4} \\ P_r(c = \pm 11) &= 2^{-5} \\ P_r(c = \pm 13, \pm 15) &= 2^{-6}. \end{aligned} \tag{7}$$

If we use this probability mapping again in (1) for transmission rates $R = 2.0$ and 3.0 b/dim, we achieve gains of 0.682 and 0.948 dB, which are quite close to the capacity gains of the MB distribution achieved in (5) and (6). Moreover, these probabilities can easily be implemented by using a table that maps equiprobable input words of six bits into nonequiprobable words of four bits having the probabilities specified in (7). Table I shows a way to do it. The columns $b_0, b_1, \ldots, b_5$ represent the input bits. The signal points in the first column show

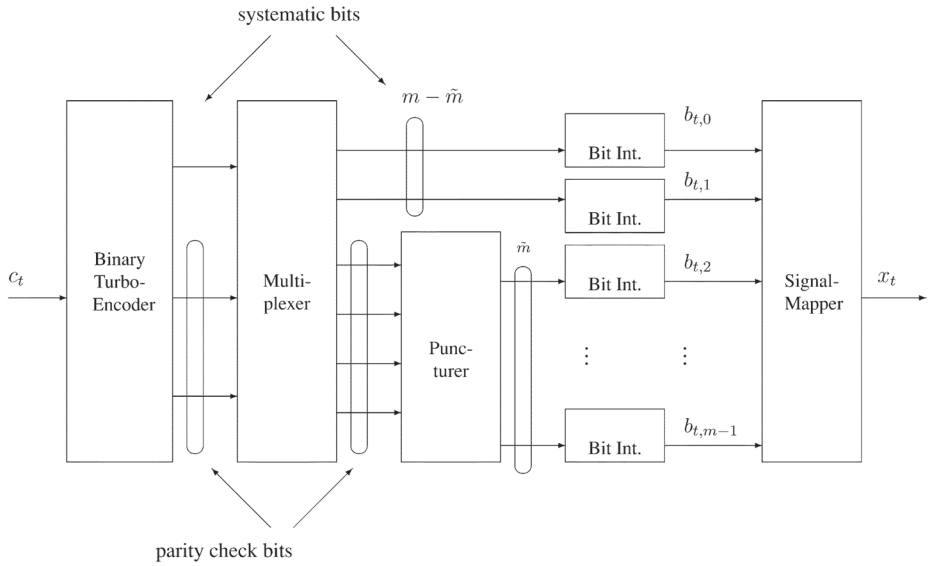


Fig. 1. Pragmatic binary TCM encoder.

TABLE I
SIGNAL MAPPER WITH BINARY PROBABILITIES OF TYPE $2^{-k}, k = 3, 4, 5,$ AND 6, FOR A 16-PAM CONSTELLATION

Signal Point	b_0	b_1	b_2	b_3	b_4	b_5
15	0	0	0	0	0	0
13	0	0	0	0	0	1
11	0	0	0	0	1	$\times 2$
9	0	0	0	1	$\times 2$	$\times 2$
7	0	0	1	1	$\times 2$	$\times 2$
5	0	0	1	0	$\times 2$	$\times 2$
3	0	1	1	$\times 2$	$\times 2$	$\times 2$
1	0	1	0	$\times 2$	$\times 2$	$\times 2$
-1	1	1	0	$\times 2$	$\times 2$	$\times 2$
-3	1	1	1	$\times 2$	$\times 2$	$\times 2$
-5	1	0	1	0	$\times 2$	$\times 2$
-7	1	0	1	1	$\times 2$	$\times 2$
-9	1	0	0	1	$\times 2$	$\times 2$
-11	1	0	0	0	1	$\times 2$
-13	1	0	0	0	0	1
-15	1	0	0	0	0	0

how to map each input word into one of the 16 signals. The notation $[\times 2]$ in the table means that a certain input bit in that location can take on the values zero or one. In this way, four words are mapped, for example, to the signal point 9.0, and eight are mapped to 1.0, and so on. Clearly, the probability of each input word is $1/64$, whereas probabilities of the output words become $8/64, 4/64, 2/64$, and $1/64$. As requested, the output probabilities are equal to the binary probabilities in (7).

It should be noticed that Table I actually performs prefix code mapping onto the constellation. This can be seen by disregarding the $[\times 2]$ entries of each input word. What is left is a variable-length Huffman prefix code.

B. Applying to TCM

We now apply the nonequiprobable distribution derived above to TCM. In pragmatic binary TCM [4], a single binary turbo code of rate $1/3$ is used as the component code. Its encoder outputs are suitably multiplexed and punctured to obtain $\tilde{m}$ parity bits and $m - \tilde{m}$ information bits, as shown in Fig. 1. The encoded bits are mapped onto an M-ary phase-shift keying (PSK) or M-QAM signal set. For simplicity, we used an M-PAM signal set, which is equivalent to an M^2-QAM having a spectral efficiency of $2(m - \tilde{m})$ b/s/Hz.

The signal mapper associates each word of m encoded bits to one of the M-PAM channel symbols available in the modulator. In an equiprobable signaling scheme, we map m encoded bits onto one of the $M = 2^m$ symbols using Gray code. Otherwise, in a nonequiprobable scheme, we apply a table (e.g., Table I) that maps m-bits equiprobable input words onto nonequiprobable M-PAM symbols.

It is clear that the mapping through the table onto the nonequiprobable constellation is a form of an additional puncturing because of the $[\times 2]$ ambiguity of some of the bits. On the other hand, as long as we keep the systematic bits unpunctured, the gain achieved by the nonequiprobable signaling scheme more than compensates for this loss in code strength. Thus, our scheme actually implements a variable-rate turbo code, because the number of parity bits given to each information bit varies as a function of the input combination.

The receiver, shown in Fig. 2, calculates the LLR calculation block for each encoded bit based on the received noisy symbol. The stream of the bit-likelihood values is then bit deinterleaved, demultiplexed, and depunctured before passing to the binary turbo decoder which is based on the maximum *a posteriori* (MAP) algorithm, e.g., [13]. As suggested in [11], the LLR calculation block is used in the turbo decoder iterations. The extrinsic coded data shown in Fig. 2 are the new values of the output turbo decoder MAP LLRs, for both systematic and parity bits, in each turbo iteration. This data will be used by the LLR calculation block as *a priori* input to the next iteration. To illustrate this, consider the calculation of the LLR for each encoded bit b_t

$$\Lambda(b_t) = \log \frac{\sum_{x:b_t=1} \exp\left(-\frac{1}{2\sigma^2}(r-x)^2\right) \cdot P_r(x \mid b_t = 1)}{\sum_{x:b_t=0} \exp\left(-\frac{1}{2\sigma^2}(r-x)^2\right) \cdot P_r(x \mid b_t = 0)} \tag{8}$$

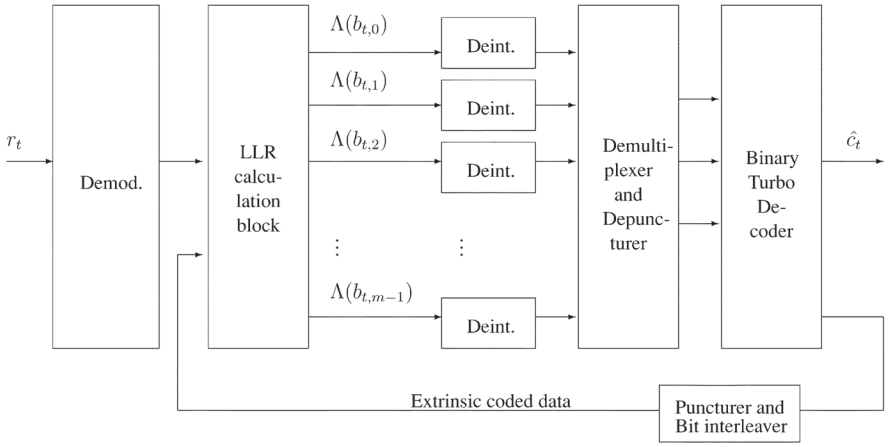


Fig. 2. Pragmatic binary TCM decoder.

where x is a symbol at the output of the mapping table, having inputs $b_t = 0$ or 1, r is the received symbol, and σ^2 is the noise variance. Each new turbo iteration will update the variable $P_r(x \mid b_t)$ and thus improve the stream of bit LLRs entering the decoder for the next iteration.

IV. Simulation Results

We used the standard rate-1/3 turbo-encoder, e.g., [14], made up of two elementary encoders with memory size four and the same generator polynomial 37-23 (octal number 23 represents feedback connections, and 37 represents feed-forward connections). The generator polynomial was taken from [15], which states the optimal encoders for various turbo-code rates and memory sizes. Turbo decoding was performed in 18 iterations on blocks of 32 768, 16 384, and 8192 information bits using pseudorandom interleaving. We applied two schemes for spectral efficiencies of 2 and 3 b/dim. The first one used a rate-1/3 turbo encoder and nonequiprobable signaling. This scheme applied Table I for a mapping of six-bit input words including two information bits onto 16-PAM symbols having a binary distribution, as in (7). It was compared to a rate-2/3 turbo code using equiprobable signaling with three-bit 8-PAM symbols, as in the standard pragmatic binary TCM technique [4]. The second scheme used a rate-1/2 turbo encoder and a similar nonequiprobable signaling technique, where this time, three information bits were mapped onto six-bit input words. It was compared with a rate-3/4 equiprobable 16-PAM pragmatic binary TCM. The bit-error rate (BER) versus E_b/N_0 for the two schemes are shown in Figs. 3 and 4. The capacity limits for the 16-PAM constellation and the continuous-input AWGN channel at both transmission rates are also reported.

The error-floor effect we have encountered occurred at BERs below 10^{-5} for the information block lengths we used. We can notice that for rate-2.0 b/dim and $P_b(e) = 10^{-5}$, the nonequiprobable scheme produces gains of 0.59 dB ($N = 32\,768$), 0.477 dB ($N = 16\,384$), and 0.57 dB ($N = 8192$) compared with the equiprobable one. The only power-constrained, continuous-input channel-capacity limit of the AWGN channel is $E_b/N_0 = 5.74$ dB. The performance of our decoder at $P_b(e) = 10^{-5}$ for the longest block length is about 1.1 dB from this limit. At 3.0 b/dim, the nonequiprobable

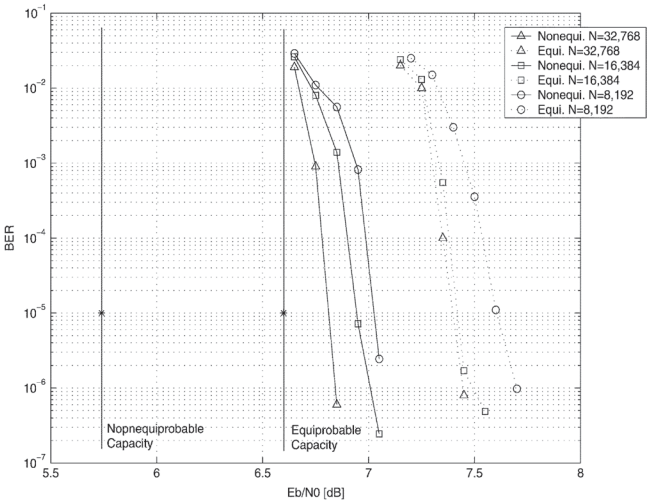


Fig. 3. Performance comparison between two schemes of nonequiprobable and equiprobable signaling at rate-2 b/dim using pragmatic binary TCM with 18 iterations and block lengths $N = 32\,768, N = 16\,384$, and $N = 8192$ b. Channel capacity limit is 5.74 dB, equiprobable 16-PAM capacity limit is 6.6 dB.

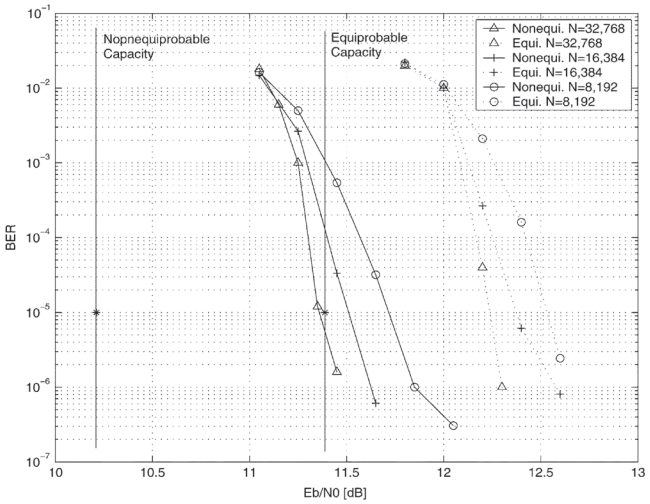


Fig. 4. Performance comparison between two schemes of nonequiprobable and equiprobable signaling at rate-3 b/dim using pragmatic binary TCM with 18 iterations and block lengths $N = 32\,768, N = 16\,384$, and $N = 8192$ b. Channel capacity limit is 10.2 dB, equiprobable 16-PAM capacity limit is 11.38 dB.

scheme produces gains of 0.87 dB ($N = 32\,768$), 0.86 dB ($N = 16\,384$), and 0.82 dB ($N = 8192$) compared with the equiprobable one for the same BER, the channel capacity limit is $E_b/N_0 = 10.2$ dB, and we achieve $P_b(e) = 10^{-5}$ for the longest block length within 1.1 dB of this limit.

It may be interesting to compare our results with the recent results of [7], where the authors used an 8-PAM TTCM scheme and shaping using nonuniform constellations for rate-2 b/dim. Using an input block size of 16 384 bits, they achieved $P_b(e) = 10^{-5}$ at SNR of $E_b/N_0 = 7.05$ dB, which is about 0.15 dB higher than our results. By increasing the block length to $N = 32\,768$ and the number of decoder iterations, our results are better within 0.25 dB.

V. Conclusion

In this letter, we presented a new scheme for improving the performance of pragmatic binary TCM by using nonequiprobable signaling. We described a nonequiprobable signaling technique that makes it possible to approach the maximum capacity gain of a finite-constellation AWGN channel. Our nonuniform signaling scheme is very easy to implement, and adds negligible load on the turbo decoder. We showed for an example of 6 b/QAM symbol, a gain of 0.9 dB relative to the equiprobable scheme performance, and transmission within 1.1 dB of the Shannon limit. Note that the difference between the capacities of the equiprobable and nonequiprobable schemes is 1.07 dB.

References

[1] G. D. Forney, Jr. and L. F. Wei, "Multidimensional constellations—Part I: Introduction, figures of merit, and generalized cross constellations," *IEEE J. Select. Areas Commun.*, vol. 7, pp. 877–892, Aug. 1989.

[2] P. Robertson and T. Woerz, "Bandwidth-efficient turbo trellis-coded modulation using punctured component codes," *IEEE J. Select. Areas Commun.*, vol. 16, pp. 206–218, Feb. 1998.

[3] U. Wachsmann, R. F. H. Fischer, and J. B. Huber, "Multilevel codes: Theoretical concepts and practical design rules," *IEEE Trans. Inform. Theory*, vol. 45, pp. 1361–1391, July 1999.

[4] S. Le Goff, A. Glavieux, and C. Berrou, "Turbo codes and high-efficiency modulation," in *Proc. IEEE Int. Conf. Communications*, New Orleans, LA, May 1994, pp. 645–649.

[5] C. Fragouli and R. D. Wesel, "Turbo encoder design for symbol-interleaved parallel concatenated trellis-coded modulation," *IEEE Trans. Commun.*, vol. 49, pp. 425–430, Mar. 2001.

[6] D. Sommer and G. Fettweis, "Signal shaping by nonuniform QAM for AWGN channels and applications using turbo coding," in *Proc. ITG Conf. Source and Channel Coding*, Jan. 2000, pp. 81–86.

[7] C. Fragouli, R. D. Wesel, D. Sommer, and P. Fettweis, "Turbo codes with nonuniform constellations," in *Proc. IEEE Int. Conf. Communications*, vol. 1, 2001, pp. 70–73.

[8] G. D. Forney, Jr., "Trellis shaping," *IEEE Trans. Inform. Theory*, vol. 38, pp. 281–300, Mar. 1992.

[9] R. G. Gallager, *Information Theory and Reliable Communication*. New York: Wiley, 1968.

[10] F. R. Kschischang and S. Pasupathy, "Optimal nonuniform signaling for Gaussian channels," *IEEE Trans. Inform. Theory*, vol. 39, pp. 913–929, May 1993.

[11] S. Benedetto and G. Montorsi, "Generalized concatenated codes with interleavers," in *Proc. IEEE Int. Symp. Turbo Codes*, Brest, France, Sept. 3–5, 1997, pp. 32–39.

[12] N. Varnica, X. Ma, and A. Kavcic, "Capacity of power-constrained memoryless AWGN channels with fixed input constellations," in *Proc. IEEE Global Telecommunications Conf.*, vol. 2, Nov. 17–21, 2002, pp. 1339–1343.

[13] L. Bahl, J. Cocke, F. Jelinek, and J. Raviv, "Optimal decoding of linear codes for minimizing symbol-error rate," *IEEE Trans. Inform. Theory*, vol. IT-20, pp. 284–287, Mar. 1974.

[14] C. Berrou, A. Glavieux, and P. Thitimajshima, "Near-optimum error-correcting coding and decoding: Turbo codes," *IEEE Trans. Commun.*, vol. 44, pp. 1261–1271, Oct. 1996.

[15] S. Benedetto, R. Garello, and G. Montorsi, "A search for good convolutional codes to be used in the construction of turbo codes," *IEEE Trans. Commun.*, vol. 46, pp. 1101–1105, Sept. 1998.

APPENDIX SOMMER03

Shaping Gain by Non-Uniform QAM Constellation with Binary Turbo Coded Modulation

Fei Zesong
Dept. of E.E.
Beijing Institute of Technology
Beijing, China
feizesong@bit.edu.cn

Kuang Jingming ,Yang Yu
Dept. of E.E.
Beijing Institute of Technology
Beijing, China

Abstract—**A non-uniform signal constellation can be used to obtain shaping gain. One typical way to design non-uniform constellation is make the output signal follow a Gaussian distribution by using equally like signals with unequal spacing. However, for binary Turbo coded modulation (BTCM) with M-QAM system, this non-uniform constellation design criteria can be modified based on different impacts of various Turbo encoded bits sequence on BER performance. In this paper, author points out that shaping gain for M-QAM with BTCM can be achieved integrated with optimization of mapping rule, performance of the proposed scheme outperforms over BTCM with uniform constellation, especially under low and moderate SNR region. Meanwhile, the effects of code rate, order of QAM constellation on shaping gain are investigated. Numeral results are provided to support the proposed scheme and analysis. The proposed scheme can be applied to high rate data service with Hybrid ARQ, such as HSDPA system.**

Keywords-Shaping gain, non-uniform constellation, M-QAM, Binary Turbo coded modulation,Mapping rule

I. INTRODUCTION

It is known from information theory that, in addition to coding gain, shaping gain of AWGN channel can be obtained while the amplitudes of output signals follow Gaussian distribution. One typical method to achieve shaping gain is to use a uniformly spaced constellation with different transmitted probability for each signal point, this idea is initial investigated in [1]. Recently, D. Raphaeli and A. Gurevitz designed one non-uniform signaling in pragmatic binary Turbo coded modulation environment with 16QAM constellation in [2].

Another way to get shaping gain is using non-uniform constellation with the same transmitted probability for each point. Non-uniform constellation has been utilized widely in many applications. For instance, to create a signal set for rate adaptive transmission in [3,4]; trellis codes employ a non-uniform constellation to get shaping gain in [5,6]. In [7], authors pointed out that when each constellation point is transmitted with the same probability and the distance between the constellation points varies in such a way that the output signal approximately follows a Gaussian distribution. Christine Fragouli presented a parallel concatenated Turbo codes employing a non-uniform constellation to achieve shaping gain [8].

In this paper, we investigate the design of non-uniform M-QAM constellation with BTCM to achieve shaping gain. In [7], author proposed a method to design a non-uniform constellation that its signal amplitude approximates Gaussian distribution for various ASK constellations and simulation results showed that for high order Gray M-QAM with Turbo code, non-uniform constellation outperforms about 0.5 - 1.0 dB over uniform constellation. Here, a novel non-uniform constellation design criteria is presented to achieve maximum shaping gain for Turbo code with M-QAM modulation.

For both Gray uniform 16QAM constellation and non-uniform constellation, it can provide fundamentally two-level error protections, in other words, there are high reliable positions and low reliable positions provided by constellation. The difference between non-uniform constellation and uniform constellation is the bit error probability difference provided by high reliable positions and low reliable positions. On the other hand, for a standard code rate R=1/3 Turbo encoder, its output bits consist of one information bit and two parity bits. For bit error ratio (BER) performance, in general, the information bit is more important. Therefore, various bits sequences of Turbo encoder output have various impacts on BER performance. To enhance BER performance, the mapping rule can be optimized in the following way: information bits of Turbo encoder output should be mapped onto high reliable positions of M-QAM constellation as more as possible, while the less important parity bits are mapped onto low reliable positions [9]. If the difference of bit error probability provided by high reliable positions and low reliable positions can match the different impacts of information bits sequence and parity bits sequence on BER perfectly, the optimal BER performance can be achieved and the largest shaping gain is obtained. Therefore, if the amplitudes of signal points in M-QAM constellation only follow Gaussian distribution, not matching the difference of various bits sequence on BER performance well, no significant shaping gain can be obtained. However, this isn't considered in [7].

Therefore, the shaping gain of M-QAM constellation with BTCM can be achieved integrated with the optimization of mapping rule design. Furthermore, the impacts of some parameters, such as code rate, the order of QAM constellation and the receiver structure on shaping gain are also investigated in this paper.

This research activity was in part supported by ERICSSON

0-7803-7822-9/03/$17.00 © 2003 IEEE.

Authorized licensed use limited to: Fish & Richardson PC. Downloaded on August 22,2022 at 14:22:15 UTC from IEEE Xplore. Restrictions apply.

The rest parts of this paper are organized as follows. System model and some fundamental analysis are given in section II. The proposed scheme achieving shaping gain integrated with optimization of mapping rule for BTCM with M-QAM is presented in Section III. Furthermore, the influences of channel code rate, order of modulation lever are analyzed in Section IV. Finally some conclusions are drawn in section V.

II. SYSTEM MODEL

In this section, system model and some fundamental analysis are introduced. Firstly transmitter and receiver structures of BTCM with M-QAM are given; second the uncoded BER property of uniform and non-uniform 16QAM Gray constellation is analyzed. Then the mapping rule can be optimized based on the influences of various Turbo encoded bits sequence on decoding performance. Finally the performance comparison of uniform and non-uniform constellation proposed in [7] is presented.

A. Binary Turbo Coded Modulation (BTCM)

BTCM is proposed in [10] as a bandwidth efficient modulation using Turbo codes. Fig 1 shows a code rate R=(m-m')/m turbo encoder built from a binary standard turbo encoder using rate matching with M-QAM modulation.

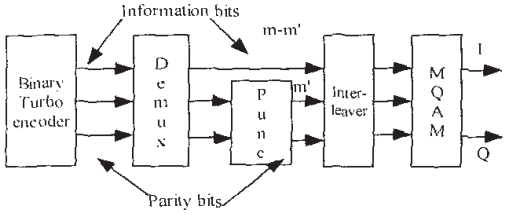


Figure 1. BTCM with M-QAM modulation

Non-iterative receiver is showed in Fig.2 ignoring the dotted line, from observation of modulation symbols, the Logarithm of Likelihood (LLR) associated with each bit can be calculated and sent to binary Turbo decoder as a relevant soft decision. In this paper, only the case of square Gray M-QAM constellation is considered and the calculation of LLR is in accordance with that in [10].

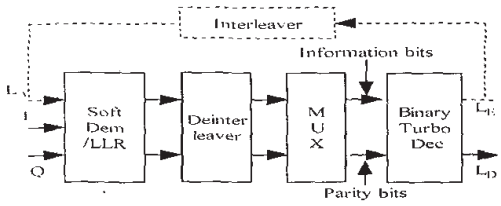


Figure 2. Receiver structure of BTCM scheme

B. Uniform & Non-Uniform QAM Constellation

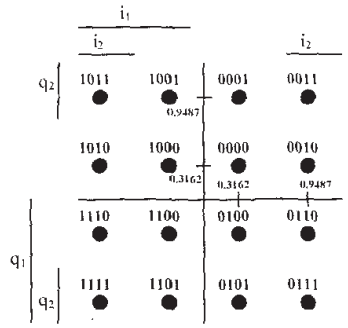
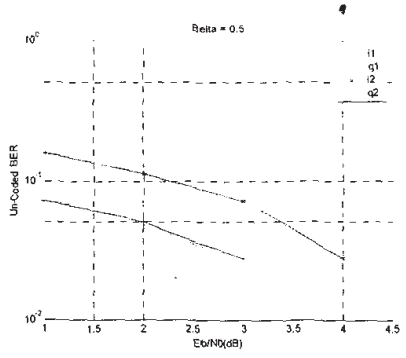


Figure 3. Gray uniform constellation of 16QAM

Square Gray uniform constellation of 16QAM is showed in Fig. 3, the bit error probability of bit position: i1 and q1 is the same and different from that of bit positions: i2 and q2. And higher error protections are provided for bits positions: i1 and q1, namely high reliable positions. Therefore, there are two-level error protections provided by uniform constellation [11]. While for non-uniform 16QAM constellation as mentioned in [7], the spaces of various signal points are unequal as listed in Table 1. The average constellation energy is normalized. Uncoded BER performances of each bit position of constellation are showed in Fig. 4, it's clear that the performance difference of high reliable positions and low reliable positions of uniform & non-uniform constellation is different.

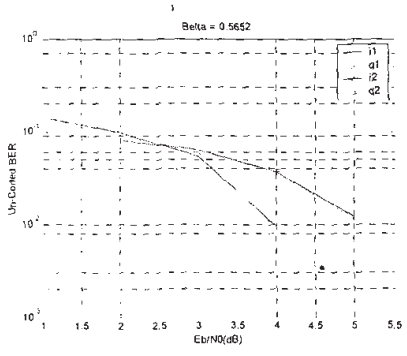
TABLE I. SIGNAL POINTS OF 16QAM (4-ASK)

Uniform constellation	±0.3162	±0.9487
Non-uniform constellation	±0.2677	±0.9635



(a) Uniform Constellation

Authorized licensed use limited to: Fish & Richardson PC. Downloaded on August 22,2022 at 14:22:15 UTC from IEEE Xplore. Restrictions apply.



(b) Non-Uniform Constellation in [7]

Figure 4. Bit error probability of different bit positions of uniform and non-uniform Gray 16QAM constellation

C. *Different Influences of VariousEncoded Bits Sequences on Turbo Decoding Performance*

As mentioned in previous section, information bits are usually more important than parity bits for decoding BER performance. Therefore, output coded bits sequence of Turbo encoder can be divided into at least two sub-flows, that is information bits sequence and parity bits sequence based on their different influences on decoding performance. Some related simulation results with 1/3 code rate while encoded block length is 400 are shown in Fig 5, we can see that information bits sequence denoted by "s" is more important than parity bits sequence. Although the Turbo codes performance itself is independent of the specific mapping, it is advantageous to offer the most reliable bits to the first decoder. Therefore, parity bits sequence of the first component encoder denoted by "p1" is slightly important that parity bits sequence of the second component encoder denoted by "p2".

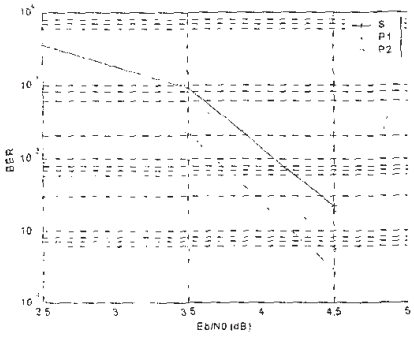


Figure 5. Importance of different bit sequences with 1/3 code rate

Note: We get the Fig. 5 through the following way. For example, when only information bits are transmitted through AWGN channel and parity bits are sent through error-free channel, the curve, BER versus Eb/N0, denoted by legend "s" can be obtained after 8 iterations SOVA decoding. Other two curves can be obtained by similar way. Under the same Eb/N0, the BER value of the curve denoted by legend "s" is higher than that of either of other two curves. In other words, if information bits received in error, it'll result in a higher BER than BER caused by receiving parity bits in error. Therefore, information bits sequence has a more important impact on BER performance.

D. *Performance Comparison of Uniform & Non-Uniform QAM Constellations*

From above analysis, it's clear that to get better BER performance of BTCM with M-QAM system, the mapping rule should be optimized as presented in [9]. In this section, BER performances of BTCM with uniform & non-uniform constellation in [7] with and without optimization of mapping rule are showed in Fig. 6. From simulation results, it can be seen that first scheme with optimization outperforms over the scheme without optimization; secondly integrating with optimization of mapping rule, uniform constellation is better than non-uniform one in [7]. Therefore, the criteria presented in [7] achieving shaping gain is no longer valid.

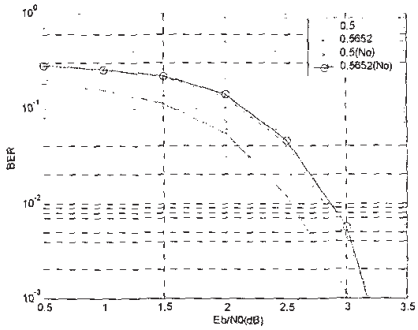


Figure 6. Performance of BTCM with uniform & non-uniform constellation with and without mapping rule optimization

III. SHAPING GAIN ACHIEVEMENT BY NON-UNIFORM CONSTELLATION WITH MAPPING RULE OPTIMIZATION

A. *Non-uniform Constellation Construction*

In previous section, a non-uniform 16QAM constellation that its signal amplitude approximately follows Gaussian distribution is used to achieve shaping gain. However, from simulation results, it can be seen that isn't good with 1/3 code rate. Therefore, in this section, a method to construct a kind of non-uniform 16QAM constellations [11] is introduced that the spaces of signal points can be arbitrarily variable, and the difference of error probability of various bit positions can be arbitrary. Then we can select the optimal non-uniform constellation through a rough search, which can achieve the largest shaping gain.

The non-uniform constellation can be construct as outlined in following. The basis is a square 4-QAM constellation defined by formula (1), and the scaled versions of the basis are defined by formula (2).

$$S_1 = c \cdot \{1+j, -1+j, -1-j, 1-j\} \quad (1)$$

Authorized licensed use limited to: Fish & Richardson PC. Downloaded on August 22,2022 at 14:22:15 UTC from IEEE Xplore. Restrictions apply.

$$S_i = \beta \cdot S_{i-1}, \qquad i = 2, \cdots, m \tag{2}$$

Where c is a constant established by constellation average energy normalization, and $4^m = M$.

The points of the constellation are obtained by summing one symbol from each of the m alphabets, defined by formula (3), where $s_{i,k}$ is a symbol from the symbol alphabet s_i .

$$a_k = \sum_{i=1}^{m} s_{i,k}, \qquad k = 0, \cdots, M-1 \tag{3}$$

B. *Shaping Gain Achievement with the Optimization of Mapping Rule*

From above analysis and simulation results, it's clear that to achieve shaping for BTCM with M-QAM constellation, the design criteria proposed in [7] isn't optimal, it should be in conjunction with the optimization of mapping rule for Turbo coded signal. To find the non-uniform 16QAM constellation that can provide the largest shaping gain with 1/3 code rate, a rough search for non-uniform constellations with different spaces of signal points by changing the value of β in (2). While $\beta = 0.5$, uniform constellation is obtained. The encoded block length of simulations in this section is 400.

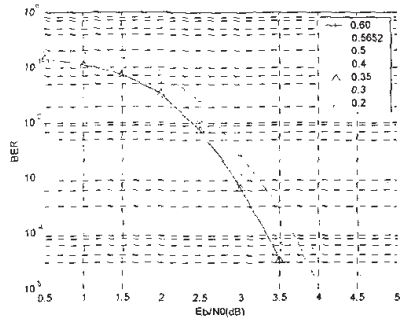


Figure 7. BER performances with different values of β (R=1/3)

From Fig. 7, it's clear that when $\beta = 0.35$, the largest shaping gain can be obtained, if the value of β is higher or lower than 0.35, the shaping gain available is less than that of $\beta = 0.35$. In other words, when $\beta = 0.35$, the difference of bit error probability provided by high reliable positions and low reliable positions of non-uniform constellation can match the different impacts of information bits sequence and parity bits sequence on BER best, the optimal BER performance can be achieved and the largest shaping gain is obtained, although the improvement of shaping gain is not obvious.

IV. Influence of Some Parameters on Shaping Gain Achievement of BTCM System

Based on the results and analysis of previous section, the influences of some parameters, such as code rate, order of modulation level on shaping gain achievement are analyzed in this section.

A. *Impact of Code Rate on Shaping Gain*

Up to now, the analysis and results are focused on Turbo code with 1/3 code rate, in this subsection the influence of code rate on the achievement of shaping gain is investigated. Our scheme is based on the fact of different encoded bits have various impacts on BER performance. However, there is another fact that the importance of each kind of encoded bits sequence to BER performance is changed with code rate. Fig. 8 shows the similar result with 1/2 code rate compared to the results with 1/3 code rate illustrated in Fig. 5. As we know, only parity bits are punctured to get different code rate code. For different puncture ratio, the proportion of information bits sequence of the total code bits sequence is various. For those links with very high puncture rates, it is most likely that the proportion of the information bits of the output bits sequence become large. And the influence of left parity bits sequence on BER becomes comparable with that of information bits sequence. The difference impacts of various bits sequences on decoding performance can be ignored. Therefore, we can expect that the role of optimized mapping rule becoming slighter with code rate increasing. For 1/3 code rate, we can see different bits sequences have various impacts on decoding performance clearly. While code rate increase to 1/2, the difference impacts of various bits sequences become much slight.

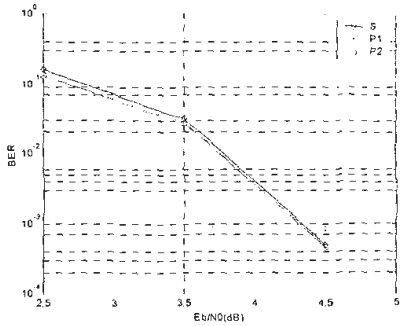


Figure 8. Importance of different bit sequences with 1/2 code rate

Since the importance of each kind of encoder output b sequence of 1/2 code rate is different from that of 1/3, the val of β chosen for 1/3 code rate to achieve the largest shapi gain isn't optimal for 1/2 code rate. Through similar search f 1/3 code rate, the optimal value can be found.

Compared with Fig. 9, we can find that the optimal BI performance is achieved using non-uniform constellati with $\beta = 0.5$, instead of $\beta = 0.35$. The reason lies in t bits sequence importance to BER performance with 1/2 cc rate is variable compared with that of 1/3, as mentior previously.

Authorized licensed use limited to: Fish & Richardson PC. Downloaded on August 22,2022 at 14:22:15 UTC from IEEE Xplore. Restrictions apply.

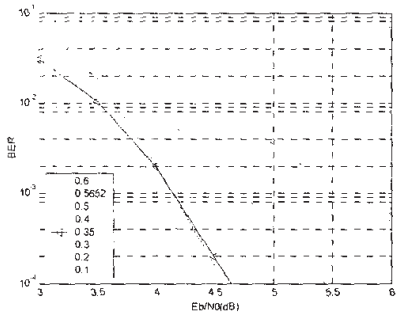


Figure 9. BER performances with different values of β (R=1/2)

B. *Impact of Order of M-QAM Constellation on Shaping Gain*

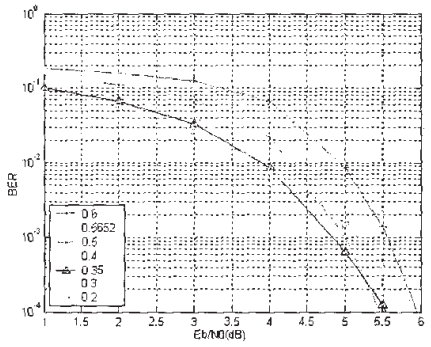


Figure 10. BER performances with different values of β (R=1/3,64QAM)

Compared with 16QAM, 64QAM can provide three levels error protection, i.e. high reliable, middle reliable and low reliable positions. Similar with the mapping rule optimization of 16QAM, the mapping rule of 64QAM is optimized to get better performance. While extended to 64QAM, larger shaping gain obtained by non-uniform constellation. From Fig. 10, we can see that the optimal BER performance can be achieved through non-uniform constellation with the value of β between 0.3 and 0.4. For 64QAM, under low and middle SNR range, non-uniform constellation outperforms over uniform constellation significantly, larger than 0.5dB; while channel condition becomes good, non-uniform constellation isn't so advantageous as under poor channel conditions.

V. CONCLUSIONS

To achieve the shaping gain for Turbo code signal, conventional method is to make the amplitudes of output signals follow Gaussian distribution. In this paper, author points out that this criteria should be modified, taking into account the different influences of various encoded bits sequence on channel decoding performance. Integrated with the optimization of mapping rule for Turbo coded signal, it can be found that the conventional method can't achieve large shaping gain. Therefore a simple search method is introduced to find the optimal non-uniform constellation to achieve largest shaping gain. In the meanwhile, the effects of Turbo code rate and the order of QAM constellation on shaping gain are analyzed. Simulation results show that the optimal non-uniform constellation outperforms over uniform constellation, and the order of QAM constellation is higher, the larger gain can be achieved, especially under low and middle SNR values with high order QAM modulation about 0.5-1.0dB gain can be achieved. The scheme proposed in this paper can applied to high rate data service with HARQ protocol, such as high speed downlink packet access (HSDPA).

ACKNOWLEDGMENT

The authors are grateful to the anonymous reviewers for their careful reading and comments. In addition, the authors would like to acknowledge the continuing contributions of Wan Lei, Zhao Shenghui, Liu Linnan, Yang Xiaoqian.

REFERENCE

[1] A. R. Calderbank, L. H. Ozarow, "Nonequiprobable Signalling on the Gaussian Channel", IEEE Trans. On Info. , vol. 36, pp. 726-740, July 1990.

[2] D. Raphaeli, A. Gurevitz, "Constellation shaping for pragmatic turbo coded modulation", Electronics Letters, vol. 38, pp. 717-719, July, 2002.

[3] K. Fazel, M. Ruf, "combined multilevel coding and multiresolution modulation", ICC'93, pp. 1081-1085, Sept, 1993.

[4] T. Todmann, "Optimierung von signalraumaufteiungen fur eine hierarchische ubeertragung", ITG Fachtagung fur codierung, Quelle, anal and Ubertragung, Mar, 1998.

[5] W. Betts, A. Calderbank, "Performance of nonuniform constellations on the gaussian channel", IEEE Trans. On Info. Theory, Vol 40, pp 1633-1638, Sept, 1993.

[6] F. Sun and H. Tilborg, "Approaching capacity by equiprobable signaling on the gaussian channel", IEEE Trans. on Info. Theory, pp 1714-1716.

[7] G. Fettweis, D. Sommer, "Signal shaping by non-uniform qam fr awgn channels and applications using turbo coding", ITG Conference Source and Chanel coding, pp 81-86, Jan, 2000.

[8] Christine Fragouli, Richard D.Wesel, " Turbo codes with non-uniform QAM constellation", ICC 2001, pp

[9] Fei Zesong, Wan Lei and Kuang Jingming, "Improved Binary Turbo Coded Modulation with 16QAM in HSDPA", WCNC 2003, (Accepted), March, 2003.

[10] S. Le Goff, A. Glavieux, and C. Berrou, "Turbo codes and high spectral efficiency modulation", in Proc. ICC '94, New Orleans, 1994, pp. 645-649.

[11] Roald Otnes, Torleiv Maseng, "Adaptive data rate using ARQ and Nonuniform constellations", IEEE VTC 2001, pp. 1211-1215.

Authorized licensed use limited to: Fish & Richardson PC. Downloaded on August 22,2022 at 14:22:15 UTC from IEEE Xplore. Restrictions apply.

APPENDIX SOMMER04

Constellation Shaping for Bandwidth-Efficient Turbo-Coded Modulation With Iterative Receiver

Stéphane Y. Le Goff, Boon Kien Khoo, Charalampos C. Tsimenidis, *Member, IEEE,* and Bayan S. Sharif, *Senior Member, IEEE*

***Abstract*— This paper introduces a new technique for combining constellation shaping and bit-interleaved turbo-coded modulation (BITCM) over additive white Gaussian noise channel. The proposed scheme consists of serial concatenation of a binary turbo code, short-length binary shaping code, and mapping function using Gray labeling. The corresponding receiver is made up of four blocks (demapper, shaping decoder, and two constituent RSC decoders) exchanging extrinsic information in order to optimize error performance. A BITCM scheme employing 16-PAM constellation to achieve a rate of 3 bits/dim is considered as an example. It is shown that, by careful selection of the shaping code parameters, shaping gains almost equal to 0.8 dB can be obtained at a little cost in terms of system complexity.**

***Index Terms*— Constellation shaping, iterative receiver, shaping code, turbo-coded modulation.**

I. Introduction

CONSTELLATION shaping refers to techniques used in bandwidth-efficient communication schemes to reduce the average transmitted signal power (see, e.g., [1]-[8]). The idea is to transmit constellation signal points with low energy more frequently than those with high energy. The resulting power saving, called shaping gain, is achieved while affecting neither the data rate nor the error performance of the whole system. For bandwidth-efficient communications over additive white Gaussian noise (AWGN) channels, it is interesting to investigate the combination of constellation shaping and turbo coding [9], [10]. Some techniques have recently been proposed to apply shaping principles to the design of turbo-coded modulation by employing either a multi-level coding (MLC) approach [11]-[13] or a bit-interleaved coded modulation (BICM) approach [14]-[17].

In MLC, shaping and coding algorithms operate independently of each other because the information bits that are not channel-encoded can be used for shaping [3], [4]. It is thus relatively easy to integrate coding and shaping within a common MLC scheme. For practical applications, MLC is, however, less attractive than BICM; indeed BICM schemes are generally simpler to implement, more flexible, and have less decoding delay and simpler design rules than MLC systems. Note that, in the context of this paper, the adjective *flexible* refers to the ability of a system to accommodate different data rates without requiring any change in the modulation and basic channel coding functions. Despite its simplicity, BICM is, in most cases, as power-efficient as MLC provided that near-capacity channel codes, such as turbo codes, are employed [18]. All these features have recently made BICM a very popular approach for designing coded modulation schemes.

The error performance of BICM schemes could be further improved by using constellation shaping. A major difference between MLC and BICM is that, in BICM, all information bits are channel-encoded, which means that coding and shaping algorithms can no longer be separated. This makes the integration of shaping and coding in the same system a more challenging issue in BICM than in MLC.

Sommer and Fettweis were the first to apply constellation shaping principles to BICM schemes using turbo coding, hereafter referred to as *bit-interleaved turbo-coded modulation* (BITCM) schemes [14]. Their idea consisted of employing non-uniform pulse-amplitude modulation (PAM) constellations for which signal points are transmitted with equal probabilities but are placed on the one-dimensional (1-D) axis according to a Gaussian distribution [19]. Recently, Raphaeli and Gurevitz introduced a more sophisticated, and also more power-efficient, method in which a variable-rate turbo code is followed by a Huffman code mapping onto non-equiprobable signal points of a PAM constellation. The turbo code rate is matched to the Huffman code using time-varying puncturing so that both data rate and transmitted signal rate remain constant [15]-[17]. It was shown that, with such technique applied to 16-PAM, shaping gains of approximately 0.6 and 0.9 dB can be achieved for data rates equal to 2 and 3 bits/dim, respectively.

In this paper, we propose and investigate another method for combining shaping and BITCM. Our approach, which is radically different from those presented in [14]-[17], consists of partitioning the basic constellation into several equal-sized sub-constellations of increasing average energy. A shaping code is then used to specify the sequence of sub-constellations so that low-energy signals are transmitted more often than high-energy signals [4]. The partitioning method preserves the Gray mapping, and is therefore suitable for BITCM design, provided that only one level of partition is considered, i.e. the basic constellation is divided into two sub-constellations. This relative compatibility between shaping and Gray mapping

Manuscript received October 12, 2005; revised June 28, 2006 and October 31, 2006; accepted November 15, 2006. The associate editor coordinating the review of this paper and approving it for publication was T. Duman. This paper was presented in part at IEEE GLOBECOM'04, Dallas, Texas, 29 November- 3 December 2004, and in part at the International Symposium on Turbo Codes and Related Topics, Munich, Germany, 3-7 April 2006.

The authors are with the School of Electrical, Electronic, and Computer Engineering at the University of Newcastle upon Tyne, United Kingdom (e-mail: stephane.le-goff@ncl.ac.uk; b.k.khoo@ncl.ac.uk; charalampos.tsimenidis@ncl.ac.uk; bayan.sharif@ncl.ac.uk).

Digital Object Identifier 10.1109/TWC.2007.05780.

1536-1276/07$25.00 © 2007 IEEE

constitutes a crucial point since it is well known that BICM schemes using near-capacity channel codes, such as turbo codes, perform optimally when Gray mapping is used to label constellation signal points [18], [20]. It is worthwhile mentioning that, when using low-complexity convolutional codes instead of turbo codes, there are other labeling techniques that perform better than Gray mapping (see, e.g., [21]-[27]). The application of such techniques to BICM with shaping is, however, beyond the scope of this paper because our goal is primarily to design very power-efficient coding schemes whose complexity is not necessarily the critical issue.

Throughout this work, we assume an AWGN channel and only consider the case of 2^m-ary 1-D constellations, referred to as 2^m-PAM constellations. The results given in this paper are therefore directly applicable to the design of BITCMs based on square quadrature-amplitude modulation (QAM) constellations since any square 2^{2m}-QAM modulation using Gray mapping is actually made up of two independent 2^m-PAM modulations in quadrature.

The organization of this paper is as follows. In Section II, the general structure of the proposed BITCM scheme is presented. Particular attention is paid to the description of the iterative decoding algorithm that involves several constituent blocks at the receiver side. Then, we consider in Section III an example for which we give various theoretical and computer simulation results. In the same section, we also show that it is possible to simplify tremendously the receiver structure without any significant error performance degradation. Finally, Section IV presents conclusions of this work.

II. Structure of the Proposed BITCM System

In this section, we present the structure of the BITCM transmitter and receiver proposed in this paper. Before proceeding further, let us stipulate a convention: A notation in the form $V = (v_i)_I$ shall be used hereafter to denote a block/sequence V composed of I scalar quantities $v_i, i \in \{1, ..., I\}$, that can be either bits or log-likelihood ratios (LLRs) associated to bits.

The block diagrams of the proposed BITCM transmitter and receiver are shown in Fig. 1.

A. BITCM Transmitter Structure

A frame $U = (u_p)_{N_f}$ composed of N_f information bits $u_p, p \in \{1, ..., N_f\}$, is encoded by a rate-$R_c$ binary turbo encoder made up of two parallel-concatenated recursive and systematic convolutional (RSC) codes separated by a random interleaver [9], [10]. The coded sequence E is divided, using a serial-to-parallel (S/P) converter, into m parallel sequences which are then bit-interleaved separately in a random fashion ($\pi_j, j \in \{1, ..., m\}$). The bit stream available at the first interleaver output (π_1) is broken into L successive K-bit blocks $M = (m_k)_K$. Each block M is fed into a block shaping encoder (S-ENC) which generates a corresponding N-bit codeword $C = (c_n)_N$, with $N > K$. The rate of this encoder is thus $R_s = \frac{K}{N}$. The sequence of codewords at the shaping encoder output, whose length is equal to LN bits, is then randomly interleaved (π_s). The S/P converter is designed so that the length of the $(m-1)$ sequences fed into interleavers $\pi_j, j \in \{2, ..., m\}$, is also equal to LN bits. This S/P converter

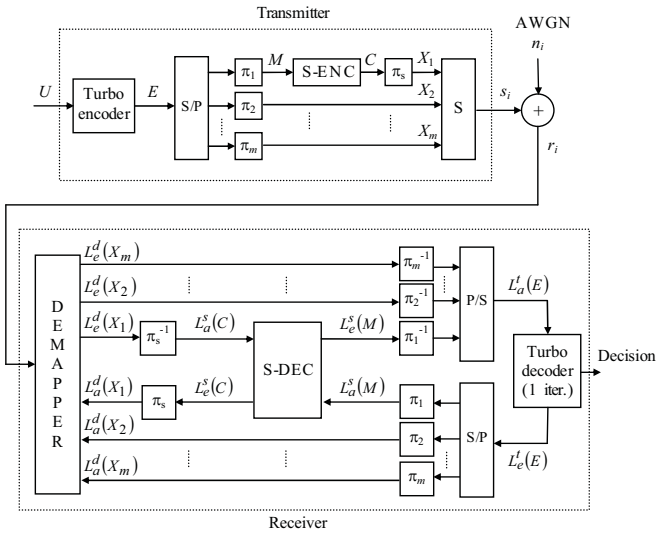


Fig. 1. Structure of the proposed BITCM scheme.

is therefore not a standard one since the first sequence (to be interleaved by π_1) contains only LK coded bits, i.e. fewer bits than the other $(m-1)$ sequences. Hereafter, we use the notations $X_1 = (x_{i,1})_{LN}$ and $X_j = (x_{i,j})_{LN}, j \in \{2, ..., m\}$, to designate the binary sequences at the output of interleavers π_s and π_j, respectively. Finally, a vector $(x_{i,1}, x_{i,2}, ..., x_{i,m})$, where $x_{i,j}$ denotes the i-th bit in sequence $X_j, j \in \{1, ..., m\}$, is mapped onto a signal point of a 2^m-PAM constellation, called S, according to Gray labeling.

The transmission of a frame of $N_f = R_c L[K + N(m-1)]$ information bits is performed by emitting LN successive signal points $s_i, i \in \{1, ..., LN\}$. The data rate R obtained with such system is thus given by

$$R = R_c(R_s + m - 1) \text{ bits/dim}, \tag{1}$$

and is lower than the rate $R' = mR_c$ bits/dim obtained with an equivalent BITCM scheme without shaping code. Hence, the use of a shaping encoder in our BITCM transmitter results in a loss in data rate that must be compensated for by increasing either the number of signal points in S or the code rate R_c. In our BITCM system, the simplest way to keep the data rate constant consists of increasing the rate R_c by changing the puncturing pattern at the turbo encoder output.

The constellation S is partitioned into two sub-constellations S_0 and S_1 so that S_0 contains the 2^{m-1} signal points of lowest energies, whereas S_1 is composed of the 2^{m-1} signal points of highest energies [4]. The Gray mapping is performed in such a way that bits $x_{i,1}$, which are originally generated by the shaping encoder, are used to select one of these sub-constellations. Assuming that $x_{i,1} = 0$ leads to the selection of S_0, the shaping encoder is designed so that $\Pr\{x_{i,1} = 0\} > \Pr\{x_{i,1} = 1\}$, i.e. S_0 is emitted more frequently than S_1. Since the average energy of signal points in S_0 is lower than that in S_1, it results in some energy saving at the transmitter output with respect to the case where S_0 and S_1 are used with equal probabilities (no shaping). The resulting energy saving E_s, in

decibels (dB), can be evaluated using

$$E_s = 10\log_{10}\left[\frac{E_0+E_1}{2(P_0E_0+[1-P_0]E_1)}\right], \quad (2)$$

where E_0 and E_1 are the average signal energies in sub-constellations S_0 and S_1, respectively, and P_0 designates the average value of $\Pr\{c_n=0\}$ at the shaping encoder output:

$$P_0 = \frac{1}{N}\sum_{n=1}^{N}\Pr\{c_n=0\}. \quad (3)$$

The shaping gain, which represents the actual energy saving, is obtained after the loss in data rate has been compensated for.

B. BITCM Receiver Structure

In order to optimize the error performance of the receiver, demapping, shaping decoding and channel decoding are performed according to an iterative algorithm [28], [29]. This receiver is made up of several soft-input soft-output (SISO) modules, connected through interleavers/de-interleavers, that exchange information in order to improve the reliability of the LLRs flowing through them. A particular SISO module processes LLR sequences, called *a priori* information, produced by the other modules in order to generate updated versions of those input sequences, called *a posteriori* information. An extrinsic knowledge is then obtained by subtracting an *a priori* LLR from the corresponding *a posteriori* LLR. This extrinsic information is then passed as an *a priori* knowledge to the other modules for further iterative decoding steps.

In our BITCM receiver, there are four iterative loops operating in parallel and allowing for information exchange between demapper and turbo decoder, demapper and shaping decoder, turbo decoder and shaping decoder, and finally both constituent decoders inside the turbo decoder. At first glance, such structure may seem complicated, but we will see later that it is possible to simplify it tremendously without any significant error performance degradation.

In this sub-section, the operation and the role of the different modules used in the BITCM receiver are explained. Note that, hereafter, the notation $L_\alpha^\beta(v), \alpha\in\{a,e\}, \beta\in\{d,s,t,t_1,t_2\}$, is used to denote the LLR of v, v being either a bit or a block/sequence of bits.

1) The Demapper: For each transmitted frame of LN signal points $s_i, i\in\{1,...,LN\}$, the corresponding received frame is composed of LN channel samples r_i that can be expressed as $r_i = s_i + n_i$, where n_i is a Gaussian noise sample with zero mean and variance $\sigma^2 = \frac{N_0}{2}$, N_0 being the one-sided power spectral density of white Gaussian noise. The role of the demapper is to compute, for each index i, the extrinsic LLRs $L_e^d(x_{i,j}), j\in\{1,...,m\}$. To this end, it processes, at each iteration, sample r_i as well as m *a priori* LLRs $L_a^d(x_{i,j}), j\in\{1,...,m\}$, representing the extrinsic information generated by both shaping and turbo decoders at the previous iteration. The computation of LLRs $L_e^d(x_{i,j})$ is performed using

$$L_e^d(x_{i,j}) = \ln\left[\frac{\Pr\{x_{i,j}=1, r_i, L_a^d(x_{i,1}),...,L_a^d(x_{i,m})\}}{\Pr\{x_{i,j}=0, r_i, L_a^d(x_{i,1}),...,L_a^d(x_{i,m})\}}\right] - L_a^d(x_{i,j}). \quad (4)$$

To further develop (4), let us assume that each LLR $L_a^d(x_{i,j})$ is a Gaussian sample with a mean equal to $(2x_{i,j}-1+L_{i,j})$ and a certain variance δ^2, where the parameter $L_{i,j}$ represents the *a priori* knowledge regarding bit $x_{i,j}$ already available before the first decoding iteration starts. The value of parameter $L_{i,j}, i\in\{1,...,LN\}$, is computed using

$$L_{i,j} = \ln\left[\frac{1-\Pr\{x_{i,j}=0\}}{\Pr\{x_{i,j}=0\}}\right]. \quad (5)$$

In practice, the variance δ^2 can be given any suitable empirical value. Using Bayes' rule and taking $\delta^2=2$, it can then be shown that (4) is equivalent to

$$L_e^d(x_{i,j}) = \ln\left[\frac{\sum_{s\in S_j^1} P\{r_i|s\}\Pr\{L_a^d(x_{i,1\to m,\neq j})|s\}\Pr\{s\}}{\sum_{s\in S_j^0} P\{r_i|s\}\Pr\{L_a^d(x_{i,1\to m,\neq j})|s\}\Pr\{s\}}\right] - L_{i,j}, \quad (6)$$

where S_j^t denotes the subset of signals $s\in S$ whose labels have the value $t\in\{0,1\}$ in position $j\in\{1,...,m\}$, and $L_a^d(x_{i,1\to m,\neq j})$ refers to the set composed of all *a priori* LLRs except $L_a^d(x_{i,j})$. The term $P\{r_i|s\}$ designates the transition probability density function of the AWGN channel given by

$$P\{r_i|s\} = \frac{1}{\sqrt{\pi N_0}}\exp\left\{-\frac{(r_i-s)^2}{N_0}\right\}. \quad (7)$$

In (6), the terms $\Pr\{L_a^d(x_{i,1\to m,\neq j})|s\}, s\in S_j^t$, can be computed using

$$\Pr\{L_a^d(x_{i,1\to m,\neq j})|s\} = \left(\frac{1}{\sqrt{4\pi}}\right)^{m-1}\exp\left\{-\frac{1}{4}\sum_{l=1,\neq j}^{m}[L_a^d(x_{i,l})-(2s_l-1)-L_{i,l}]^2\right\}, \quad (8)$$

where $s_l\in\{0,1\}$ is the value of the label of signal s in position l.

To find the expression of the extrinsic LLR $L_e^d(x_{i,j})$, we also need to determine in (6) the probability, $\Pr\{s\}$, of transmitting a particular signal s. It can easily be shown that $\Pr\{s\} = \frac{\Pr\{x_{i,1}=0\}}{2^{m-1}}$ if $s\in S_0$ and $\Pr\{s\} = \frac{1-\Pr\{x_{i,1}=0\}}{2^{m-1}}$ if $s\in S_1$. The average value of $\Pr\{x_{i,1}=0\}$ over a frame of LN transmitted signals s_i is equal to P_0. The LN probabilities $\Pr\{x_{i,1}=0\}$ are obviously known by the receiver. By combining (6), (7), and (8), and performing a few simplifications, we obtain:

$$L_e^d(x_{i,j}) = \ln\left[\frac{\sum_{s\in S_j^1}\exp\left\{A\right\}}{\sum_{s\in S_j^0}\exp\left\{A\right\}}\right] - L_{i,j}, \quad (9)$$

where

$$A = -\frac{(r_i-s)^2}{N_0} + s_1L_{i,1} + \sum_{l=1,\neq j}^{m} s_l(L_a^d(x_{i,l})-L_{i,l}). \quad (10)$$

In our system, the parameters $L_{i,l}, l \in \{2, ..., m\}$, are actually equal to zero. This is not the case for parameters $L_{i,1}$ since the bits $x_{i,1}$ generated by the shaping encoder are more likely to be equal to zero than one. The resulting simplification of (9) yields

$$L_e^d(x_{i,j}) = \ln \left[\frac{\sum_{s \in \mathrm{S}_j^1} \exp\left\{ -\frac{(r_i - s)^2}{N_0} + \sum_{l=1, \neq j}^{m} s_l L_a^d(x_{i,l}) \right\}}{\sum_{s \in \mathrm{S}_j^0} \exp\left\{ -\frac{(r_i - s)^2}{N_0} + \sum_{l=1, \neq j}^{m} s_l L_a^d(x_{i,l}) \right\}} \right]. \tag{11}$$

It is worth mentioning that, in practice, the computational complexity of the demapper can be reduced at a very negligible cost in terms of error performance by approximating (11) with the following expression:

$$\begin{aligned} L_e^d(x_{i,j}) \quad = \quad & \max_{s \in \mathrm{S}_j^1} \left(-\frac{(r_i - s)^2}{N_0} + \sum_{l=1, \neq j}^{m} s_l L_a^d(x_{i,l}) \right) \\ & - \max_{s \in \mathrm{S}_j^0} \left(-\frac{(r_i - s)^2}{N_0} + \sum_{l=1, \neq j}^{m} s_l L_a^d(x_{i,l}) \right). \end{aligned} \tag{12}$$

Note that, at the first iteration, the initial values of *a priori* LLRs are set as follows: $L_a^d(x_{i,1}) = L_{i,1}$ and $L_a^d(x_{i,j}) = 0, j \in \{2, ..., m\}$.

2) The Shaping Decoder: For each frame of LN received channel samples r_i, the demapper produces m parallel sequences $L_e^d(X_j) = (L_e^d(x_{i,j}))_{LN}, j \in \{1, ..., m\}$. The first sequence $L_e^d(X_1)$ is de-interleaved (π_s^{-1}) and broken into L blocks $L_a^s(C) = (L_a^s(c_n))_N$. At each iteration, the task of the SISO shaping decoder (S-DEC) is to produce both extrinsic LLRs $L_e^s(M) = (L_e^s(m_k))_K$ and $L_e^s(C) = (L_e^s(c_n))_N$. The LLRs $L_e^s(M)$ are to be processed by the turbo decoder at the same iteration, whereas LLRs $L_e^s(C)$ will be used by the demapper at the next iteration. The shaping decoder is not only fed with *a priori* LLRs $L_a^s(C)$ produced by the demapper, but also with *a priori* LLRs $L_a^s(M)$ representing the extrinsic information generated by the turbo decoder at the previous iteration. Since shaping codes typically operate on very short-length blocks, it is realistic to use the MAP algorithm for the shaping decoding. Hence, in order to compute $L_e^s(M)$, the SISO shaping decoder evaluates, for $k \in \{1, ..., K\}$, the expression

$$L_e^s(m_k) = \ln \left[\frac{\Pr\{m_k = 1, L_a^s(M), L_a^s(C)\}}{\Pr\{m_k = 0, L_a^s(M), L_a^s(C)\}} \right] - L_a^s(m_k), \tag{13}$$

which is equivalent to

$$L_e^s(m_k) = \ln \left[\frac{\sum_{M \in \Omega_k^1} \Pr\{L_a^s(C), L_a^s(m_{1 \to K, \neq k}) | M\}}{\sum_{M \in \Omega_k^0} \Pr\{L_a^s(C), L_a^s(m_{1 \to K, \neq k}) | M\}} \right], \tag{14}$$

where $\Omega_k^t, t \in \{0, 1\}$, denotes the set of all blocks M for which $m_k = t \left(|\Omega_k^0| = |\Omega_k^1| \right)$, and $\Pr\{L_a^s(C), L_a^s(m_{1 \to K, \neq k}) | M\}$ designates the probability of receiving all input LLRs except $L_a^s(m_k)$ given the transmission of a particular block M.

Using an approach similar to that employed to obtain (11), one can show that extrinsic LLRs $L_e^s(m_k), k \in \{1, ..., K\}$, are given by

$$L_e^s(m_k) = \ln \left[\frac{\sum_{M \in \Omega_k^1} \exp\{B\}}{\sum_{M \in \Omega_k^0} \exp\{B\}} \right], \tag{15}$$

where

$$B = \sum_{l=1, \neq k}^{K} t_l L_a^s(m_l) + \sum_{n=1}^{N} t_n \left(L_a^s(c_n) - L_n \right), \tag{16}$$

$t_l \in \{0, 1\}$ is the value of the l-th bit in the block M under consideration, and $t_n \in \{0, 1\}$ is the value of the n-th bit in the codeword C associated to this particular block. Parameters $L_n, n \in \{1, ..., N\}$, represent the *a priori* knowledge regarding bits c_n available before the first decoding iteration starts, and are computed using

$$L_n = \ln \left[\frac{1 - \Pr\{c_n = 0\}}{\Pr\{c_n = 0\}} \right]. \tag{17}$$

In a similar fashion, it can be shown that the expressions of extrinsic LLRs $L_e^s(c_n), n \in \{1, ..., N\}$, are given by

$$L_e^s(c_n) = \ln \left[\frac{\sum_{C \in \Delta_n^1} \exp\{D\}}{\sum_{C \in \Delta_n^0} \exp\{D\}} \right], \tag{18}$$

where

$$D = \sum_{k=1}^{K} t_k L_a^s(m_k) + \sum_{l=1, \neq n}^{N} t_l \left(L_a^s(c_l) - L_l \right), \tag{19}$$

and $\Delta_n^t, t \in \{0, 1\}$, designates the set of all codewords C for which $c_n = t$. In this expression, $t_l \in \{0, 1\}$ is the value of the l-th bit in the codeword C under consideration, and $t_k \in \{0, 1\}$ is the value of the k-th bit in the block M associated to this codeword. It is worthwhile mentioning that $|\Delta_n^0| > |\Delta_n^1|$ since there are more zeros than ones in codewords generated by the shaping encoder.

Expressions (15) and (18) indicate that the computational complexity of the MAP decoding algorithm can become prohibitive for high values of K and N. In particular, the number of additions required for the evaluation of these expressions increases exponentially with K since $|\Omega_k^0| + |\Omega_k^1| = |\Delta_n^0| + |\Delta_n^1| = 2^K$. However, for small values of parameters K and N, the implementation of (15) and (18) remains of reasonable complexity. This is a crucial point since it is, fortunately, possible to obtain significant shaping gains when using codes with small values of K and N. To illustrate this statement, let us consider an example. Fig. 2 shows the variation of the energy saving, E_s, as a function of the codeword length N, achieved when a rate-1/2 shaping code is combined to 16-PAM constellation according to the configuration considered in this paper. A computer program was written to generate automatically the shaping code for any rate R_s and codeword length N so that the average probability P_0, i.e. the energy

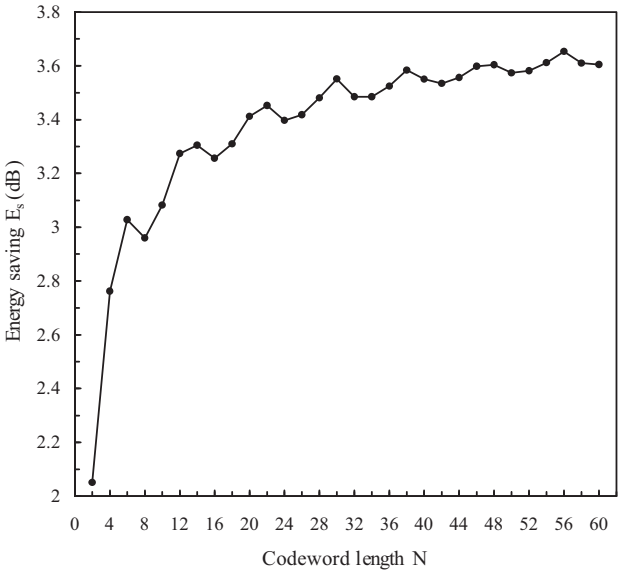


Fig. 2. Energy saving E_s as a function of the codeword length N, for a 16-PAM constellation combined to a rate-$\frac{1}{2}$ shaping code according to the configuration considered in this paper (one level of partition).

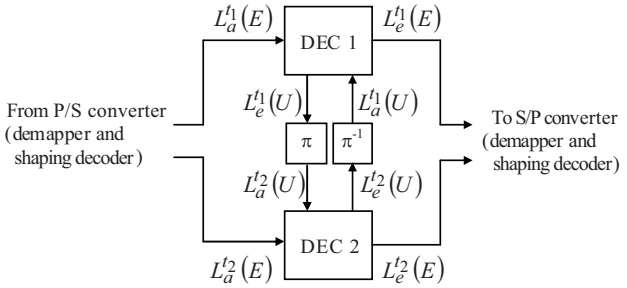


Fig. 3. Core structure of the turbo decoder made up of two SISO decoders DEC1 and DEC2 connected through an interleaving pair π/π^{-1}.

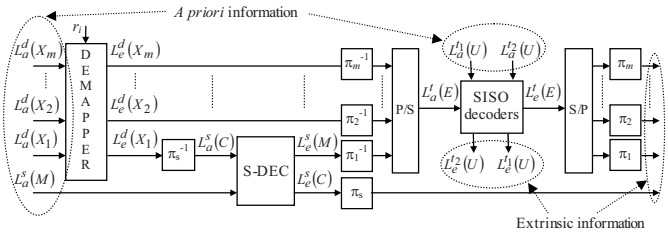


Fig. 4. Structure of a BITCM receiver module required to implement a single decoding iteration. This module processes $(m+3)$ *a priori* LLR sequences and generate their corresponding extrinsic LLRs. For clarity sake, the delay elements required for proper operation are omitted.

saving E_s, is maximized. Note that the energy saving plotted in Fig. 2 is achieved while decreasing the constellation entropy from 4 bits/dim to 3.5 bits/dim.

The results in Fig. 2 show that the value of the energy saving "saturates" as N increases. This indicates that, in practice, there is not much to be gained by increasing the codeword length N beyond a certain value. For instance, the energy saving achieved by using the moderate-complexity ($N = 14, K = 7$) code is 3.30 dB (corresponding to $P_0 \approx 0.854$), which is only 0.18 dB less than that obtained with the much more complex ($N = 32, K = 16$) code ($P_0 \approx 0.866$), and 0.30 dB less than that of the unpractical ($N = 60, K = 30$) code ($P_0 \approx 0.874$). Note that the number of possible codewords for these three rate-1/2 shaping codes is $2^7 = 128$ for $N = 14$, $2^{16} = 65536$ for $N = 32$, and $2^{30} \approx 10^9$ for $N = 60$. From Fig. 2, it can be concluded that, if any significant shaping gain is to be achieved, it will be without having to employ complex shaping codes, which is an encouraging result as far as the system complexity is concerned. Finally, note that the small irregularities in the curve plotted in Fig. 2 mean that a slight increase in the codeword length N does not always result in a higher energy saving. In other words, for a given rate R_s, some shaping codes clearly achieve a better "energy saving-complexity" trade-off than others.

3) The Turbo Decoder: The sequences $L_e^d(X_j) = (L_e^d(x_{i,j}))_{LN}, j \in \{2, ..., m\}$, as well as that composed of L blocks $L_e^s(M)$ are de-interleaved separately ($\pi_j^{-1}, j \in \{1, ..., m\}$), and then combined together through the P/S converter to form a single LLR stream $L_a^t(E)$ used as an *a priori* information by the turbo decoder. The latter is made up of two SISO constituent decoders separated by an interleaving pair π/π^{-1} corresponding to the interleaving embedded in the turbo encoder [9], [10], [28], [29]. The core of this decoder is depicted in Fig. 3.

The SISO constituent decoder DEC-$x, x \in \{1, 2\}$, processes the part of stream $L_a^t(E)$ that is relevant to it, denoted as $L_a^{t_x}(E)$ in Fig. 3, as well as some *a priori* information $L_a^{t_x}(U)$, regarding the sequence U of information bits, which was produced by the other constituent decoder at the previous iteration. Based on both sequences, decoder DEC-x generates two extrinsic sequences $L_e^{t_x}(E)$ and $L_e^{t_x}(U)$ to be used at next iteration by the demapper-shaping decoder pair and the other constituent decoder, respectively. The reader is referred to [30], [31] for more details regarding the algorithm used to produce LLR sequences $L_e^{t_x}(E)$ and $L_e^{t_x}(U)$. Finally, the turbo decoder generates the extrinsic sequence $L_e^t(E)$ representing the *added value* of this decoder to the *a priori* sequence $L_a^t(E)$.

After S/P conversion of this LLR stream and interleaving of the m parallel sequences thus generated ($\pi_j, j \in \{1, ..., m\}$), we obtain the sequences $L_a^d(X_j), j \in \{2, ..., m\}$, and that composed of L blocks $L_a^s(M)$ to be used as *a priori* information at the next iteration by the demapper and the shaping decoder, respectively.

As a summary, Fig. 4 shows the structure of a BITCM receiver module that implements, in practice, a single decoding iteration. Each module processes $(m+3)$ sequences of *a priori* LLRs, all of them generated by the previous module, in order to produce the corresponding streams of extrinsic LLRs that will be used by the next module.

III. Performance of the Proposed BITCM System

The error performance of our BITCM system is investigated in this section. To this end, we consider the example of a 3-bit/dim 16-PAM BITCM scheme for which the achievable shaping gains are evaluated and computer simulation results are given. It is also shown that it is possible to simplify the receiver structure without significant error performance degradation.

A. Achievable Shaping Gains

Let $s \in \mathrm{S}$ and r denote respectively the transmitted signal and the corresponding received signal. Information theory tells us that the mutual information I of the discrete-input Gaussian channel, expressed in bits/dim, is given by [15]-[17]

$$I = \sum_{s\in \mathrm{S}} \int_{-\infty}^{+\infty} \Pr\{s\} P(r|s) \log_2 \left[\frac{P(r|s)}{\sum_{s\in \mathrm{S}} P(r|s)\Pr\{s\}} \right] dr, \tag{20}$$

where $P(r|s)$ denotes the transition probability density function of the AWGN channel. It can be seen from (20) that the mutual information depends both on the terms $P(r|s)$, i.e. the signal-to-noise ratio, and also on the probabilities $\Pr\{s\}$ of transmitting the different signals $s \in \mathrm{S}$. Consider a particular value I of the mutual information. When all probabilities $\Pr\{s\}$ are equal, this mutual information value is obtained for a certain SNR, called γ_0, which represents the channel capacity limit of the system in the absence of constellation shaping. If we apply a shaping algorithm that makes the probabilities $\Pr\{s\}$ unequal, it is possible to achieve the same mutual information I with a SNR value, denoted as γ_1, which is smaller than γ_0. When γ_1 and γ_0 are both expressed in dB, the potential shaping gain that can be obtained with the shaping algorithm is simply equal to $(\gamma_0 - \gamma_1)$ dB. Therefore, the concept of mutual information allows us to determine the shaping gains achievable with the method proposed in this paper. Based on (20), it could be shown that the mutual information for the system described in this paper can be expressed as

$$I = E_{s,r} \left[\log_2 \left(\frac{2^{m-1} \exp\left\{ -\dfrac{3\gamma_s (r-s)^2}{4^{m-1}(7-6P_0)-1} \right\}}{\sum_{x\in \mathrm{S}} p(x) \exp\left\{ -\dfrac{3\gamma_s (r-x)^2}{4^{m-1}(7-6P_0)-1} \right\}} \right) \right], \tag{21}$$

where $E_{s,r}[.]$ denotes expectation of "." with respect to s and r, γ_s is the average signal-to-noise ratio (SNR) per transmitted signal, and the term $p(x)$ is equal to P_0 for $x \in \mathrm{S}_0$ and equal to $(1 - P_0)$ for $x \in \mathrm{S}_1$.

Numerical integration of (21) via the Monte Carlo method allows us to determine the achievable shaping gain for any desired mutual information I and any values of parameters m and P_0. Fig. 5 shows the variation of the shaping gain as a function of P_0, when I = 3 bits/dim and m = 4 (16-PAM). It is seen that the method described in this paper can offer shaping gains larger than 0.7 dB provided that the shaping code is designed so that P_0 ranges from 0.69 to 0.85. The maximal value of the shaping gain is equal to 0.80 dB, and is obtained when $P_0 \approx 0.78$. Such value is 0.14 dB less than that obtained with the method introduced by Raphaeli and Gurevitz which is based on a partitioning of 16-PAM into four sub-constellations [15]-[17].

B. Choice of Coding Rates R_c and R_s

To guarantee the best error performance at the receiver output, it is important to select carefully the values of parameters

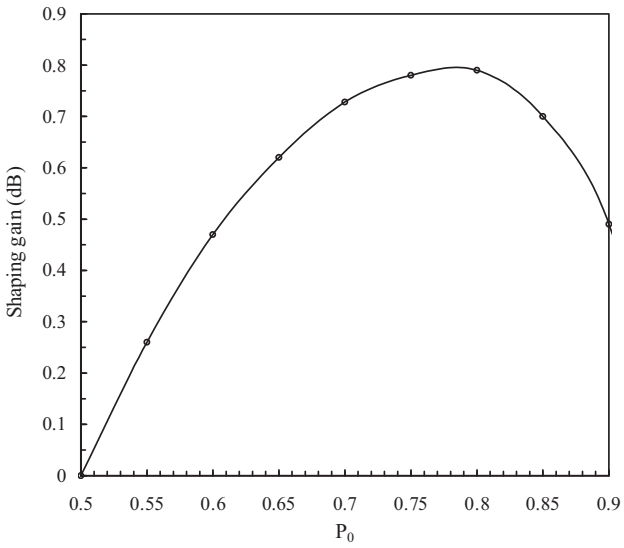


Fig. 5. Variation of the achievable shaping gain as a function of P_0 for the proposed system, when $I = 3$ bits/dim and $m = 4$ (16-PAM).

TABLE I
SEVERAL POSSIBLE CONFIGURATIONS FOR DESIGNING A 3-BIT/DIM 16-PAM BITCM SCHEME

R_c	R_s	K	N	P_0	E_s (dB)
4/5	3/4	3	4	0.687	1.44
		6	8	0.717	1.72
5/6	3/5	3	5	0.775	2.32
		6	10	0.806	2.69
6/7	1/2	1	2	0.750	2.05
		2	4	0.812	2.76
		3	6	0.833	3.03
		4	8	0.828	2.96
		5	10	0.837	3.08
		6	12	0.851	3.27
		7	14	0.854	3.30
		8	16	0.850	3.26
7/8	3/7	3	7	0.875	3.61
		6	14	0.875	3.61

R_s and R_c. We indicate in Table 1 a number of configurations that are of particular interest for the practical design of our 3-bit/dim 16-PAM BITCM scheme since they correspond to turbo code rates R_c in the form $R_c = \frac{n}{n+1}$, n being an integer. For complexity reasons, only shaping codes with a number of codewords smaller than or equal to $2^8 = 256$ ($K \leq 8$) are considered.

The results in Table 1 indicate that all listed configurations for which $R_c = \frac{4}{5}, \frac{5}{6}$, and $\frac{6}{7}$ are potentially suitable since they are associated with values of P_0 that fall within the appropriate range previously determined by the theoretical analysis ($0.69 < P_0 < 0.85$). On the other hand, the case $R_c = \frac{7}{8}$ and $R_s = \frac{3}{7}$ corresponds to values of P_0 which are outside this range, and should therefore not be considered any further. Obviously, this would also be the case for any other configuration with $R_c > \frac{7}{8}$ and $R_s < \frac{3}{7}$. This simple analysis shows that a good design strategy consists of finding the right balance between the rates of both codes so that the total available amount of redundancy (1 bit/dim in our example) is properly shared between shaping coding and channel coding.

Once suitable configurations have been identified, we can select the values of K and N that produce the highest energy saving E_s for each configuration. Note that, for a given value of R_s, increasing K (or N) does not necessarily result in a larger energy saving (as indicated in Fig. 2). For instance, for the case $R_s = \frac{1}{2}$, the $(N = 12, K = 6)$ code provides the same energy saving as the $(N = 16, K = 8)$ code despite being four times simpler to implement (four times lesser codewords).

C. Simulation Results

We simulated the error performance of several 3-bit/dim 16-PAM BITCMs made up of five different shaping codes identified to be potentially the most attractive ones according to the results given in Table 1. The $(N = 6, K = 3)$ code was also considered despite providing a smaller energy saving than the $(N = 12, K = 6)$ and $(N = 14, K = 7)$ codes because it is interesting to assess the shaping gain that can be achieved using a very low complexity shaping code.

The rate-$\frac{4}{5}$, -$\frac{5}{6}$, and -$\frac{6}{7}$ turbo codes are obtained by puncturing a rate-1/3 turbo code built from two parallel-concatenated 16-state RSC codes with polynomials (23, 31). To ensure optimal error performance, only parity bits are punctured. We adopted the puncturing patterns proposed in [32]. The size of the pseudo-random interleaver separating both RSC codes, i.e. the length N_f of a frame of information bits, can be either large (N_f = 10000 bits) or small (N_f = 2000 bits). After transmission of a frame of N_f information bits, the trellis of the first RSC encoder is reset to the all-zero state. Turbo decoding is performed in 10 iterations, and the log-MAP algorithm is used for the decoding of each RSC code. In all cases, Gray mapping is such that maximum protection is offered to parity bits. Figs. 6 and 7 show graphs of BER versus $\frac{E_b}{N_0}$ for several 3-bit/dim 16-PAM BITCM schemes, for large and small frames, respectively. The BER curves obtained without shaping are also displayed for comparison purposes.

From Figs. 6 and 7, it is seen that the shaping technique described in this paper allows for significant error performance improvement for both frame sizes. For instance, at a BER of 10^{-5}, we achieve, with the $(N = 14, K = 7)$ code, shaping gains equal to 0.72 dB and 0.78 dB, for N_f = 10000 and 2000 bits, respectively. These simulation results indicate that the best shaping code is the $(N = 14, K = 7)$ code, closely followed by the $(N = 12, K = 6)$ and $(N = 10, K = 6)$ codes. As expected, smaller, but still significant, shaping gains of 0.42 and 0.50 dB are achieved when using the very low-complexity $(N = 6, K = 3)$ code, for N_f = 10000 and 2000 bits, respectively.

D. Simplification of Receiver Structure

The receiver structure depicted in Figs. 1 and 4 may seem complicated due to the four iterative loops operating in parallel. It is therefore desirable to simplify such structure. Hereafter, we propose to show that, in most practical cases, it is possible to remove the demapper from the iterative decoding loop without degrading the overall error performance. This obviously results in a tremendous simplification of the receiver structure since two iterative loops are then eliminated.

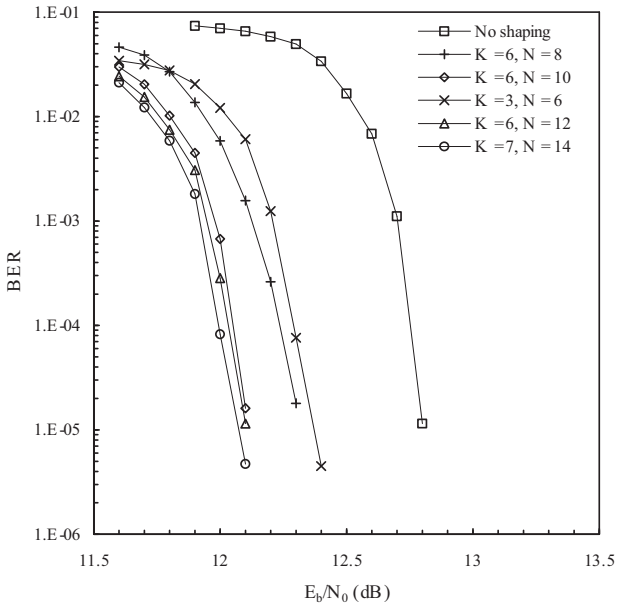


Fig. 6. BER performance comparison over AWGN channel between several 3-bit/dim 16-PAM BITCM schemes operating on large frames (N_f = 10000 bits). Turbo decoding is performed in 10 iterations. The results are given for five different shaping codes. For comparison purposes, the BER curve obtained with the equivalent BITCM system without shaping is also plotted.

In the existing literature about convolutional-coded BICM, it has been widely reported that iterative demapping is not beneficial when Gray mapping is employed (see, e.g., [21], [25]). On the other hand, some studies have reached opposite conclusions since they have indicated that iterative demapping with Gray mapping can actually bring some substantial performance improvement [14], [28], [29]. It is thus necessary to further clarify this point.

To this end, let us focus on a particular extrinsic LLR $L_e^d(x_{i,j})$ generated by the demapper, and assume that, in addition to the channel sample r_i, some *a priori* information $L_a^d(x_{i,1\to m,\neq j})$ regarding the values of bits $x_{i,l}, l \in \{1, ..., j-1, j+1, ..., m\}$ is made available to this demapper. It is well known that the demapper produces an *erroneous* LLR $L_e^d(x_{i,j})$, i.e. an LLR $L_e^d(x_{i,j})$ that would generate a bit error after hard decision, when the detected signal s_i^d is different from the transmitted signal s_i^t and the j-th bits in the labels of s_i^d and s_i^t are different.

Consider first the case where s_i^d and s_i^t are nearest neighbor signal points. With Gray mapping, the labels of two nearest neighbor signal points can differ by only one bit. This implies that the $(m-1)$ bits in positions $l, l \in \{1, ..., j-1, j+1, ..., m\}$, in the labels of s_i^d and s_i^t are identical. Therefore, any *a priori* knowledge regarding the values of bits $x_{i,l}, l \in \{1, ..., j-1, j+1, ..., m\}$ cannot help the demapper in producing a more reliable LLR $L_e^d(x_{i,j})$. In such case, iterative demapping does not improve the error performance of the whole BITCM system.

The situation is different when s_i^d and s_i^t are not nearest neighbor signal points. In this case, the $(m-1)$ bits in positions $l, l \in \{1, ..., j-1, j+1, ..., m\}$, in the labels of these particular signal points are not all identical. As a result, some *a priori* knowledge $L_a^d(x_{i,1\to m,\neq j})$ generally allows the demapper to

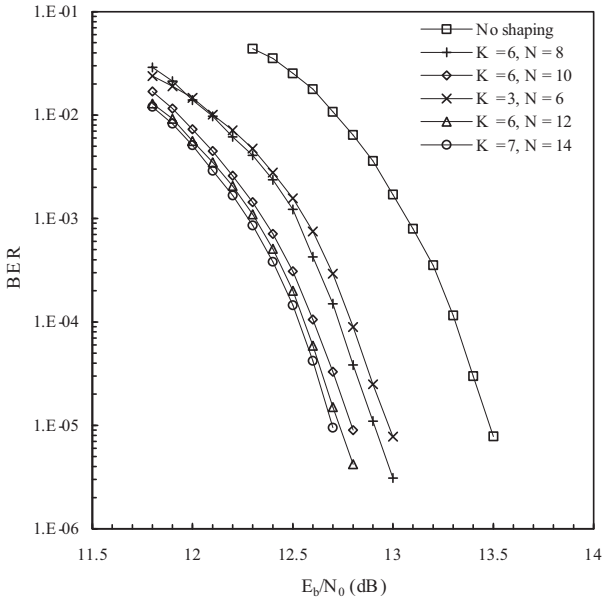


Fig. 7. BER performance comparison over AWGN channel between several 3-bit/dim 16-PAM BITCM schemes operating on small frames (N_f = 2000 bits). Turbo decoding is performed in 10 iterations. The results are given for five different shaping codes. For comparison purposes, the BER curve obtained with the equivalent BITCM system without shaping is also plotted.

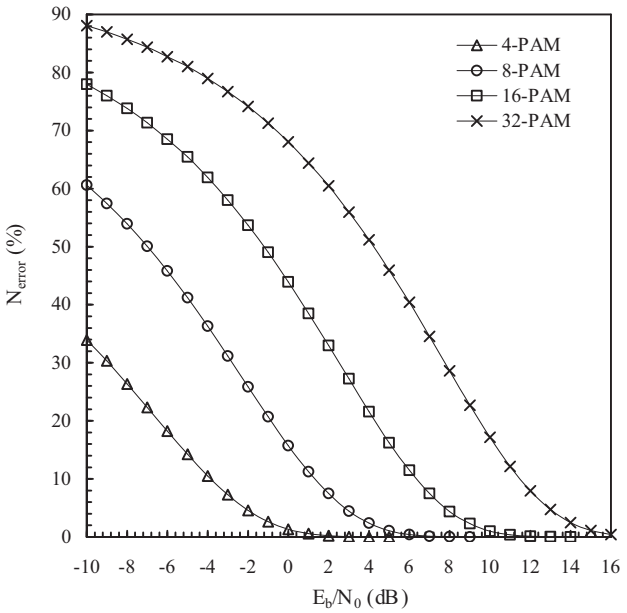


Fig. 8. Percentage, N_{error}, of error events due to a confusion between two signal points that are not nearest neighbors as a function of $\frac{E_b}{N_0}$, for four uncoded 2^m-PAM constellations and transmission over AWGN channel.

perform a better distinction between both signal points, and thus generate a more reliable estimate $L_e^d(x_{i,j})$.

We conclude that, when Gray mapping is employed, iterative demapping does improve performance only if there is a significant percentage of error events that are due to some confusion between non-nearest neighbor signal points. On AWGN channels, these error events only occur at low SNR. To illustrate this statement, we evaluated via computer simulations the percentage, N_{error}, of such error events as a function of the SNR $\frac{E_b}{N_0}$, for four different uncoded 2^m-PAM constellations. The results, plotted in Fig. 8, confirm that the probability that transmitted and detected signals are not nearest neighbors is significant only at low SNR values. Hence, iterative demapping can only be beneficial for BITCM systems operating at these low SNR values. By exploiting the results given in Fig. 8, we found that, as a rule of thumb, the error performance of a 2^m-PAM BITCM scheme can be improved by iterative demapping as long as the data rate R is less than or equal to $(m-2)$ bits/dim. On the other hand, if the desired rate is $R = (m-1)$ bits/dim, then iterative demapping is not beneficial.

As an example, Fig. 9 displays the BER curves obtained with two 16-PAM BITCM schemes using turbo codes with rates $R_c = \frac{1}{2}$ and $\frac{3}{4}$ in order to achieve data rates of 2 bits/dim and 3 bits/dim, respectively. No shaping code is employed in both cases. From Fig. 9, it is clearly seen that the use of iterative demapping does improve the error performance of the 2-bit/dim scheme by approximately 0.3 dB, but does not affect that of the 3-bit/dim system.

Shannon theory tells us that the best choice for designing a $(m-1)$-bit/dim coding scheme based on PAM signalling consists of employing a constellation with 2^m signal points. In fact, the use of a larger signal set would only increase the system complexity while keeping the error performance unchanged [33]. This is the reason why 2^m-PAM constellations are, in practice, seldom used for transmitting information at rates of $(m-2)$ bits/dim or less. Taking into account the conclusions reached earlier, we can therefore state that, in most cases of practical interest, it is possible to remove the demapper from the iterative decoding loop without degrading the error performance of the whole system.

Fig. 10 shows the corresponding simplified receiver structure. The only difference between such block diagram and that of a classical BITCM receiver (see, e.g., [34]) is the presence of a SISO shaping decoder fed, at each iteration, with blocks $L_a^s(C)$ and $L_a^s(M)$ generated by demapper and turbo decoder, respectively. The task of this shaping decoder is to generate the extrinsic information $L_e^s(M)$ to be processed at next iteration by the turbo decoder. Note that, with such simplified structure, both SISO constituent decoders DEC-$x, x \in \{1,2\}$, embedded inside the turbo-decoder are no longer required to produce extrinsic LLRs of the parity bits since, in practice, only LLRs of the information bits are exchanged between turbo and shaping decoders. This further simplifies the receiver structure.

To check the conclusions reached in this sub-section, we performed some computer simulations on a 3-bit/dim 16-PAM BITCM system using a $(N = 14, K = 7)$ shaping code. The results, which are not displayed here due to the lack of space, clearly confirmed that the demapper can be removed from the iterative decoding loop without any noticeable performance degradation.

Finally, it is interesting to compare the error performance of the 3-bit/dim 16-PAM system proposed in [15]-[17], hereafter referred to as Raphaeli′s scheme, with that of our system with $N = 14$ and $K = 7$. We have represented in Fig. 11 six BER plots obtained using both approaches, for frame sizes N_f equal to 2000, 1000, and 500 bits. All these systems employ

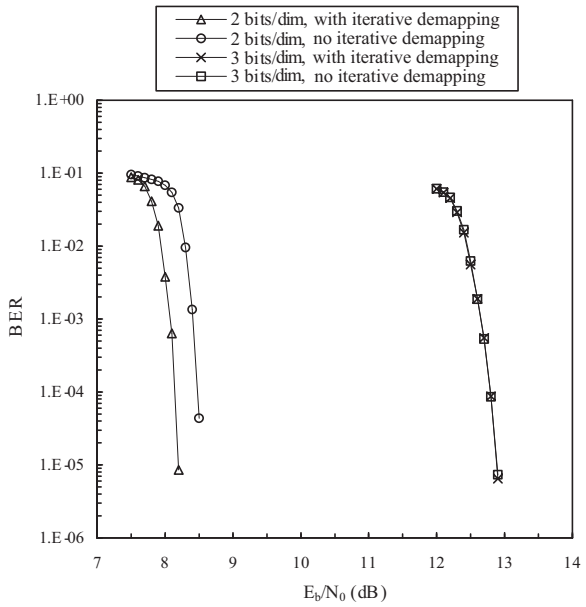


Fig. 9. BER performance comparison over AWGN channel between several 16-PAM BITCM schemes using turbo codes with rates $R_c = \frac{1}{2}$ and $\frac{3}{4}$ in order to achieve data rates of 2 bits/dim and 3 bits/dim, respectively, with and without iterative demapping. The frame size is 10000 bits and turbo decoding is performed in 8 iterations.

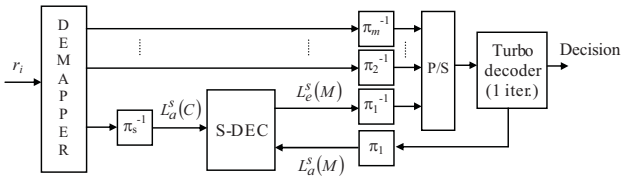


Fig. 10. Structure of the simplified BITCM receiver. The demapper has been removed from the iterative decoding loop.

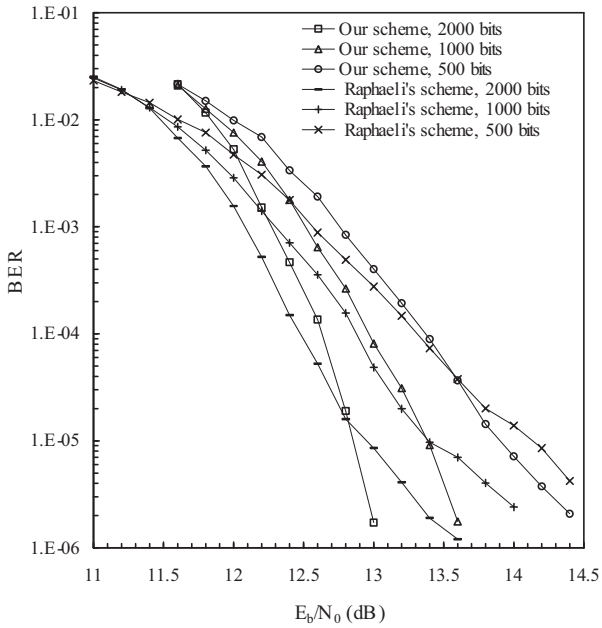


Fig. 11. BER performance comparison over AWGN channel between several 3-bit/dim 16-PAM BITCM systems designed using either Raphaeli's method or the technique proposed in this paper with $N = 14$ and $K = 7$. The schemes operate on frame sizes N_f equal to 2000, 1000, and 500 bits. All systems employ the same turbo code built from two parallel-concatenated 16-state RSC codes with polynomials (23, 31). In all cases, both RSC codes are decoded using the log-MAP algorithm and 10 iterations are used at the receiver side without including the demapper inside the decoding loop.

the same turbo code built from two parallel-concatenated 16-state RSC codes with polynomials (23, 31). In all cases, both RSC codes are decoded using the log-MAP algorithm and 10 iterations are used at the receiver side without including the demapper inside the decoding loop. By examining these results, it is seen that Raphaeli′s scheme outperforms our system at high-to-medium error rates. However, as the SNR is increased, the performance gap between both approaches diminishes. For BERs smaller than approximately $10^{-4} - 10^{-5}$, our scheme actually turns out to be the most power-efficient.

The method introduced in [15]-[17] is based on a partitioning of 16-PAM into four sub-constellations. It provides a potential shaping gain which is between 0.1 and 0.2 dB higher than that achieved with our technique. However, this is not the main reason behind the superiority of Raphaeli′s scheme at low SNR. From Fig. 11, we observe that the convergence threshold of our BITCM receiver is about 0.5 dB higher than that of Raphaeli′s receiver. We recall that the convergence threshold is defined as the minimal SNR at which the iterative decoding algorithm is able to converge, i.e. decrease the bit error rate between two successive iterations. In fact, the higher convergence threshold obtained with our method is essentially due to the presence of a shaping decoder inside the receiver. To understand the negative impact of this decoder on the convergence threshold, one must remember that a shaping code is neither an error-correcting code nor a systematic code. This is why the error probability at the output of a shaping decoder is significantly greater than the error probability at its input. As a direct consequence, the insertion of such decoder inside an iterative decoding loop does increase the convergence threshold of the receiver. The fact that Raphaeli′s scheme does not use any shaping code makes it more power-efficient than our scheme in the low SNR region.

At larger SNR, Raphaeli′s scheme is outperformed by our system. In the 3-bit/dim 16-PAM Raphaeli′s scheme, a time-varying puncturing device is placed at the output of a rate-1/2 turbo encoder. Such device operates on groups of six coded bits composed of three information bits and three parity bits. The puncturing pattern applied to the three parity bits depends on the values of the three corresponding information bits, and is therefore random. In some cases (one in four), none of the three parity bits are actually transmitted. The problem with such a random puncturing strategy is that some sequences of information bits are left completely unprotected since they are associated with no parity bit at all. The number of these sequences is low compared to the total number of possible sequences, which explains why the turbo decoder still performs very well at low SNR. However, it is well known in coding theory that the existence of a few unprotected sequences is very detrimental to the asymptotic performance of the decoder. The error floors exhibited by the BER curves in Fig. 11 are a clear indication of the existence of these

unprotected sequences in Raphaeli′s system. On the other hand, our system uses a regular puncturing pattern at the turbo-encoder output. This conventional puncturing strategy guarantees a good asymptotic behaviour, and therefore makes our system more suitable than Raphaeli′s scheme when low BER values ($< 10^{-4}$) are targeted.

As for the complexity issue, the comparison between both approaches is quite straightforward. Assume that a classical BITCM without shaping is taken as a reference. To implement the shaping method proposed in [15]-[17], we just need to slightly modify the demapping function in order to cope with the fact that several groups of coded bits can be associated with the same constellation signal point. If we assume that this demapping function is not even part of the iterative decoding loop, i.e. used only once no matter how many iterations are performed, Raphaeli′s scheme can be considered as only marginally more complicated than a traditional BITCM system without shaping. It is therefore less complex than our system because the implementation of the latter requires the insertion of a shaping decoder inside the iterative decoding loop. However, as long as this shaping decoder operates on short blocks, we can state that the complexity difference between both approaches remains quite moderate.

IV. Conclusions

A novel method to combine constellation shaping and BITCM has been proposed and studied in this paper. Our technique consists of inserting a single short-length binary shaping code between turbo coding and modulation blocks. The corresponding receiver structure is originally made up of four main blocks (demapper, shaping decoder, and two constituent RSC decoders) exchanging extrinsic information. Simulation results carried out on a 3-bit/dim BITCM employing 16-PAM constellation, or equivalently a 6-bit/s/Hz BITCM using 256-QAM signal set, indicated that, by carefully selecting the shaping code parameters, it is possible to achieve shaping gains almost equal to 0.8 dB. It has also been shown that the demapper can be removed from the iterative decoding loop while keeping this shaping gain value unchanged, thus resulting in a tremendous simplification of the receiver structure at no cost in terms of error performance. All results achieved throughout this work lead to the conclusion that our shaping technique can substantially improve the performance of high spectral efficiency BITCM schemes over AWGN channels while adding little complexity to these schemes. Finally, note that the method introduced here can be applied in a straightforward manner to BICM systems employing low-density parity-check codes [35], [36] in place of turbo codes.

Acknowledgment

The authors would like to thank the reviewers for their helpful comments which improved the presentation of the paper.

References

[1] G. D. Forney, Jr., R. G. Gallager, G. R. Lang, F. M. Longstaff, and S. U. Qureshi, "Efficient modulation for band-limited channels," *IEEE J. Select. Areas Commun.*, vol. 2, pp. 632-647, Sep. 1984.

[2] G. D. Forney, Jr., and L. F. Wei, "Multidimensional constellations - Part I: Introduction, figures of merit, and generalized cross constellations," *IEEE J. Select. Areas Commun.*, vol. 7, pp. 877-892, Aug. 1989.

[3] G. D. Forney, Jr., "Multidimensional constellations - Part II: Voronoi constellations," *IEEE J. Select. Areas Commun.*, vol. 7, pp. 941-958, Aug. 1989.

[4] A. R. Calderbank and L. H. Ozarow, "Nonequiprobable signaling on the Gaussian channel," *IEEE Trans. Inform. Theory*, vol. 36, pp. 726-740, July 1990.

[5] A. R. Calderbank and M. Klimesh, "Balanced codes and nonequiprobable signaling," *IEEE Trans. Inform. Theory*, vol. 38, pp. 1119-1122, May 1992.

[6] F. R. Kschischang and S. Pasupathy, "Optimal nonuniform signaling for Gaussian channels," *IEEE Trans. Inform. Theory*, vol. 39, pp. 892-903, May 1993.

[7] A. K. Khandani and P. Kabal, "Shaping multidimensional signal spaces - Part I: Optimum shaping, shell mapping," *IEEE Trans. Inform. Theory*, vol. 39, pp. 1799-1808, Nov. 1993.

[8] A. K. Khandani and P. Kabal, "Shaping multidimensional signal spaces - Part II: Shell-addressed constellations," *IEEE Trans. Inform. Theory*, vol. 39, pp. 1809-1819, Nov. 1993.

[9] C. Berrou, A. Glavieux, and P. Thitimajshima, "Near Shannon limit error correcting coding and decoding: Turbo codes," in *Proc. IEEE ICC*, May 1993, pp. 1064-1070.

[10] S. Benedetto and G. Montorsi, "Unveiling turbo codes: Some results on parallel concatenated coding schemes," *IEEE Trans. Inform. Theory*, vol. 42, pp. 409-428, Mar. 1996.

[11] U. Wachsmann, R. F. H. Fischer, and J. B. Huber, "Multilevel codes: Theoretical concepts and practical design rules," *IEEE Trans. Inform. Theory*, vol. 45, pp. 1361-1391, July 1999.

[12] A. K. Khandani and W. Tong, "Application of shaping technique to multi-level turbo-coded modulation," in *Proc.* 21*st Biennial Symposium Commun.*, June 2002, pp. 20-24.

[13] A. K. Khandani and W. Tong, "Application of shaping technique with turbo coset codes," *IEEE Trans. Veh. Technol.*, to appear.

[14] D. Sommer and G. P. Fettweis, "Signal shaping by non-uniform QAM for AWGN channels and applications using turbo coding," in *Proc. ITG Conf. Source Channel Coding*, Jan. 2000, pp. 81-86.

[15] D. Raphaeli and A. Gurevitz, "Constellation shaping for pragmatic turbo-coded modulation," *IEEE Electron. Lett.*, vol. 38, pp. 717-719, July 2002.

[16] D. Raphaeli and A. Gurevitz, "An improved pragmatic turbo encoding scheme for high spectral efficiency using constellation shaping," in *Proc. IEEE ICC*, May 2003, pp. 2738-2742.

[17] D. Raphaeli and A. Gurevitz, "Constellation shaping for pragmatic turbo-coded modulation with high spectral efficiency," *IEEE Trans. Commun.*, vol. 52, pp. 341-345, Mar. 2004.

[18] G. Caire, G. Taricco, and E. Biglieri, "Bit-interleaved coded modulation," *IEEE Trans. Inform. Theory*, vol. 44, pp. 927-946, May 1998.

[19] F. W. Sun and H. C. A. van Tilborg, "Approaching capacity by equiprobable signaling on the Gaussian channel," *IEEE Trans. Inform. Theory*, vol. 39, pp. 1714-1716, Sep. 1993.

[20] S. Y. Le Goff, "Signal constellations for bit-interleaved coded modulation," *IEEE Trans. Inform. Theory*, vol. 49, pp. 307-313, Jan. 2003.

[21] X. Li and J. Ritcey, "Bit-interleaved coded modulation with iterative decoding using soft feedback," *IEEE Electron. Lett.*, vol. 34, pp. 942-943, May 1998.

[22] S. ten Brink, J. Speidel, and R. Yan, "Iterative demapping and decoding for multilevel modulation," in *Proc. IEEE Globecom Conf.*, Nov. 1998, pp. 579-584.

[23] X. Li, A. Chindapol and J. Ritcey, "Bit-interleaved coded modulation with iterative decoding and 8PSK signaling," *IEEE Trans. Commun.*, vol. 50, pp. 1250-1257, Aug. 2002.

[24] F. Schreckenbach, N. Görtz, J. Hagenauer, and G. Bauch, "Optimization of symbol mappings for bit-interleaved coded modulation with iterative decoding," *IEEE Commun. Lett.*, vol. 7, pp. 593-595, Dec. 2003.

[25] J. Tan and G. L. Stüber, "Analysis and design of symbol mappers for iteratively decoded BICM," *IEEE Trans. Wireless Commun.*, vol. 4, pp. 662-672, Mar. 2005.

[26] N. H. Tran and H. H. Nguyen, "Design and performance of BICM-ID systems with hypercube constellations," *IEEE Trans. Wireless Commun.*, vol. 5, pp. 1169-1179, May 2006.

[27] F. Simoens, H. Wymeersch, and M. Moeneclaey, "Multi-dimensional mapping for bit-interleaved coded modulation with BPSK/QPSK signaling," *IEEE Commun. Lett.*, vol. 9, pp. 453-455, May 2005.

[28] S. Benedetto and G. Montorsi, "Generalized concatenated codes with interleavers," in *Proc. International Symposium Turbo Codes*, Sep. 1997, pp. 32-39.

[29] S. Benedetto, D. Divsalar, G. Montorsi, and F. Pollara, "Soft-input soft-output modules for the construction and distributed iterative decoding of code networks," *Europ. Trans. Telecommun.*, vol. 9, pp. 155-172, Mar.-Apr. 1998.
[30] S. Benedetto, D. Divsalar, G. Montorsi, and F. Pollara, "A soft-input soft-output APP module for iterative decoding of concatenated codes," *IEEE Commun. Lett.*, vol. 1, pp. 22-24, Jan. 1997.
[31] S. Benedetto, D. Divsalar, G. Montorsi, and F. Pollara, "Serial concatenation of interleaved codes: Performance analysis, design, and iterative decoding," *IEEE Trans. Inform. Theory*, vol. 44, pp. 909-926, May 1998.
[32] O. F. Acikel and W. E. Ryan, "Punctured turbo codes for BPSK/QPSK channels," *IEEE Trans. Commun.*, vol. 47, pp. 1315-1323, Sep. 1999.
[33] G. Ungerboeck, "Channel coding with multilevel/phase signals," *IEEE Trans. Inform. Theory*, vol. 28, pp. 56-67, Jan. 1982.
[34] S. Y. Le Goff, A. Glavieux, and C. Berrou, "Turbo codes and high spectral efficiency modulation," in *Proc. IEEE ICC*, May 1994, pp. 645-649.
[35] R. G. Gallager, *Low-Density Parity-Check Codes*. Cambridge, MA: MIT Press, 1963.
[36] D. J. C. MacKay, "Good error-correcting codes based on very sparse matrices," *IEEE Trans. Inform. Theory*, vol. 45, pp. 399-431, Mar. 1999.



Stéphane Y. Le Goff received the BSc, MSc, and PhD degrees, all in electrical engineering, from the University of Western Brittany, Brest, Brittany, France, in 1990, 1991, and 1995, respectively. From 1995 to 1997, he worked as a teacher at the Institut Supérieur d'Electronique de Bretagne in Brest. During 1999-2003, Dr. Le Goff was an Assistant Professor at the Emirates Telecommunications Corporation (Etisalat) College of Engineering, UAE. In 2003, he joined the Department of Physics and Electronics at the University of Waikato, Hamilton, New Zealand, as a Senior Lecturer in Electronics. Since March 2005, he has been a Lecturer in the School of Electrical, Electronic, and Computer Engineering at the University of Newcastle upon Tyne, UK. Dr. Le Goff also held visiting positions at the Eastern Mediterranean University, Cyprus, during the academic year 1998-1999 and at the Sultan Qaboos University, Oman, from September to December 2004. His research interests include information theory, channel coding, and wireless communication systems.



Boon Kien Khoo received the B.Eng. degree from the University of Northumbria, Newcastle, UK, in 2003. During 2003-2004, he worked as a research and development engineer at Agilent Technologies in Malaysia. Since October 2004, he has been working towards the PhD degree in the School of Electrical, Electronic, and Computer Engineering at the University of Newcastle upon Tyne, UK. His research interests include coded modulation, iterative decoding, and peak power reduction for multicarrier communication systems.



Charalampos Tsimenidis (M'05) received his MSc and PhD degrees in 1999 and 2002, respectively, from the University of Newcastle upon Tyne where he is working now as a Lecturer in Signal Processing for Communications in the School of Electrical, Electronic, and Computer Engineering. His main research interests are in the area of adaptive array receivers for wireless multiple access communications. He has published over 40 conference and journal papers. During the last five year he has also made contributions in the area of receiver design to several European funded research projects including LOTUS, SWAN, and ACME.



Bayan Sharif (M'92-SM'02) is Professor of Digital Communications and Head of the School of Electrical, Electronic and Computer Engineering. He received the bachelor and doctorate degrees from Queen's University of Belfast and Ulster University, N. Ireland, in 1984 and 1988, respectively. He then held a Research Fellowship at Queen's University of Belfast before he was appointed as Lecturer at Newcastle University in 1990, and then as Senior Lecturer and Professor in Digital Communications in 1999 and 2000, respectively. Prof. Sharif has research interests in digital communications with a focus on wireless receiver structures and optimisation of wireless networks. He has published over 200 journal and conference papers, and held UK and EU research grants in digital communications, underwater acoustics and signal processing worth over £3M. He is a Chartered Engineer and Fellow of the IEE.

APPENDIX SOMMER05

An Improved Bit-Interleaved Turbo-Coded Modulation Scheme using Constellation Shaping and Iterative Decoding

Stéphane Y. Le Goff, Boon Kien Khoo, Charalampos C. Tsimenidis, and Bayan S. Sharif
School of Electrical, Electronic, and Computer Engineering
University of Newcastle upon Tyne, NE1 7RU, United Kingdom
Email: stephane.le-goff@ncl.ac.uk

***Abstract*— We present an improved version of the bit-interleaved turbo-coded modulation (BITCM) scheme with constellation shaping originally introduced in [3]. Simulation results carried out on a 3-bit/dim 16-PAM BITCM indicate that, by implementing an iterative decoding algorithm at the receiver side, it is possible to obtain shaping gains almost equal to 0.8 dB, which is very close to the maximal achievable values predicted by theory. It is also shown that, in most practical cases, the receiver structure can be simplified by removing the demapper from the iterative decoding loop, without any performance degradation.**

I. Introduction

For power- and bandwidth-efficient communications over additive white Gaussian noise (AWGN) channels, some techniques have recently been proposed to apply constellation shaping principles to the design of bit-interleaved turbo-coded modulation (BITCM) [1] - [3]. Sommer and Fettweis were the first to consider the use of constellation shaping for improving the error performance of BITCM schemes [1]. Their idea consisted of employing non-uniform pulse-amplitude modulation (PAM) constellations for which signal points are transmitted with equal probabilities but are placed on the one-dimensional (1-D) axis according to a Gaussian distribution [4]. Recently, Raphaeli and Gurevitz introduced a more power-efficient method in which a variable-rate turbo code is followed by a Huffman code mapping onto non-equiprobable signal points of a PAM constellation [2]. The turbo code rate is matched to the Huffman code using time-varying puncturing so that both data rate and transmitted signal rate remain constant. With such technique applied to 16-PAM, shaping gains of approximately 0.6 and 0.9 dB can be achieved for data rates equal to 2- and 3-bits/dim, respectively. A third method to combine constellation shaping and BITCM was introduced in [3]. It relies on the partitioning of a Gray-mapped constellation into several equal-sized sub-constellations of increasing average energy, and the use of a shaping code specifying the sequence of sub-constellations so that low-energy signals are transmitted more often than high-energy signals [5]. This technique is quite simple to implement and requires very little change in the classical BITCM structure. However, it achieves shaping gains that are approximately 0.3 - 0.4 dB smaller than those obtained using Raphaeli's method.

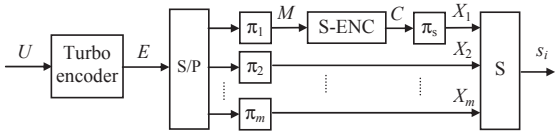


Fig. 1. Structure of the BITCM transmitter using constellation shaping.

In this paper, we propose to modify the BITCM structure originally introduced in [3] so as to improve its error performance, and thus attempt to bridge the gap with Raphaeli's approach, while keeping its complexity low. The main idea consists of designing the transmitter differently so that an efficient iterative decoding strategy can be implemented.

The organization of this paper is as follows. In Section II, the general structure of the modified BITCM scheme is presented. Particular attention is paid to the description of the iterative decoding algorithm that involves several constituent blocks at the receiver side. Then, we consider in Section III an example for which various computer simulation results are given, and show that the receiver structure can be simplified in most practical cases without any significant performance degradation. Finally, Section IV presents conclusions of this work.

II. Structure of the Modified BITCM System

In this Section, a notation in the form $V = (v_i)_I$ shall be used to denote a block/sequence V composed of I scalar quantities $v_i, i \in \{1, ..., I\}$, that can be either bits or log-likelihood ratios (LLRs) associated to bits.

A. BITCM transmitter structure

The proposed BITCM transmitter structure is shown in Fig. 1. A frame $U = (u_p)_{N_f}$ composed of N_f information bits $u_p, p \in \{1, ..., N_f\}$, is encoded by a rate-$R_c$ binary turbo encoder made up of two parallel-concatenated recursive and systematic convolutional (RSC) codes separated by a random interleaver [6]. The coded sequence E is divided, using a serial-to-parallel (S/P) converter, into m parallel sequences which are then bit-interleaved separately in a random fashion ($\pi_j, j \in \{1, ..., m\}$). The bit stream available at the first interleaver output (π_1) is broken into L successive K-bit

Authorized licensed use limited to: Fish & Richardson PC. Downloaded on August 22,2022 at 14:23:12 UTC from IEEE Xplore. Restrictions apply.

blocks $M = (m_k)_K$. Each block M is fed into a block shaping encoder (S-ENC) which generates a corresponding N-bit codeword $C = (c_n)_N$, with $N > K$. The rate of this encoder is thus $R_s = \frac{K}{N}$. The sequence of codewords at the shaping encoder output, whose length is equal to LN bits, is then randomly interleaved (π_s). The S/P converter is designed so that the length of the $(m-1)$ sequences fed into interleavers $\pi_j, j \in \{2, ..., m\}$, is also equal to LN bits. This S/P converter is therefore not a standard one since the first sequence contains only LK coded bits, i.e. fewer bits than the other $(m-1)$ sequences. Hereafter, we use the notations $X_1 = (x_{i,1})_{LN}$ and $X_j = (x_{i,j})_{LN}, j \in \{2, ..., m\}$, to designate the binary sequences at the output of interleavers π_s and π_j, respectively. Finally, a vector $(x_{i,1}, x_{i,2}, ..., x_{i,m})$, where $x_{i,j}$ denotes the i-th bit in sequence $X_j, j \in \{1, ..., m\}$, is mapped onto a signal point of a 2^m-PAM constellation, called S, according to Gray labeling. The transmission of a frame of $N_f = R_c L[K + N(m-1)]$ information bits is performed by emitting LN successive signal points $s_i, i \in \{1, ..., LN\}$. The data rate R is thus given by $R = R_c(R_s + m - 1)$ bits/dim, and is lower than the rate $R' = mR_c$ bits/dim obtained with an equivalent BITCM scheme without shaping code. Hence, the use of a shaping encoder results in a loss in data rate that can simply be compensated for by changing the puncturing pattern at the turbo encoder output.

The constellation S is partitioned into two sub-constellations S_0 and S_1 so that S_0 contains the 2^{m-1} signal points of lowest energies, whereas S_1 is composed of the 2^{m-1} signal points of highest energies [5]. The Gray mapping is performed in such a way that bits $x_{i,1}$, which are originally generated by the shaping encoder, are used to select one of these sub-constellations. Assuming that $x_{i,1} = 0$ leads to the selection of S_0, the shaping encoder is designed so that $\Pr\{x_{i,1} = 0\} > \Pr\{x_{i,1} = 1\}$, i.e. S_0 is emitted more frequently than S_1. Since the average energy of signal points in S_0 is lower than that in S_1, it results in some energy saving at the transmitter output with respect to the case where S_0 and S_1 are used with equal probabilities. The energy saving E_s, in decibels (dB), can be evaluated using

$$E_s = 10 \log_{10} \left[\frac{E_0 + E_1}{2(P_0 E_0 + [1 - P_0] E_1)} \right], \qquad (1)$$

where E_0 and E_1 are the average signal energies in S_0 and S_1, respectively, and P_0 designates the average value of $\Pr\{c_n = 0\}$ at the shaping encoder output. The shaping gain, which represents the actual energy saving, is obtained after the loss in data rate has been compensated for.

B. BITCM receiver structure

The block diagram of the BITCM receiver is depicted in Fig. 2. In order to optimize the error performance, demapping, shaping decoding and channel decoding are performed according to an iterative algorithm [7]. In our receiver, there are four iterative loops operating in parallel and allowing for information exchange between demapper and turbo decoder, demapper and shaping decoder, turbo decoder and shaping

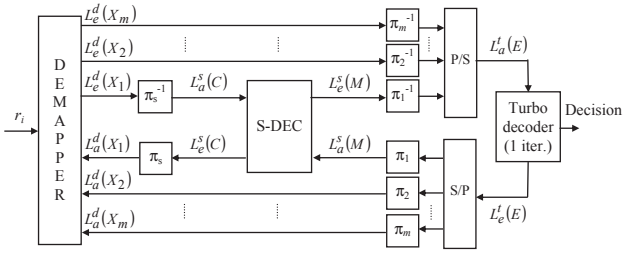


Fig. 2. Structure of the ierative BITCM receiver.

decoder, and finally both constituent decoders inside the turbo decoder. In this Sub-section, the operation and the role of the different modules used in the receiver is explained. Note that, hereafter, the notation $L_\alpha^\beta(v), \alpha \in \{a, e\}, \beta \in \{d, s, t\}$, is used to denote the LLR of v, v being either a bit or a block/sequence of bits.

1) The demapper: For each transmitted frame of LN signal points $s_i, i \in \{1, ..., LN\}$, the corresponding received frame is composed of LN channel samples r_i that can be expressed as $r_i = s_i + n_i$, where n_i is a Gaussian noise sample with zero mean and variance $\sigma^2 = \frac{N_0}{2}$, N_0 being the one-sided power spectral density of white Gaussian noise. The role of the demapper is to compute, for each index i, the extrinsic LLRs $L_e^d(x_{i,j}), j \in \{1, ..., m\}$. To this end, it processes, at each iteration, sample r_i as well as m *a priori* LLRs $L_a^d(x_{i,j}), j \in \{1, ..., m\}$, representing the extrinsic information generated by both shaping and turbo decoders at the previous iteration. Using a calculation similar to that in [8] - [10], we could show that the computation of LLRs $L_e^d(x_{i,j})$ is performed using

$$L_e^d(x_{i,j}) = \ln \left[\frac{\sum_{s \in S_j^1} \exp\left\{ -\frac{(r_i - s)^2}{N_0} + \sum_{l=1, \neq j}^{m} s_l L_a^d(x_{i,l}) \right\}}{\sum_{s \in S_j^0} \exp\left\{ -\frac{(r_i - s)^2}{N_0} + \sum_{l=1, \neq j}^{m} s_l L_a^d(x_{i,l}) \right\}} \right]. \qquad (2)$$

where S_j^t denotes the subset of signals $s \in S$ whose labels have the value $t \in \{0, 1\}$ in position $j \in \{1, ..., m\}$, and $s_l \in \{0, 1\}$ is the value of the label of signal s in position l.

Note that, at the first iteration, the initial value of *a priori* LLR $L_a^d(x_{i,1})$ is not equal to zero since, due to the presence of a shaping encoder, there is already some preliminary knowledge about the value of bit $x_{i,1}$ before the first iteration starts. The initial value of LLR $L_a^d(x_{i,1}), i \in \{1, ..., LN\}$, is computed using

$$L_a^d(x_{i,1}) = \ln \left[\frac{1 - \Pr\{x_{i,1} = 0\}}{\Pr\{x_{i,1} = 0\}} \right]. \qquad (3)$$

The average value of $\Pr\{x_{i,1} = 0\}$ over a frame of LN transmitted signals s_i is equal to P_0. The LN probabilities $\Pr\{x_{i,1} = 0\}$ are known to the receiver.

Authorized licensed use limited to: Fish & Richardson PC. Downloaded on August 22,2022 at 14:23:12 UTC from IEEE Xplore. Restrictions apply.

2) The shaping decoder: For each frame of LN received channel samples r_i, the demapper produces m parallel sequences $L_e^d(X_j) = (L_e^d(x_{i,j}))_{LN}, j \in \{1, ..., m\}$. The first sequence $L_e^d(X_1)$ is de-interleaved (π_s^{-1}) and broken into L blocks $L_a^s(C) = (L_a^s(c_n))_N$. At each iteration, the task of the SISO shaping decoder (S-DEC) is to produce both extrinsic LLRs $L_e^s(M) = (L_e^s(m_k))_K$ and $L_e^s(C) = (L_e^s(c_n))_N$. The LLRs $L_e^s(M)$ are to be processed by the turbo decoder at the same iteration, whereas LLRs $L_e^s(C)$ will be used by the demapper at the next iteration. The shaping decoder is not only fed with *a priori* LLRs $L_a^s(C)$ produced by the demapper, but also with *a priori* LLRs $L_a^s(M)$ representing the extrinsic information generated by the turbo decoder at the previous iteration. Since shaping codes typically operate on very short-length blocks, it is realistic to use the MAP algorithm for the shaping decoding. Hence, in order to compute $L_e^s(M)$, the SISO shaping decoder evaluates, for $k \in \{1, ..., K\}$, the expression

$$L_e^s(m_k) = \ln\left[\frac{\Pr\{m_k = 1, L_a^s(M), L_a^s(C)\}}{\Pr\{m_k = 0, L_a^s(M), L_a^s(C)\}}\right] - L_a^s(m_k), \quad (4)$$

which is equivalent to

$$L_e^s(m_k) = \ln\left[\frac{\sum_{M \in \Omega_k^1} \Pr\{L_a^s(C), L_a^s(m_{1\to K, \neq k})|M\}}{\sum_{M \in \Omega_k^0} \Pr\{L_a^s(C), L_a^s(m_{1\to K, \neq k})|M\}}\right], \quad (5)$$

where Ω_k^t, $t \in \{0, 1\}$, denotes the set of all blocks M for which $m_k = t$ ($|\Omega_k^0| = |\Omega_k^1|$), and $\Pr\{L_a^s(C), L_a^s(m_{1\to K, \neq k})|M\}$ designates the probability of receiving all input LLRs except $L_a^s(m_k)$ given the transmission of a particular block M. Developing (5), one could show that extrinsic LLRs $L_e^s(m_k), k \in \{1, ..., K\}$, are given by

$$L_e^s(m_k) = \ln\left[\frac{\sum_{M \in \Omega_k^1} \exp\left\{\sum_{l=1, \neq k}^{K} t_l L_a^s(m_l) + \sum_{n=1}^{N} t_n \tilde{L_a^s}(c_n)\right\}}{\sum_{M \in \Omega_k^0} \exp\left\{\sum_{l=1, \neq k}^{K} t_l L_a^s(m_l) + \sum_{n=1}^{N} t_n \tilde{L_a^s}(c_n)\right\}}\right] \quad (6)$$

where $t_l \in \{0, 1\}$ is the value of the l-th bit in the block M under consideration and $t_n \in \{0, 1\}$ is the value of the n-th bit in the codeword C associated to this particular block. The LLR $\tilde{L_a^s}(c_n)$ is defined as $\tilde{L_a^s}(c_n) = L_a^s(c_n) - L_n$, where the term $L_n, n \in \{1, ..., N\}$, accounts for the *a priori* knowledge regarding bits c_n available before the first decoding iteration starts, and is computed using

$$L_n = \ln\left[\frac{1 - \Pr\{c_n = 0\}}{\Pr\{c_n = 0\}}\right]. \quad (7)$$

The expressions of extrinsic LLRs $L_e^s(c_n), n \in \{1, ..., N\}$, are very similar to (6) but are not given here due to the lack of space. Equation (6) indicates that the computational complexity of the MAP decoding algorithm can become prohibitive for high values of K and N. In particular, the number of additions required for the evaluation of this expression increases exponentially with K since $|\Omega_k^0| = |\Omega_k^1| = 2^{K-1}$. However, for small values of parameters K and N, the computational complexity of (6) remains of reasonable complexity. We will see later that shaping gains close to the maximal values predicted by theory can be achieved using small values of K and N.

3) The turbo decoder: The sequences $L_e^d(X_j) = (L_e^d(x_{i,j}))_{LN}, j \in \{2, ..., m\}$, as well as that composed of L blocks $L_e^s(M)$ are de-interleaved separately ($\pi_j^{-1}, j \in \{1, ..., m\}$), and then combined together through the P/S converter to form a single LLR stream $L_a^t(E)$ used as an *a priori* information by the turbo decoder. The latter is made up of two SISO constituent decoders separated by an interleaving pair corresponding to the interleaving embedded in the turbo encoder [6]. A constituent decoder processes the part of stream $L_a^t(E)$ that is relevant to it as well as some *a priori* information, regarding the sequence U of information bits, produced by the other constituent decoder at the previous iteration. Based on both sequences, each decoder generates two extrinsic sequences to be used at next iteration by the demapper-shaping decoder pair and the other constituent decoder. The reader is referred to [11] for more details regarding the algorithm used to produce LLR sequences. Finally, the turbo decoder generates the extrinsic sequence $L_e^t(E)$ representing the *added value* of this decoder to the *a priori* sequence $L_a^t(E)$.

After S/P conversion of this LLR stream and interleaving of the m parallel sequences thus generated ($\pi_j, j \in \{1, ..., m\}$), we obtain the sequences $L_a^d(X_j), j \in \{2, ..., m\}$, and that composed of L blocks $L_a^s(M)$ to be used as *a priori* information at the next iteration by the demapper and the shaping decoder, respectively.

III. Performance of the Modified BITCM System

We now consider the example of a 3-bit/dim 16-PAM BITCM scheme for which computer simulation results are given. We recall that, for such scheme, the potential shaping gain achievable with our technique can be larger than 0.7 dB provided that the shaping code is designed so that P_0 ranges from 0.69 to 0.85. Its maximal value is equal to 0.80 dB, and is obtained for $P_0 \approx 0.78$ [3].

A. Choice of coding rates R_c and R_s

To guarantee the best error performance at the receiver output, it is important to select carefully the values of parameters R_s and R_c. We indicate in Table I a number of configurations that are of particular interest for the practical design of our 3-bit/dim 16-PAM BITCM scheme since they correspond to turbo code rates R_c in the form $R_c = \frac{n}{n+1}$, n being an integer. For complexity reasons, only shaping codes with a number of codewords smaller than or equal to $2^8 = 256$ ($K \leq 8$) are considered. The results in Table I indicate that all listed configurations for which $R_c = \frac{4}{5}, \frac{5}{6}$, and $\frac{6}{7}$ are potentially

Authorized licensed use limited to: Fish & Richardson PC. Downloaded on August 22,2022 at 14:23:12 UTC from IEEE Xplore. Restrictions apply.

TABLE I

SEVERAL POSSIBLE CONFIGURATIONS FOR DESIGNING A 3-BIT 16-PAM BITCM SCHEME

R_c	R_s	K	N	P_0	E_s (dB)
4/5	3/4	3	4	0.687	1.44
		6	8	0.717	1.72
5/6	3/5	3	5	0.775	2.32
		6	10	0.806	2.69
6/7	1/2	1	2	0.750	2.05
		2	4	0.812	2.76
		3	6	0.833	3.03
		4	8	0.828	2.96
		5	10	0.837	3.08
		6	12	0.851	3.27
		7	14	0.854	3.30
		8	16	0.850	3.26
7/8	3/7	3	7	0.875	3.61
		6	14	0.875	3.61

suitable since they are associated with values of P_0 that fall within the appropriate range ($0.69 < P_0 < 0.85$). On the other hand, the case $R_c = \frac{7}{8}$ and $R_s = \frac{3}{7}$ corresponds to values of P_0 which are outside this range, and should therefore not be considered any further. This would also be the case for any other configuration with $R_c > \frac{7}{8}$ and $R_s < \frac{3}{7}$. This simple analysis shows that a good design strategy consists of finding the right balance between the rates of both codes so that the total available amount of redundancy (1 bit/dim in our example) is properly shared between shaping coding and channel coding. Once suitable configurations have been identified, we can select the values of K and N that produce the highest energy saving E_s for each configuration. Note that, for a given value of R_s, increasing K (or N) does not necessarily result in a larger energy saving. For instance, for the case $R_s = \frac{1}{2}$, the $(N = 12, K = 6)$ code provides slightly more energy saving than the $(N = 16, K = 8)$ code despite being four times simpler to implement (four times lesser codewords).

B. Simulation results

We simulated the error performance of several 3-bit/dim 16-PAM BITCMs made up of five different shaping codes identified to be potentially the most attractive ones according to the results given in Table I. The $(N = 6, K = 3)$ code was also considered despite providing a smaller energy saving than the $(N = 12, K = 6)$ and $(N = 14, K = 7)$ codes because it is interesting to assess the shaping gain achieved using a very low complexity shaping code. The rate-$\frac{4}{5}$, -$\frac{5}{6}$, and -$\frac{6}{7}$ turbo codes are obtained by puncturing a rate-1/3 turbo code built from two 16-state RSC codes with polynomials (23, 31). We adopt the puncturing patterns proposed in [12]. The size of the pseudo-random interleaver separating both RSC codes, i.e. the length N_f of a frame of information bits, can be either large (N_f = 10000 bits) or small (N_f = 2000 bits). After transmission of a frame of N_f information bits, the trellis of the first RSC encoder is reset to the all-zero state. Turbo decoding is performed in 10 iterations, and the log-

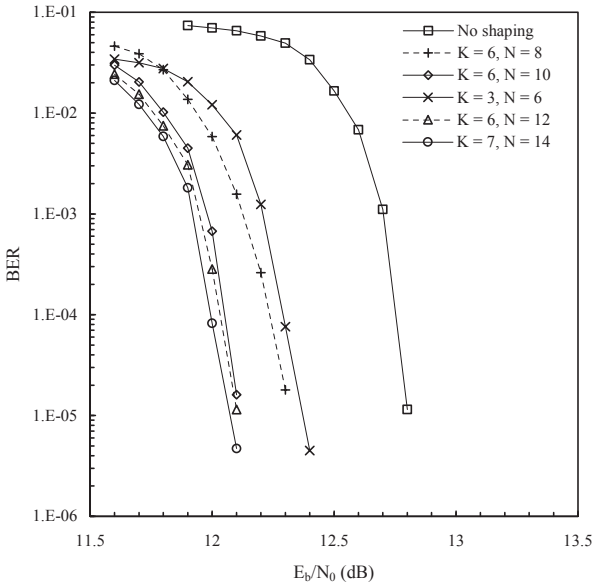


Fig. 3. BER performance comparison over AWGN channel between several 3-bit/dim 16-PAM BITCM schemes operating on large frames (N_f = 10000 bits). Turbo decoding is performed in 10 iterations. The results are given for five different shaping codes. For comparison purposes, the BER curve obtained with the equivalent BITCM system without shaping is also plotted.

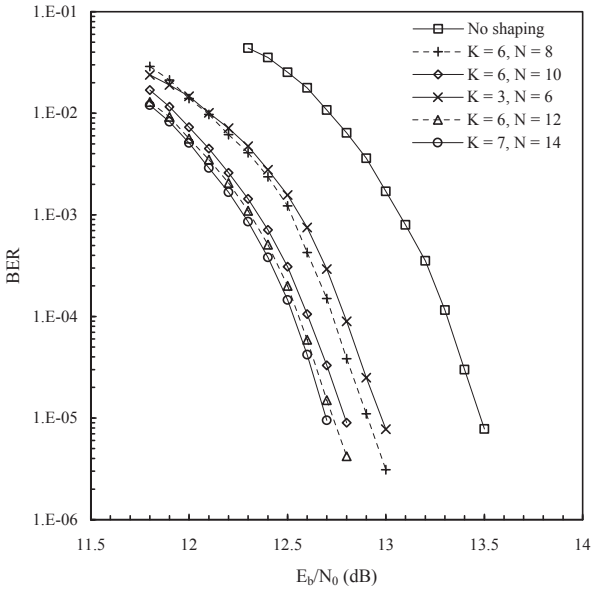


Fig. 4. BER performance comparison over AWGN channel between several 3-bit/dim 16-PAM BITCM schemes operating on small frames (N_f = 2000 bits). Turbo decoding is performed in 10 iterations. The results are given for five different shaping codes. For comparison purposes, the BER curve obtained with the equivalent BITCM system without shaping is also plotted.

Authorized licensed use limited to: Fish & Richardson PC. Downloaded on August 22,2022 at 14:23:12 UTC from IEEE Xplore. Restrictions apply.

MAP algorithm is used for the decoding of each RSC code. In all cases, Gray mapping is such that maximum protection is offered to parity bits. Figs. 3 and 4 show graphs of BER versus $\frac{E_b}{N_0}$ for several 3-bit/dim 16-PAM BITCM schemes, for large and small frames, respectively. The BER curves obtained without shaping are also displayed for comparison purposes.

From Figs. 3 and 4, it is seen that the shaping technique described in this paper allows for significant error performance improvement for both frame sizes. For instance, at a BER of 10^{-5}, we achieve, with the $(N = 14, K = 7)$ code, shaping gains equal to 0.72 dB and 0.78 dB, for N_f = 10000 and 2000 bits, respectively. These simulation results indicate that the best shaping code is the $(N = 14, K = 7)$ code, closely followed by the $(N = 12, K = 6)$ and $(N = 10, K = 6)$ codes. As expected, smaller, but still significant, shaping gains of 0.42 and 0.50 dB are achieved when using the very low-complexity $(N = 6, K = 3)$ code, for N_f = 10000 and 2000 bits, respectively. The shaping algorithm proposed by Raphaeli and Gurevitz can improve the performance of a 3-bit/dim 16-PAM BITCM scheme by almost 0.9 dB [2]. Such gain is approximately 0.1 dB higher than that obtained with our method. This small performance difference is due to the more refined partitioning of 16-PAM employed by Raphaeli (four sub-constellations instead of only two with our method).

C. Simplification of receiver structure

The receiver structure depicted in Fig. 2 may seem complicated due to the four iterative loops operating in parallel. Hereafter, we propose to show that, in most practical cases, it is possible to remove the demapper from the iterative decoding loop without degrading the error performance of the system. This obviously results in a simplification of the receiver structure since two iterative loops are then suppressed. In the literature on bit-interleaved coded modulation, it has been widely reported that iterative demapping is not beneficial when Gray mapping is employed (see, e.g., [8] - [10]). On the other hand, some studies have reached opposite conclusions since they have indicated that iterative demapping with Gray mapping can actually bring some substantial performance improvement [1], [7]. To further clarify this point, let us focus on a particular extrinsic LLR $L_e^d(x_{i,j})$ generated by the demapper, and assume that, in addition to the channel sample r_i, some *a priori* information $L_a^d(x_{i,1\rightarrow m,\neq j})$ regarding the values of bits $x_{i,l}, l \in \{1, ..., j-1, j+1, ..., m\}$ is made available to this demapper. It is well known that the demapper produces an *erroneous* LLR $L_e^d(x_{i,j})$, i.e. an LLR $L_e^d(x_{i,j})$ that would generate a bit error after hard decision, when the detected signal s_i^d is different from the transmitted signal s_i^t and the j-th bits in the labels of s_i^d and s_i^t are different.

Consider first the case where s_i^d and s_i^t are nearest neighbor signal points. With Gray mapping, the labels of two nearest neighbor signal points can differ by only one bit. It implies that the $(m-1)$ bits in positions $l, l \in \{1, ..., j-1, j+1, ..., m\}$ in the labels of s_i^d and s_i^t are identical. Therefore, any *a priori* knowledge regarding the values of bits $x_{i,l}, l \in \{1, ..., j-1, j+1, ..., m\}$ cannot help the demapper to produce a more reliable LLR $L_e^d(x_{i,j})$. In such case, iterative demapping does not improve the error performance of the BITCM system. The situation is different when s_i^d and s_i^t are not nearest neighbor signal points. In this case, the $(m-1)$ bits in positions $l, l \in \{1, ..., j-1, j+1, ..., m\}$ in the labels of these particular signal points are not all identical. As a result, some *a priori* knowledge $L_a^d(x_{i,1\rightarrow m,\neq j})$ generally allows the demapper to perform a better distinction between both signal points, and thus generate a more reliable estimate $L_e^d(x_{i,j})$.

We conclude that, when Gray mapping is employed, iterative demapping does improve performance only if there is a significant percentage of error events that are due to some confusion between non-nearest neighbor signal points. On AWGN channels, these error events only occur at low SNR. Hence, iterative demapping can only be beneficial for BITCM systems operating at sufficiently low SNR values. In particular, we found that, as a rule of thumb, the error performance of a 2^m-PAM BITCM scheme can be improved by iterative demapping as long as the data rate R is less than or equal to $(m-2)$ bits/dim. On the other hand, if the desired rate is $R = (m-1)$ bits/dim, then iterative demapping is not beneficial. As an example, Fig. 5 displays the BER curves obtained with two 16-PAM BITCM schemes using turbo codes with rates $R_c = \frac{1}{2}$ and $\frac{3}{4}$ in order to achieve data rates of 2 bits/dim and 3 bits/dim, respectively. No shaping code is employed in either case. From Fig. 5, it is clearly seen that the use of iterative demapping does improve the error performance of the 2-bit/dim scheme by approximately 0.3 dB, but does not affect that of the 3-bit/dim system. In any case, it is well known that the best choice for designing a practical m-bit/dim coding scheme based on PAM signaling consists of employing a constellation with 2^{m+1} signal points [13]. We therefore conclude that, in cases of practical interest, it is possible to remove the demapper from the iterative decoding loop without degrading the error performance of the whole system.

Fig. 6 shows the corresponding simplified receiver structure. The only difference between such block diagram and that of a classical BITCM receiver is the presence of a SISO shaping decoder fed, at each iteration, with blocks $L_a^s(C)$ and $L_a^s(M)$ generated by demapper and turbo decoder, respectively. The task of this shaping decoder is to generate the extrinsic information $L_e^s(M)$ to be processed at next iteration by the turbo decoder. With such simplified structure, both constituent decoders embedded inside the turbo decoder are no longer required to produce extrinsic LLRs of the parity bits since, in practice, only LLRs of the information bits are exchanged between turbo and shaping decoders. This further simplifies the receiver structure.

To confirm the results obtained in this Sub-section, we have represented in Fig. 7 the BER performance achieved with and without iterative demapping, for two 3-bit/dim 16-PAM BITCM schemes operating on either large (N_f = 10000 bits) or small (N_f = 2000 bits) frames. Both schemes employ a shaping code with $K = 7$ and $N = 14$ as well as 10 decoding iterations. The BER plots depicted in Fig. 7 confirm that iterative demapping does not improve the error performance

Authorized licensed use limited to: Fish & Richardson PC. Downloaded on August 22,2022 at 14:23:12 UTC from IEEE Xplore. Restrictions apply.

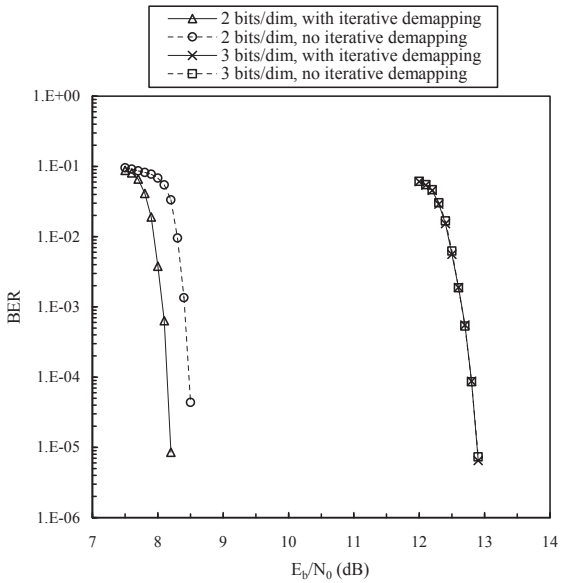


Fig. 5. BER performance comparison over AWGN channel between several 16-PAM BITCM schemes using turbo codes with rates $R_c = \frac{1}{2}$ and $\frac{3}{4}$ in order to achieve data rates of 2 bits/dim and 3 bits/dim, respectively, with and without iterative demapping. The frame size is 10000 bits and turbo decoding is performed in 8 iterations.

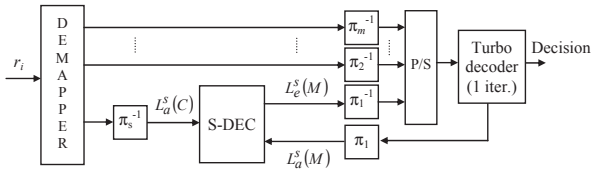


Fig. 6. Structure of the simplified iterative BITCM receiver.

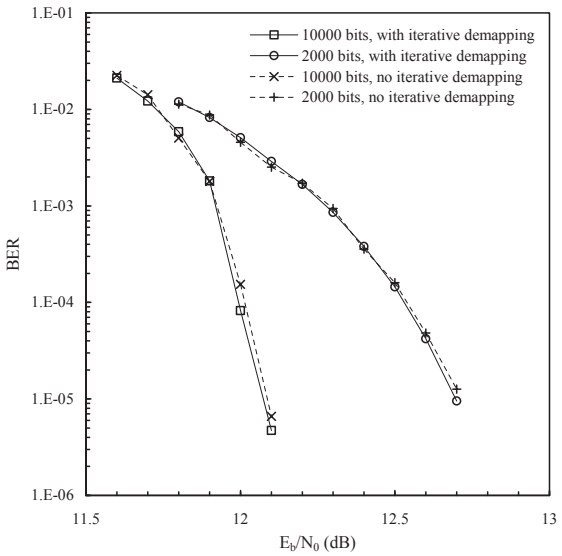


Fig. 7. BER performance achieved over AWGN channel with and without iterative demapping, for two 3-bit/dim 16-PAM BITCM schemes operating on either large (N_f = 10000 bits) or small (N_f = 2000 bits) frames. Both schemes employ a shaping code with $K = 7$ and $N = 14$ as well as 10 decoding iterations.

of a 3-bit/dim 16-PAM scheme for both frame sizes. In other words, the simplified receiver structure shown in Fig. 6 is sufficient to obtain the shaping gains previously evaluated from Figs. 3 and 4.

IV. Conclusions

The scheme originally introduced in [3] is modified so as to improve its error performance. Simulation results carried out on a 3-bit/dim 16-PAM BITCM indicate that, by implementing an iterative decoding algorithm at the receiver side, performance very close to the theoretical shaping gain values of 0.7 - 0.8 dB can be achieved. It is also shown that we can remove the demapper from the iterative decoding loop, i.e. simplify the receiver structure, without degrading the error performance of the whole system.

Note that the work described in this paper is, in fact, applicable to any square QAM constellation because, provided that Gray mapping is employed, a 2^{2m}-QAM signal set can be viewed as two independent 2^m-PAM constellations in quadrature. In particular, this implies that the work carried out on our 3-bit/dim 16-PAM BITCM can be directly applied to the design of a 6-bit/s/Hz 256-QAM BITCM.

References

[1] D. Sommer and G. P. Fettweis, "Signal shaping by non-uniform QAM for AWGN channels and applications using turbo coding," *in Proc. ITG Conf. Source and Channel Coding*, Munich, Germany, Jan. 2000, pp. 81-86.

[2] D. Raphaeli and A. Gurevitz, "Constellation shaping for pragmatic turbo-coded modulation with high spectral efficiency," *IEEE Trans. Commun.*, vol. 52, pp. 341-345, March 2004.

[3] S. Y. Le Goff, B. S. Sharif, and S. A. Jimaa, "Bit-interleaved turbo-coded modulation using shaping coding," *IEEE Commun. Letters*, vol. 9, pp. 246-248, March 2005.

[4] F. W. Sun and H. C. A. van Tilborg, "Approaching capacity by equiprobable signaling on the Gaussian channel," *IEEE Trans. Inform. Theory*, vol. 39, pp. 1714-1716, Sept. 1993.

[5] A. R. Calderbank and L. H. Ozarow, "Nonequiprobable signaling on the Gaussian channel," *IEEE Trans. Inform. Theory*, vol. 36, pp. 726-740, July 1990.

[6] C. Berrou, A. Glavieux, and P. Thitimajshima, "Near Shannon limit error correcting coding and decoding: Turbo codes," *in Proc. IEEE ICC*'93, Geneva, Switzerland, May 1993, pp. 1064-1070.

[7] S. Benedetto, D. Divsalar, G. Montorsi, and F. Pollara, "Soft-input soft-output modules for the construction and distributed iterative decoding of code networks," *Europ. Trans. Telecommun.*, vol. 9, pp. 155-172, March-April 1998.

[8] X. Li and J. Ritcey, "Bit-interleaved coded modulation with iterative decoding using soft feedback," *Electron. Letters*, vol. 34, pp. 942-943, May 1998.

[9] S. ten Brink, J. Speidel, and R. Yan, "Iterative demapping and decoding for multilevel modulation," *in Proc. IEEE Globecom Conference*, Sydney, Australia, Nov. 1998, pp. 579-584.

[10] X. Li, A. Chindapol and J. Ritcey, "Bit-interleaved coded modulation with iterative decoding and 8PSK signaling," *IEEE Trans. Commun.*, vol. 50, pp. 1250-1257, Aug. 2002.

[11] S. Benedetto, D. Divsalar, G. Montorsi, and F. Pollara, "A soft-input soft-output APP module for iterative decoding of concatenated codes," *IEEE Commun. Letters*, vol. 1, pp. 22-24, Jan. 1997.

[12] Ö. F. Acikel and W. E. Ryan, "Punctured turbo codes for BPSK/QPSK channels," *IEEE Trans. Commun.*, vol. 47, pp. 1315-1323, Sept. 1999.

[13] G. Ungerboeck, "Channel coding with multilevel/phase signals," *IEEE Trans. Inform. Theory*, vol. 28, pp. 56-67, Jan. 1982.

Authorized licensed use limited to: Fish & Richardson PC. Downloaded on August 22,2022 at 14:23:12 UTC from IEEE Xplore. Restrictions apply.

APPENDIX SOMMER06

Constellation Design via Capacity Maximization

Maged F. Barsoum
Jet Propulsion Laboratory
California Institute of Technology
Pasadena, CA 91109
mbarsoum@jpl.nasa.gov

Christopher Jones
Jet Propulsion Laboratory
California Institute of Technology
Pasadena, CA 91109
crjones@jpl.nasa.gov

Michael Fitz
Department of Electrical Engineering
UCLA
Los Angeles, CA 90095
fitz@ee.ucla.edu

Abstract— **Traditional constellations are uniformally spaced. By giving up uniform spacing, constellations can be designed to have larger joint (i.e. overall) capacity or parallel decoding capacity. In this paper non-uniformally spaced (i.e. 'geometrically' shaped) constellations are designed to maximize either of these quantities. By way of numerical capacity computations we show that except in special cases, there are no universally optimal geometrically shaped constellations across all code rates, and that the optimization of a constellation has to target a specific code rate. Unlike joint capacity, optimizing for parallel decoding capacity is label dependent. For PAM and PSK constellations, we found the maximum parallel decoding capacity to be achieved using gray (not necessarily binary reflective gray) labels. However, for PAM constellations, not *all* gray labels can yield the highest parallel decoding capacity. Besides the conventional use of a $(log_2(M)-1)/log_2(M)$ code rate with an M-point constellation for bandwidth efficient communications, the optimized constellations could offer further non-trivial gains at lower code rates (unlike traditional constellations). An optimized constellation is used with a state-of-the-art LDPC code and simulation results are presented. This paper also draws a distinction between probabilistic shaping and geometric shaping and in fact proves under broad conditions, that any gain in capacity which can be found via probabilistic shaping can also be achieved or exceeded solely through geometric shaping.**

I. Introduction

In this paper, constellations are designed to maximize their joint or parallel decoding capacity over the Additive White Gaussian Noise (AWGN) channel. These constellations are well suited for use in conjunction with modern capacity approaching codes such as LDPC and Turbo codes.

Although the minimum distance (d_{min}) between constellation points is indicative of the capacity of a constellation only at relatively high signal-to-noise ratios (SNRs), constellations have most often been designed to maximize d_{min} [1]. Along similar lines, since increasing the dimensionality of a constellation allows larger minimum distance for constant constellation energy per dimension, several researchers have designed multi-dimensional constellations with good minimum distance properties e.g. [2][3][4][5][6]. However, in all these efforts the capacity of the constellation remained limited by a design that targeted d_{min}, a measure that is indicative of the performance of an uncoded system, but is not necessarily a good measure at low SNRs typical of coded systems, particularly with capacity approaching codes.

To optimize the capacity of the constellations presented in this paper, we allow for unequal spacing and unconstrained labels (although Agrell *et al.* showed that the binary reflected gray labeling is optimal in a probability of error sense for equally spaced constellations [7]). Other researchers have previously designed unequally spaced constellations to optimize measures other than capacity. Foschini *et al.*. used numerical optimization to design unequally spaced constellations that minimize the error rate of an uncoded system [8]. Betts *et al.* demonstrated a gain of 0.25 dB when using constellations designed by warping together with Trellis codes [9].

Sun *et al.* [10] showed that with asymptotically large M, equiprobable, but non-uniformly spaced signaling can achieve the Gaussian input distribution. This approach can be approximated for finite M in an attempt to mimic the Gaussian distribution [11][12]. However, approaches that mimic the Gaussian input distribution do not parameterize designs based on code rate, and are apparently limited to one dimensional PAM constellations. In this paper, we show that careful placement of constellation points to maximize a capacity measure at a given SNR yields more efficient constellations. For example, Sommer and Fettweis [11] achieve a 0.8 dB gain in parallel decoding capacity for PAM-32 at rate-1/2, while the proposed optimization technique yields a gain of 1.5 dB, as will be shown. Unlike the approach of [11], direct optimization of the constellation points for a given capacity measure yields different constellations depending on the SNR they are optimized at. The optimized constellations are therefore code rate dependent.

Shaping techniques provide an alternative approach for improving energy efficiency. The term shaping is traditionally applied to techniques that attempt to approximate the capacity achieving Gaussian input distribution by transmitting some constellation points with greater frequency than others, an operation which poses several practical difficulties. In section VI, we show under broad conditions that any gain in capacity that can be achieved by probabilistic shaping can also be achieved or exceeded by equiprobable but non-uniformally spaced signaling i.e. geometrical shaping.

II. Design Methodology

A constellation can be parameterized by the total number of constellation points, M, and the number of real dimensions, N_{dim} . We will see that, except for trivial cases such as BPSK, no particular constellation minimizes transmit power across all code rates. The number of user bits per dimension, η, is related

1-4244-1429-6/07/$25.00 ©2007 IEEE

Authorized licensed use limited to: Fish & Richardson PC. Downloaded on August 22,2022 at 14:20:05 UTC from IEEE Xplore. Restrictions apply.

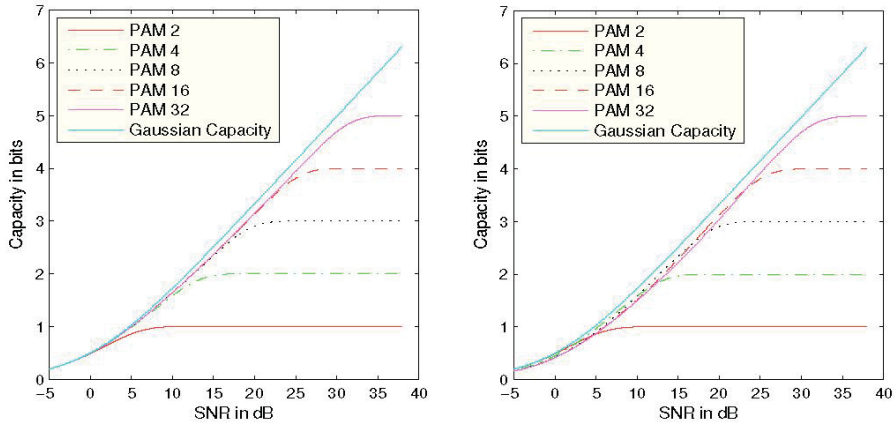


Fig. 1. (a) Capacity of PAM constellations together with the Gaussian Capacity curve.(b) Parallel Decoding Capacity of PAM constellations together with the Gaussian Capacity curve.

to code rate, R, as follows:

$$\eta = \frac{R\left(\log_2\left(M\right)\right)}{N_{\dim}}$$

In systems where there are no belief propagation iterations between the decoder and the constellation demapper, the constellation demapper can be thought of as part of the channel. The capacity of the channel defined as such is the parallel decoding (PD) capacity, given by

$$C_{PD} = \sum_{i=0}^{l-1} I(X_i; Y)$$

where X_i is the i^{th} bit of the l-bits transmitted symbol, and Y is the received symbol, and $I(A;B)$ denotes the mutual information between random variables A and B. With belief propagation iterations between the demapper and the decoder, the demapper can no longer be viewed as part of the channel, and the joint capacity of the constellation becomes the tightest known bound on the system performance.

$$C_{JOINT} = I(X;Y)$$

In this paper, we do not advocate a particular system level choice regarding the decision to iterate (or not) between decoder and detector, but recognize that in various circumstances PD capacity may be more or less relevant than joint capacity. We therefore offer designs for both capacity measures. Constellations designed to maximize the joint capacity may also be particularly suited for codes over $GF(q)$ where q equals the size of the constellation M.

Constellations and labelings were optimized jointly using a constrained non-linear optimizer by finding the optimal location for each label. Constraints included lower and upper bounds on point locations (with one constellation point fixed at the upper bound). These bounds limit the search space, but do not exclude a global optimum since feasible solutions are scale independent. It can easily be shown that an optimal constellation will have zero mean (no DC component). Explicit inclusion of a zero mean constraint helps the optimization routine to converge more quickly.

Optimizing for a particular user data rate requires an iterative process because the optimizing SNR for the to-be designed constellation is not known *a priori*. Instead, a capacity-maximizing constellation is designed for an initial SNR guess. The SNR at which this constellation gives the desired rate is then used for finding a new capacity-maximizing constellation. Given the new constellation, the SNR at which the desired rate is achieved is computed. If this SNR is no lower than the SNR used to find the constellation, the process stops (otherwise it repeats). We note that throughout this paper, SNR is defined as the ratio of the average constellation energy per dimension to the average noise energy per dimension.

We offer no proof that the solutions found herein are globally optimal. While it would be nice to be able to make such claims, we maintain that the gains provided in the cases considered are motivating enough to pursue the question of global optimality in future work. We note that in case where exhaustive search is possible, the solution provided by the constrained non-linear optimizer is in fact globally optimal (an example of this is given in section III-A.1).

III. Examples

A. PAM Constellations

This section presents different PAM constellations optimized for several user data rates. We start by presenting the joint and parallel decoding capacities for classic constellations (with the conventional binary reflective gray labels) at different SNRs. Figure 1 (a) shows the joint capacity for the classic PAM-2, 4, 8, 16 and 32, together with the Gaussian capacity.

Authorized licensed use limited to: Fish & Richardson PC. Downloaded on August 22,2022 at 14:20:05 UTC from IEEE Xplore. Restrictions apply.

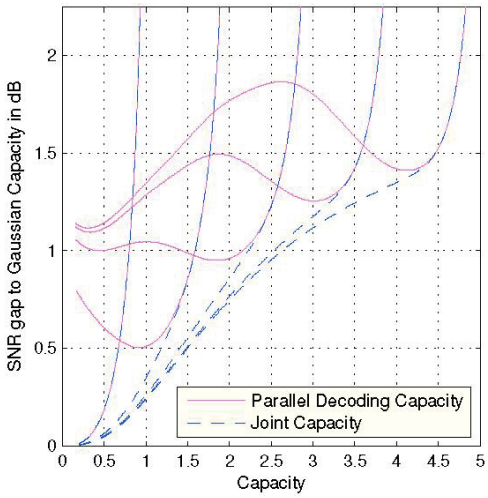


Fig. 2. SNR gap to Gaussian Capacity for the Joint Capacity and Parallel Decoding Capacity of 2,4,8,16 and 32 PAM constellations

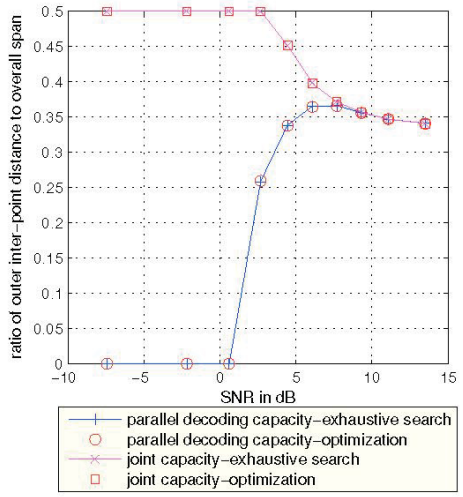


Fig. 3. r versus SNR for PAM-4 constellations optimized for joint capacity/parallel decoding capacity

Figure 1 (b) shows the parallel decoding capacity for the same constellations together with the Gaussian capacity.

In order to gain a better view of the differences between these curves at points close to the Gaussian capacity, we instead plot the SNR gap to Gaussian capacity for different values of capacity for each constellation as shown in Fig. 2. It is interesting to note that unlike the joint capacity, at the same SNR, the parallel decoding capacity does not necessarily increase with the number of constellation points. This will not be the case with the optimized constellations.

1) PAM-4: PAM-4 constellations were designed via an exhaustive search with a resolution of 0.002 with -1 and 1 as the lower and upper bounds on all constellation points. We obtained the same results using the previously described non-linear constrained optimization.

At all user data rates, we found the optimized PAM-4 constellations to be symmetric around the origin. Let $-a$, $-b$, b, a denote the location of the 4 points in the constellation from left to right. The constellation can be fully described by the ratio $r = \frac{a-b}{2*a}$.

Figure 3 shows r for PAM-4 constellations optimized for joint capacity/parallel decoding capacity at different SNRs. As seen in the figure, at low SNR's PAM-4 constellations optimized for joint capacity differ from those optimized for parallel decoding capacity. A constellation optimized for joint capacity has $b = 0$ i.e. it looks like a 3-point equally-spaced constellation with two of the four symbols mapped to zero. A constellation optimized for parallel decoding capacity has $b = a$ i.e. a BPSK constellation with two of the four symbols mapped to a and the other two mapped to $-a$.

At high SNRs it makes negligible difference whether a PAM-4 constellation is optimized for joint capacity or parallel decoding capacity (Fig. 3). As the SNR increases, r approaches $1/3$, i.e. the constellation becomes equally spaced. This illustrates that constellations designed to maximize the minimum distance between constellation points are well suited for high SNRs (as may be used, for example, in uncoded systems).

2) Other PAM constellations: After examining the design of PAM-4 constellations in detail in the previous section, we now present a summary of the results for the design of PAM-8, 16, and 32 (it should be noted that BPSK is the optimal PAM-2 constellation at all code rates). We have optimized the constellations for joint capacity and parallel decoding capacity for different target user bits per dimension (i.e. code rates). The optimized constellations are different depending on the target user bits per dimension, and also depending on whether they have been designed to maximize the joint capacity or the parallel decoding capacity. For all the PAM constellations examined and at all code rates, we found that the labels that maximize the parallel decoding capacity are gray. However, not all gray labels achieve the maximum possible decoding capacity even given the freedom to place the constellation points anywhere on the real line. Figure 4 (a) shows the SNR gap to Gaussian capacity for each constellation we optimized for joint capacity. Figure 4 (b) shows the SNR gap for each constellation we optimized for parallel decoding capacity. Again, it should be emphasized that each '+' on the plot represents a different constellation. As a brief example, Table I gives results for PAM-8 optimized for 1.5 and 2.0 bits-per-symbol.

B. PSK Constellations

This section presents one example of optimized PSK constellations. Figure 5 shows a 16 points PSK constellation optimized for joint capacity and another optimized for parallel decoding capacity at SNR=8.87 dB. The constellation optimized for joint capacity is equally spaced while the one

Authorized licensed use limited to: Fish & Richardson PC. Downloaded on August 22,2022 at 14:20:05 UTC from IEEE Xplore. Restrictions apply.

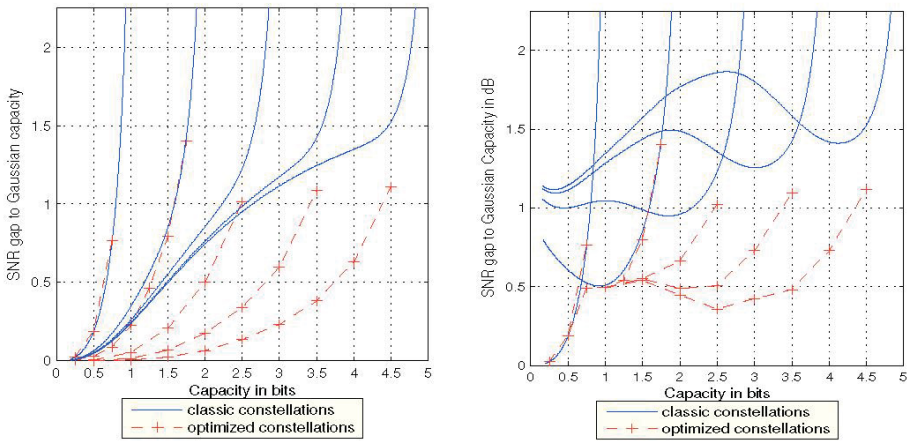


Fig. 4. (a) SNR gap to Gaussian Capacity for the joint capacity of the classic and the optimized PAM- 2, 4, 8, 16 and 32 constellations (from left to right respectively). (b) Gap between the Parallel Decoding Capacity and Gaussian Capacity for the classic and the optimized constellations.

TABLE I

C_{PD} OPTIMIZED PAM-8 CONSTELLATIONS FOR 1.5 AND 2.0 BITS/SYMBOL

PAM-8 C_{PD}			
1.5 bps		2.0 bps	
Label	Value	Label	Value
001	-0.6077	011	-0.5812
011	-0.2862	010	-0.3416
010	-0.2205	110	-0.2067
110	-0.0076	111	-0.0522
111	0.0076	101	0.0522
101	0.2205	100	0.2067
100	0.2862	000	0.3416
000	0.6077	001	0.5812

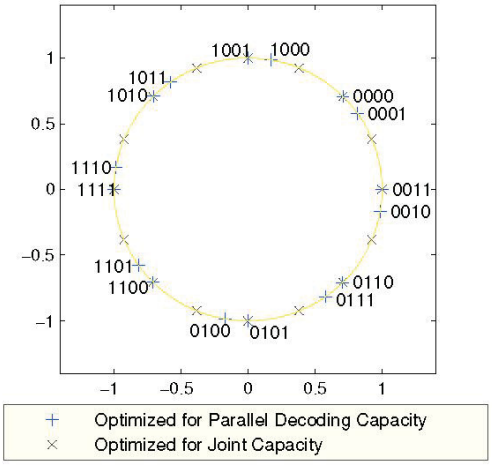


Fig. 5. A labelled 16 PSK constellation optimized for Parallel Decoding Capacity at SNR=8.87 dB along with a non-labelled constellation optimized for Joint Capacity at the same SNR

optimized for parallel decoding capacity is not. However, it is gray labeled and has interesting symmetry properties. We conjecture that all PSK or even multi-dimensional spherical (i.e. equal magnitude) constellations optimized for joint capacity will always be uniformally spaced regardless of the code rate, they are optimized for.

C. QAM and Multi-dimensional constellations

QAM/ multi-dimensional constellations can be constructed using orthogonal PAM optimized constellations. More efficient QAM/ multi-dimensional constellations may be found by joint optimization in multiple dimensions, which is more complex and has not been thoroughly investigated yet.

IV. Code Rate Rule

The joint capacity of traditional constellations suggests using a (log2(M) -1)/log2(M) code rate with an M point constellation for bandwidth efficient communication, as illustrated by Ungerboeck [13]. This rule can be readily applied to the optimized constellations. As can be seen in Fig. 4(a), a rate 4/5 optimized PAM-32 is 0.72 dB better than traditional PAM-32 in joint capacity.

In addition, however, while only marginal gains that can be found when using traditional constellations with code rates that are lower than suggested by the conventional code rate rule, larger gains can be achieved under the same circumstances with the optimized constellations. For example, a traditional PAM-32 constellation at rate 3/5 has a joint capacity that is only 0.06 dB better than a traditional PAM-16 constellation at rate 3/4. Using the optimized constellations, this difference is 0.36 dB instead, which may justify using a different code rate

Authorized licensed use limited to: Fish & Richardson PC. Downloaded on August 22,2022 at 14:20:05 UTC from IEEE Xplore. Restrictions apply.

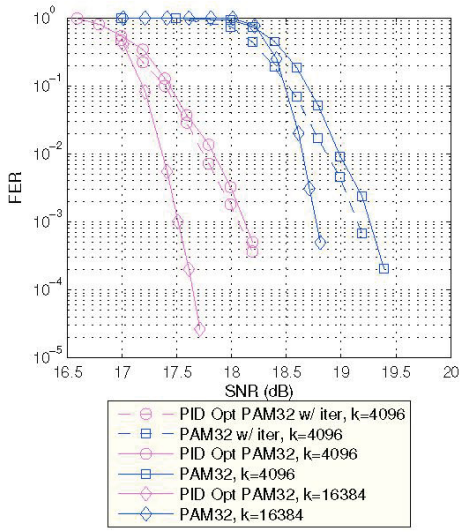


Fig. 6. Simulation results for a rate 1/2 LDPC code in conjunction with the classic versus the optimized PAM-32 constellation

rule with the optimized constellations.

V. Performance with LDPC Codes

In this section, sample simulation results of systems using LDPC codes are presented. We compare the performance of two systems, one using the classic PAM-32 constellation and the other using our C_{PD} optimized PAM-32 constellation. A rate $1/2$ Accumulate-Repeat-4-Jagged-Accumulate (AR4JA) LDPC code [14], is used with a codeword size of 8 kbits and 32 kbits. Simulation results are presented in Fig. 6. As seen in the figure there is a significant SNR gap between the two systems (around 1.2 dB). This compares to the 1.5 dB gap between the traditional PAM-32 and optimized PAM-32 in Fig. 4(b). It is also clear that performance does not improve much by iterating between the demapper and the decoder.

VI. Shaping: Geometric versus Probabilistic

Using the notation of [15] we compare the mutual information of systems with input alphabets $\mathcal{X}$ and $\mathcal{S}$ with elements x and s drawn from random variables X and S that exist in $\Re^n$ and have equal power constraints $EX^2 = ES^2 = P$. Symbols from one or the other alphabet are used to communicate across a channel that is specified only in so much that its output alphabet is given by $\mathcal{Y}$. Furthermore, the probability of symbols $x \in \mathcal{X}$ are constrained to be uniform $p(x) = \frac{1}{|\mathcal{X}|}$ while the probability of symbols $p(s)$ for all $s \in \mathcal{S}$ are only constrained to be rational fractions. Based on the above, the following proposition describes probabilistic shaping as a special case of geometric shaping:

Proposition 1 (Shaping): For any given alphabet $\mathcal{S}$ with rational $p(s) \forall s \in \mathcal{S}$ there exists an alphabet $\mathcal{X}$ with $p(x) = \frac{1}{|\mathcal{X}|}$ such that $I(X;Y) = I(S;Y)$.

Proof: Define $|\mathcal{S}|$ subgroups $\mathcal{X}_i \in \Re^n$ and let all elements of $\mathcal{X}_i = s_i$ for $i = 1, \ldots, |\mathcal{S}|$. Let $\mathcal{X} = \bigcup_{i=1}^{|\mathcal{S}|} \mathcal{X}_i$, $\frac{|\mathcal{X}_i|}{|\mathcal{X}|} = p(s_i)$, and $|\mathcal{X}|$ equal to the lowest common multiple of the denominators of the rational fractions that define $p(s_i)$ for $i = 1, \ldots, |\mathcal{S}|$. This yields $I(X;Y) = I(S;Y)$. ■

VII. Conclusion

In this paper we have shown that constellations designed to target a specific rate are able to achieve a smaller gap to the ultimate Shannon limit. No probabilistic shaping is required. The gains, instead, have been derived via judicious placement of points in the signaling space.

Acknowledgments

This research in part was carried out at the Jet Propulsion Laboratory, California Institute of Technology, under a contract with NASA.

References

[1] G. D. Forney, Jr., R. G. Gallager, G. R. Lang, F. M. Longstaff, and S. U. Qureshi, "Efficient modulation for band-limited channels," *IEEE J. on Select. Areas Commun.*, vol. SAC-2, pp. 632–647, 1984.

[2] J. H. Conway and N. J. A. Sloane, "A fast encoding method for lattice codes and quantizers," *IEEE Trans. Inform. Theory*, vol. IT-29, pp. 820–824, Nov. 1983.

[3] G. D. Forney, Jr. and L.-F. Wei, "Multidimensional constellations-Part I: Introduction, figures of merit, and generalized cross constellations," *IEEE J. Select. Areas Commun.*, vol. 7, pp. 877–892, Aug. 1989.

[4] G. D. Forney, Jr. "Multidimensional constellations-Part II: Voronoi constellations," *IEEE J. Select. Areas Commun.*, vol. 7, pp. 941–958, Aug. 1989.

[5] J. Hamkins and K. Zeger, "Asymptotically dense spherical codes," *IEEE Trans. Inform. Theory*, vol. 43, pp. 1774–1798, Nov. 1997.

[6] K. Ruotsalainen, "On the construction of the higher dimensional constellations," *IEEE Int. Symp. Information Theory*, pp. 490, July 2002.

[7] E. Agrell, J. Lassing, E. Ström and T. Ottosson, "On the optimality of the binary reflected gray code," *IEEE Trans. Inform. Theory*, vol. 50, pp. 3170–3182, Dec. 2004.

[8] G. Foschini, R. D. Gitlin, and S. B. Weinstein, "Optimization of two-dimensional signal constellations in the presence of Gaussian noise," *IEEE Trans. Commun.*, vol. 22, pp. 28–38, Jan. 1974.

[9] W. Betts, A. R. Calderbank, and R. Laroia, "Performance of nonuniform constellations on the Gaussian channel," *IEEE Trans. Inform. Theory*, vol. 40, pp. 1633–1638, Sept. 1994.

[10] F.-W. Sun, H. C. A. van Tilborg, "Approaching capacity by equiprobable signaling on the Gaussian channel," *IEEE Trans. Inform. Theory*, vol. 39, pp. 1714–1716, Sept. 1993.

[11] D. Sommer and G. P. Feitweis, "Signal shaping by non-uniform QAM for AWGN channels and applications using turbo coding," *ITG Conference on Source and Channel Coding*, pp. 81–86, Jan. 2000.

[12] C. Fragouli, R. D. Wesel, D. Sommer, and G. Fettweis, "Turbo codes with nonuniform QAM constellations," *IEEE Int. Conf. Commun.*, pp. 70–73, June 2001.

[13] G. Ungerboeck, "Channel coding with multilevel/phase signals," *IEEE Trans. Inform. Theory*, vol. 28, pp. 55–67, Sept. 1981.

[14] D. Divsalar, S. Dolinar, and C. Jones, "Low-rate LDPC codes with simple protograph structure," *IEEE Int. Symp. Inform. Theory*, pp. 1622-1626, Sept. 2005.

[15] T. M. Cover and J. A. Thomas, *Elements of Information Theory*. New York: Wiley, 1991.

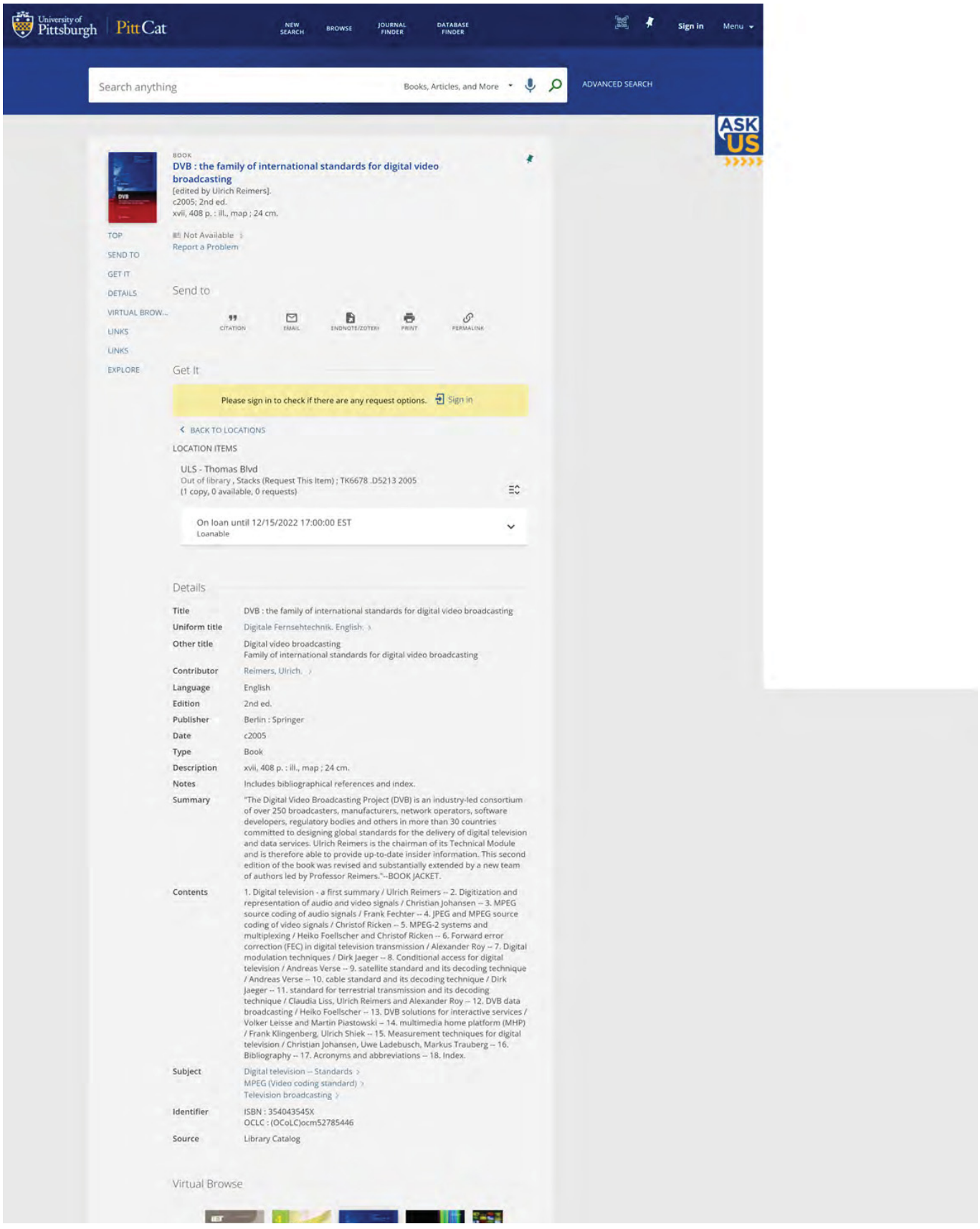
Authorized licensed use limited to: Fish & Richardson PC. Downloaded on August 22,2022 at 14:20:05 UTC from IEEE Xplore. Restrictions apply.

APPENDIX REIMERS01

screenshot-pitt.primo.exlibrisgroup.com-2022.11.18-08_40_32
https://pitt.primo.exlibrisgroup.com/discovery/sourceRecord?vid=01PITT_INST:01PITT_INST&docId=alma9944323503406236&recordOwner=01PITT_INST
18.11.2022

```
leader  03053cam a22003858a 4500
001     9944323503406236
005     20191122120705.0
008     030731s2005    gw ab    b    001 0 eng
015     ##$aGBA3-V5194
016     7#$a969712391 $2GyFmDB
020     ##$a354043545X
035     ##$a(OCoLC)ocm52785446
035     ##$a4432350
035     ##$a(ppiu)4432350-pittdb
035     ##$a(pittdb)4432350-pittdb
040     ##$aUKM $cUKM $dOCLCQ $dOHX $dHNK $dOrLoB-B $dUtOrBLW
041     1#$aeng $hger
049     ##$aPITT
072     #7$aTK $2lcco
082     04$a621.38833 $221
090     ##$aTK6678 $b.D5213 2005
130     0#$aDigitale Fernsehtechnik. $lEnglish.
245     10$aDVB : $bthe family of international standards for digital video broadcasting / $c[edited by Ulrich Reimers].
246     3#$aDigital video broadcasting
246     30$aFamily of international standards for digital video broadcasting
250     ##$a2nd ed.
260     ##$aBerlin : $bSpringer, $cc2005.
300     ##$axvii, 408 p. : $bill., map ; $c24 cm.
504     ##$aIncludes bibliographical references and index.
505     00$g1. $tDigital television - a first summary / $rUlrich Reimers --  $g2. $tDigitization and representation of audio and video signals / $rChristian Johansen --  $g
520     1#$a"The Digital Video Broadcasting Project (DVB) is an industry-led consortium of over 250 broadcasters, manufacturers, network operators, software developers, regu
650     #0$aDigital television $xStandards.
650     #0$aMPEG (Video coding standard)
650     #0$aTelevision broadcasting.
700     1#$aReimers, Ulrich.
938     ##$aOtto Harrassowitz $bHARR $nhar035023992 $c85.55 EUR
994     ##$aE0 $bPIT
906     ##$aULS
```

screenshot-pitt.primo.exlibrisgroup.com-2022.11.18-08_40_54
https://pitt.primo.exlibrisgroup.com/discovery/fulldisplay?context=L&vid=01PITT_INST:01PITT_INST&search_scope=MyInst_and_CI&tab=Everything&docid=alma9944323503406236
18.11.2022





Links

Find this Item in Google Books
Display Source Record

Syndetics Unbound

Summary Look Inside Reader Reviews
Browse Shelf

SUMMARY

This second edition provides first-hand information about the most recent developments in the exciting and fast moving field of telecommunications media and consumer electronics. The DVB group developed the standards which are being used in Europe, Australia, Southeast Asia, and many other parts of the world. Some 150 major TV broadcasting companies as well as suppliers for technical equipment (read more)

LOOK INSIDE

Digital Television - a First Summary

Digitization and Representation of Audio and Video Signals

MPEG Source Coding of Audio and Video Signals

SEE FULL TABLE OF CONTENTS COVER

READER REVIEWS

BE THE FIRST TO WRITE A REVIEW

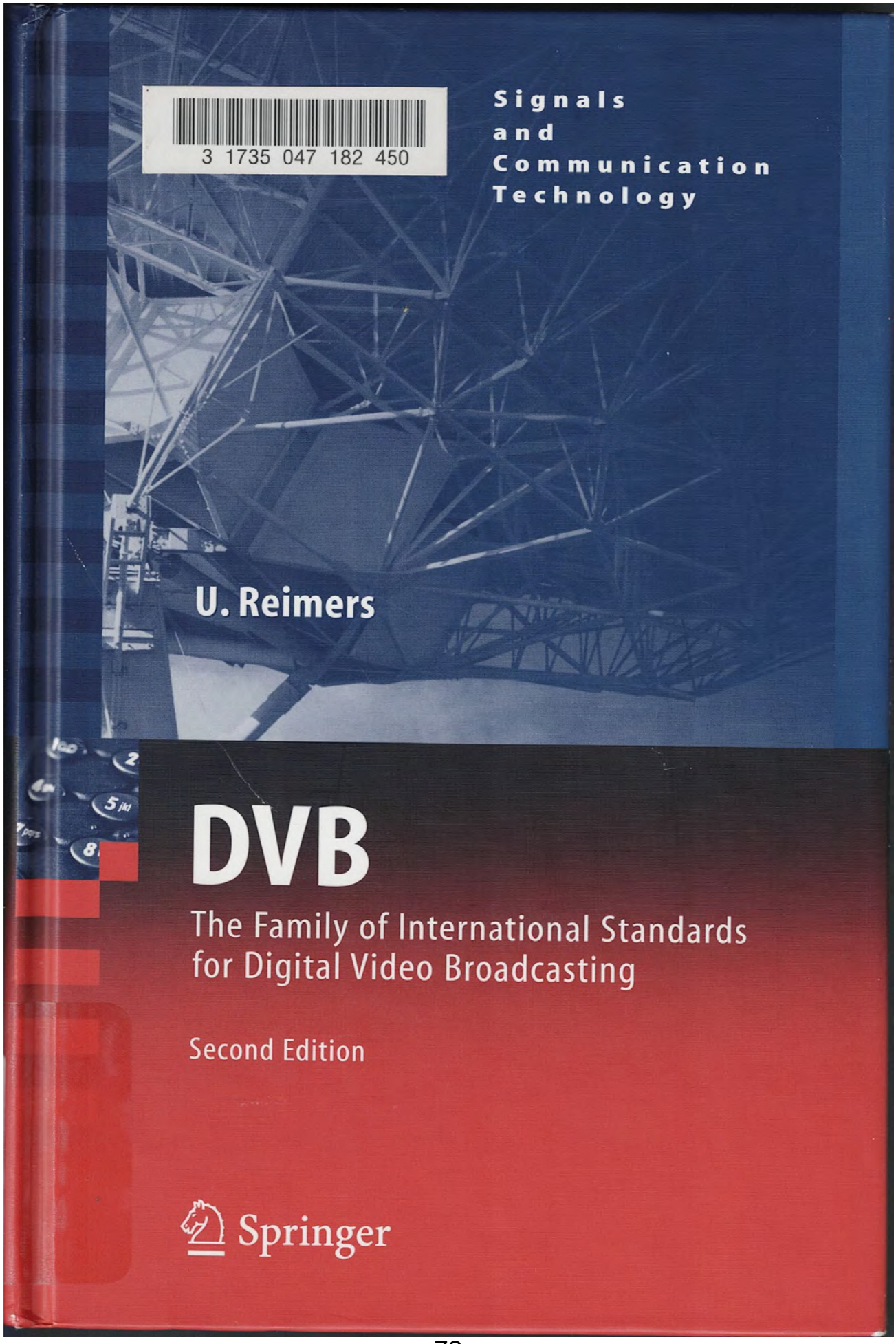
BROWSE SHELF



SEE FULL SHELF

Catalog enrichment powered by Syndetics Unbound

APPENDIX REIMERS02


3 1735 047 182 450
Signals and Communication Technology
U. Reimers
DVB
The Family of International Standards for Digital Video Broadcasting
Second Edition
Springer

Reimers
DVB
2nd Edition
INFOSCI
TK6678
D5213
2005

R09-M18-S26-T05
31735047182450
Tray ID: R09-M18-S26-T05
Call No.: TK6678 .D5213 2005
Volume:
Collection: GEN
Title: DVB : the family of internatio
Banding Label 11/16/2022 15:56:24

casting Project (DVB) is an industry-led
broadcasters, manufacturers, network
elopers, regulatory bodies and others
es committed to designing global
ry of digital television and data
is the chairman of its Technical Module
provide up-to-date insider information.
he book was revised and substantially
n of authors led by Professor Reimers.
ata Broadcasting, Solutions for Inter-
promising Multimedia Home Platform
ised are those on MPEG-2 systems
andard for terrestrial transmission and
and the first chapter, the introduction

Do Not Remove This Wrapper

University of Pittsburgh
University Library System

Storage
Facility

CIRCULATING
CIRCULATING
CIRCULATING
CIRCULATING

UNIVERSITY OF PITTSBURGH LIBRARIES

DVB

Ulrich Reimers

DVB

The Family of International Standards for Digital Video Broadcasting

Second Edition

With 261 Figures

Springer

Professor Dr.-Ing. Ulrich Reimers

Professor Dr.-Ing. Frank Fechter
Dipl.-Ing. Heiko Foellscher
Dr.-Ing. Dirk Jaeger
Dipl.-Ing. Christian Johansen
Dipl.-Ing. Frank Klinkenberg
Dr.-Ing. Uwe Ladebusch
Dipl.-Ing. Volker Leisse
Dipl.-Ing. Claudia Liss
Dr.-Ing. Martin Piastowski
Professor Dr.-Ing. Christof Ricken
Dr.-Ing. Alexander Roy
Dipl.-Ing. Ulrich Schiek
Dr.-Ing. Markus Trauberg
Dipl.-Ing. Andreas Verse

Technische Universität Braunschweig
Institut für Nachrichtentechnik
(Braunschweig Technical University
Institute for Communications Technology)
Schleinitzstr. 22
D-38092 Braunschweig
u.reimers@tu-bs.de

Originally published as a monograph

Library of Congress Control Number: 2004102304

ISBN 3-540-43545-X Springer Berlin Heidelberg New York

This work is subject to copyright. All rights are reserved, whether the whole or part of the material is concerned, specifically the rights of translation, reprinting, reuse of illustrations, recitation, broadcasting, reproduction on microfilm or in other ways, and storage in data banks. Duplication of this publication or parts thereof is permitted only under the provisions of the German Copyright Law of September 9, 1965, in its current version, and permission for use must always be obtained from Springer-Verlag. Violations are liable for prosecution under German Copyright Law.

Springer is a part of Springer Science+Business Media

springeronline.com

© Springer-Verlag Berlin Heidelberg 2005
Printed in Germany

The use of general descriptive names, registered names, trademarks, etc. in this publication does not imply, even in the absence of a specific statement, that such names are exempt from the relevant protective laws and regulations and therefore free for general use.

Typesetting: Camera ready copy from author
Cover-Design: Design & Production, Heidelberg
Printed on acid-free paper 62/3020 Rw 5 4 3 2 1 0

Table of Contents

1	**Digital Television – a First Summary** (REIMERS)	1
1.1	Definitions and Range of Application	1
1.2	The Genesis of Recommendations for Digital Television	3
1.2.1	Work in the United States of America	5
1.2.2	Work in Europe	6
1.2.3	Work in Japan	8
1.3	Objectives in the Development of Digital Television	9
1.4	Data Reduction as the Key to Success	11
1.5	Possible Means of Transmission for Digital Television	13
1.6	Standards and Norms in the World of Digital Television	17
1.7	The New DVB-Project	18
2	**Digitisation and Representation of Audio and Video Signals** (JOHANSEN)	21
2.1	Sampling and Quantising	21
2.2	Digitising Video Signals	22
2.2.1	ADCs and DACs for Video Signals	24
2.2.2	Representation of Video Signals	26
2.3	Digitising Audio Signals	29
2.3.1	Representation of Audio Signals	30
2.3.2	ADCs and DACs for Audio Signals	30
3	**MPEG Source Coding of Audio Signals** (FECHTER)	37
3.1	Basics of Bit-rate Reduction	37
3.2	Psychoacoustic Basics	39
3.2.1	Threshold of Audibility and Auditory Sensation Area	39
3.2.2	Masking	40
3.3	Source Coding of Audio Signals Utilising the Masking Qualities of the Human Ear	44
3.3.1	Basic Structure of the MPEG Coding Technique	45
3.3.2	Coding in Accordance with Layer 1	49
3.3.3	Coding in Accordance with Layer 2	51
3.3.4	Coding in Accordance with Layer 3	52
3.3.5	Decoding	54

3.3.6 The Parameters of MPEG Audio . . . 54
3.3.7 MPEG-2 Audio Coding . . . 55
3.4 Summary . . . 56

4 **JPEG and MPEG Source Coding of Video Signals** (RICKEN) . . . 59
4.1 Coding in Accordance with JPEG . . . 60
4.1.1 Block Diagram of Encoder and Decoder . . . 60
4.1.2 Discrete Cosine Transform . . . 61
4.1.3 Quantisation . . . 63
4.1.4 Redundancy Reduction . . . 65
4.1.5 Specific Modes . . . 67
4.1.6 Interchange Format . . . 70
4.2 Coding in Accordance with the MPEG Standards . . . 71
4.2.1 Block Diagrams of Encoder and Decoder . . . 73
4.2.2 Motion Estimation . . . 75
4.2.3 Reordering of Pictures . . . 78
4.2.4 Data-rate Control . . . 79
4.2.5 Special Features of MPEG-1 . . . 80
4.2.6 Special Features of MPEG-2 . . . 83
4.3 Summary . . . 89

5 **MPEG-2 Systems and Multiplexing** (FOELLSCHER, RICKEN) . . . 91
5.1 Differences between Programme Multiplex and Transport Multiplex . . . 91
5.2 Positioning of Systems in the ISO/OSI Layer Model . . . 92
5.3 End-to-end Synchronisation . . . 94
5.4 Service Information . . . 99
5.4.1 PSI/SI Tables and their Insertion into the MPEG-2 Transport Stream . . . 99
5.4.2 Section and Table Structure . . . 103
5.4.3 Examples of Table Usage: NIT and SDT . . . 105
5.4.3.1 Network Information Table (NIT) . . . 106
5.4.3.2 Service Description Table (SDT) . . . 108

6 **Forward Error Correction (FEC) in Digital Television Transmission** (ROY) . . . 111
6.1 Basic Observations . . . 111
6.2 Reed-Solomon Codes . . . 114
6.2.1 Introduction to the Arithmetic of the Galois Field . . . 115
6.2.2 Definition of the RS Code and the Encoding/Decoding in the Frequency Domain . . . 121

6.2.3 Error Correction Using the RS Code . . . 122
6.2.4 Examples of Encoding/Decoding in the Frequency Domain . . . 125
6.2.5 Encoding and Decoding in the Time Domain . . . 127
6.2.6 Efficiency of the RS Code . . . 128
6.3 Convolutional Codes . . . 129
6.3.1 Basics of the Convolutional Codes . . . 129
6.3.2 Examples of Convolutional Encoding and Decoding . . . 131
6.3.2.1 Construction of a Model Encoder . . . 131
6.3.2.2 State Diagram and Trellis Diagram of the Model Encoder . . . 132
6.3.2.3 Example of Encoding with Subsequent (Viterbi) Decoding . . . 133
6.3.3 Hard Decision and Soft Decision . . . 136
6.3.4 Puncturing of Convolutional Codes . . . 138
6.3.5 Performance of Convolutional Codes . . . 138
6.4 Code Concatenation . . . 140
6.4.1 Block-Code Concatenation . . . 140
6.4.2 Interleaving . . . 141
6.4.3 Error Correction in DVB . . . 143
6.5 Further Reading . . . 145

7 **Digital Modulation Techniques** (JAEGER) . . . 147
7.1 NRZ Baseband Signal . . . 147
7.2 Principles of the Digital Modulation of a Sinusoidal Carrier Signal 153
7.2.1 Amplitude Shift Keying (2-ASK) . . . 155
7.2.2 Frequency Shift Keying (2-FSK) . . . 157
7.2.3 Phase Shift Keying (2-PSK) . . . 158
7.3 Quadrature Phase Shift Keying (QPSK) . . . 160
7.4 Higher-level Amplitude Shift Keying (ASK) and Vestigial-Sideband Modulation (VSB) . . . 163
7.5 Digital Quadrature Amplitude Modulation (QAM) . . . 167
7.6 Orthogonal Frequency Division Multiplex (OFDM) . . . 173

8 **Conditional Access for Digital Television** (VERSE) . . . 181

9 **The Satellite Standard and Its Decoding Technique** (VERSE) . . . 187
9.1 The Basics of Satellite Transmission . . . 187
9.1.1 Transmission Distance . . . 187
9.1.2 Processing on Board a Satellite . . . 188
9.1.3 Polarisation Decoupling . . . 190
9.1.4 Energy Dispersal . . . 191
9.1.5 Signal Reception . . . 191
9.1.6 Reference Data of a Television Satellite with Astra 1D as an Example . . . 192
9.2 Requirements of the Satellite Standard . . . 192

9.3 Signal Processing at the Encoder 194
9.3.1 System Overview 194
9.3.2 Energy Dispersal 195
9.3.3 Error-protection Coding 195
9.3.4 Filtering 197
9.3.5 Modulation 197
9.4 Decoding Technique 198
9.4.1 Demodulator 199
9.4.2 Filtering and Clock Recovery 199
9.4.3 Viterbi Decoder 200
9.4.4 Sync-byte Detector 201
9.4.5 De-interleaver and RS Decoder 202
9.4.6 Energy-dispersal Remover 202
9.4.7 Baseband Interface 203
9.5 Performance Characteristics of the Standard 203
9.5.1 Useful Bit Rates 203
9.5.2 Required Carrier-to-noise Ratio in the Transmission Channel . 204
9.5.3 Antenna Diameter 205
9.6 Local Terrestrial Transmission 205

10 The Cable Standard and Its Decoding Technique (JAEGER) . . 207
10.1 Cable Transmission Based on the Example of a German CATV Network 207
10.1.1 Intermodulation 209
10.1.2 Thermal Noise 210
10.1.3 Reflections 212
10.2 User Requirements of the Cable Standard 212
10.3 Signal Processing at the Encoder 214
10.3.1 Conversion of Bytes to Symbol Words 215
10.3.2 Differential Coding of MSBs 215
10.3.3 Modulation 217
10.4 Decoding Technique 220
10.4.1 Cable Tuner 220
10.4.2 IF Interface 221
10.4.3 Recovery of the Carrier Signal 222
10.4.4 Generating the Clock Signal 224
10.4.5 Demodulation of the QAM Signal 225
10.4.6 Differential Decoding of MSBs 228
10.4.7 Conversion of Symbol Words to Bytes 228
10.4.8 Detection of MPEG Sync Bytes 229
10.5 Performance Details of the Standard 230
10.5.1 Determination of Useful Data Rates 230
10.5.2 Carrier-to-noise Ratio Required in the Transmission Channel . 232

10.6 DVB Utilisation in Master Antenna Television Networks 233
10.7 Local Terrestrial Transmission (MMDS) 235

11 **The Standard for Terrestrial Transmission and Its Decoding Technique** (LISS, REIMERS, ROY) 237
11.1 Basics of Terrestrial Television Transmission 238
11.2 User Requirements for a System for Terrestrial Transmission of DVB Signals 243
11.3 Encoder Signal Processing 245
11.3.1 Inner Interleaver and Symbol Mapping 245
11.3.2 Choosing the OFDM Parameters 248
11.3.3 Arrangement of the Transmission Frame 251
11.4 Decoding Technique 255
11.4.1 Receiver Classes 257
11.4.2 Straight Forward Technology – the Classical Approach 258
11.4.2.1 Antenna 259
11.4.2.2 Tuner 260
11.4.2.3 IF Processing 261
11.4.2.4 DVB-T Decoder Chip 263
11.4.3 Enhanced Technologies for DVB-T Reception 264
11.4.3.1 Antenna Pre-Amplifiers for DVB-T 264
11.4.3.2 One-Chip Silicon Tuner 266
11.4.3.3 Network Interface Module (NIM) Technology 267
11.4.3.4 Antenna Diversity 269
11.5 Hierarchical Modulation 270
11.6 Features of the Standard 274
11.6.1 Determination of Useful Data Rates 275
11.6.2 Required Carrier-to-noise Ratio in the Transmission Channel . . 278
11.6.3 Features Relevant for Mobile Reception 280

12 **DVB Data Broadcasting** (FOELLSCHER) 285
12.1 Basics of Data Broadcasting 285
12.2 Data Piping 286
12.3 Data Streaming 287
12.3.1 Asynchronous Data Streaming 287
12.3.2 Synchronous Data Streaming 287
12.3.3 Synchronised Data Streaming 288
12.4 Data/Object Carousel 289
12.4.1 Data Carousel 289
12.4.2 Object Carousel 292
12.5 Multiprotocol Encapsulation 295
12.5.1 IP over DVB 297
12.6 System Software Update 299

13 **DVB Solutions for Interactive Services** (LEISSE, PIASTOWSKI) . . 303
13.1 Interactive Services 303
13.2 Network-Independent Protocols for DVB Interactive Services. . 305
13.2.1 Protocol Stack 305
13.2.2 System Model 306
13.2.3 Higher Layer Protocols 307
13.3 Network-Dependent Solutions for PSTN, ISDN, DECT, GSM . . 308
13.3.1 Interaction Channel through PSTN/ISDN 309
13.3.2 Interaction Channel through DECT 310
13.3.3 Interaction Channel through GSM 311
13.4 Network-Dependent Solutions for DVB-C, DVB-S and DVB-T . 313
13.4.1 Interaction Channel for Cable TV Distribution Systems 313
13.4.2 Interaction Channel for LMDS 320
13.4.3 Interaction Channel for Satellite Distribution Systems 321
13.4.4 Interaction Channel for Satellite Master Antenna TV 323
13.4.5 Interaction Channel for Digital Terrestrial Television 325

14 **The Multimedia Home Platform (MHP)** (KLINGENBERG, SCHIEK) 331
14.1 The Role of Software Platforms in the Receiver 331
14.2 Some Non-MHP Solutions 332
14.2.1 ATVEF 333
14.2.2 Betanova 334
14.2.3 Liberate 334
14.2.4 Mediahighway 334
14.2.5 MHEG 335
14.2.6 OpenTV 336
14.2.7 Migration Concepts. 337
14.3 MHP 1.0 337
14.3.1 Basic Architecture 338
14.3.2 Transport Protocols 340
14.3.2.1 Broadcast Channel Protocols 340
14.3.2.2 Interaction Channel Protocols 341
14.3.3 Application Model and Signalling. 342
14.3.4 Content Formats 344
14.3.5 Graphics Model. 345
14.3.6 User Interface 347
14.3.7 Security Architecture 347
14.3.8 Minimum Platform Capabilities 350
14.4 MHP 1.1. 350
14.4.1 Enhancements in MHP 1.1 351
14.5 The Future of MHP 356
14.5.1 Ongoing Developments. 356
14.5.2 Aspects of a mobile MHP 356
14.6 The MHP Test Suite 357
14.7 The Globally Executable MHP 358

14.8 Other Java-Based Software Platforms 359
14.8.1 OSGi 359
14.8.2 DAB Java Specification 359
14.8.3 Mobile Information Device Profile – MIDP 360

15 **Measurement Techniques for Digital Television** (JOHANSEN, LADEBUSCH, TRAUBERG) 363
15.1 Measurement Techniques for Source-Signal Processing in the Baseband 364
15.1.1 Quality Evaluation of Video Source Coding 364
15.1.2 Checking Compressed Audio and Video Signals 366
15.1.3 Checking the MPEG-2 Transport Stream 366
15.1.4 Checking the Functionality of the Decoder 372
15.2 Measurements for Digital Transmission Technology. 373
15.2.1 Representation of the Eye Diagram 374
15.2.2 Measurements Carried out at Modulators and Demodulators . . 375
15.2.3 Measurement of Error Rate 379

16 **Bibliography** 383

17 **Acronyms and Abbreviations** 395

18 **Index** 403

1 Digital Television – a First Summary

1.1 Definitions and Range of Application

The expression "digital" is one of the elements of language which has frequently been used and very often misused in the past few years. "Digital" alone means that there are elements which can be counted on the fingers. In the everyday language of information technology the expression "digital" is often used as a synonym for "sampled, quantized and presented in binary characters". In the field of electronic media technology "digital" is a mark of quality which was first used when the compact disc (CD) was introduced on the market and offered to the general public.

The expression "digital studio" describes the introduction of digital signal forms into radio and television production. The audio and video signals are sampled by means of predetermined sampling frequencies and quantized by predetermined numbers of quantization steps. As a rule, further source coding is not used during processing and distribution, however it may take place in individual pieces of equipment.

The signals which are received by "digital" television receivers in most cases are still analogue input signals (NTSC, PAL, SECAM), which are then internally digitised and processed as digital signals. The presentation of the image, however, remains analogue.

From what has been said, it is evident that the terminology must be carefully defined in order to limit confusion to a minimum. "Digital Television", sometimes termed "Digital TeleVision (DTV)", or "Digital Video Broadcasting (DVB)", usually means the transmission of digitised audio, video and auxiliary information as data signals. However, since these data signals must in most cases be modulated onto continuous-time carrier waves in order for them to fit in the transmitting channel, the actual transmission in digital television uses analogue signals.

In the context of this book the expression "digital television" should in fact be understood as the system for the transmission of audio, video and auxiliary data described above. However, it is not possible to concentrate only on the channel coding and modulation, furthermore necessary system components must be included, in particular the technology for the source coding of audio and video signals and multiplexing. The latter is required for the co-ordination of various elementary streams to form one signal. The expression "multiplexing" is not really quite apt because this simplifies the

owing, for example, to noise in the channel – a phase is decoded which passes beyond one of the two decision thresholds (= axis in figure 9.9), there will only be one erroneous bit.

Before transmission, the IF signal is upconverted to radio frequency.

In this way two bits per symbol are transmitted; hence in ideal circumstances the utilisation of the bandwidth, referred to the gross bit rate, is $B = 2$ bit/(s · Hz). However, owing to the non-ideal filters (finite width of the filter slopes) the bandwidth utilisation is actually smaller. Depending on the configuration of the system, the ratio between bandwidth and symbol rate (BW/R_S) would be in the range of about

$$\frac{BW}{R_s} = 1.27 \frac{\text{Hz}}{\text{symbols/s}}. \tag{9.1}$$

Hence the bandwidth utilisation would be about

$$B = \frac{\text{bits per symbol}}{BW/R_s} = \frac{2 \text{ bits/symbol}}{1.27 \text{ Hz}/\frac{\text{symbols}}{\text{s}}} = 1.57 \frac{\text{bit}}{\text{s Hz}}. \tag{9.2}$$

The bandwidth utilisation can also be referred to the net bit rate, i.e. to the number of information bits only, without the error protection. In this case the calculated value, as indicated above, must be multiplied with the code rates of the outer and inner codes.

9.4 Decoding Technique

On reception of the signals transmitted from the satellite, the processing steps that were carried out at the encoder have to be reversed. In particular, the errors which occurred in the channel must be corrected. Moreover, it is necessary to recover the synchronising information, which is required for the channel decoding.

The decoder consists of the following components (figure 9.10):

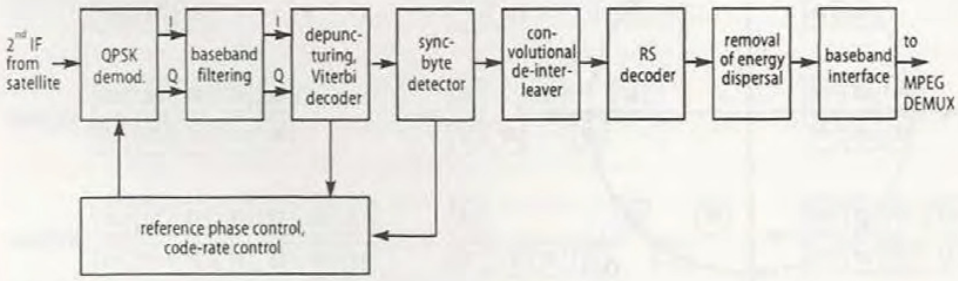


Fig. 9.10. Block diagram of signal processing at the receiving end

mitting end. The synchronisation of the clock frequency generated at the receiver is effected by means of a band-pass filter and a subsequent PLL, where the centre frequency of the oscillator corresponds with the clock frequency, which in turn corresponds with the symbol rate. After an amplitude limitation the clock signal is ready for the digital signal processing.

There are further techniques described in the literature [LEE, PROAKIS, KAMMEYER, MÄUSL] which generate the error signal for the oscillator within the analogue as well as within the digital range.

10.4.5 Demodulation of the QAM Signal

The demodulator has the task of converting the QAM signal to the baseband and simultaneously splitting it into its in-phase and quadrature components. After the temporal multiplication with two carrier signals which are orthogonal to each other in phase, the resulting sum-frequency signals of the two components must be suppressed by one low-pass filter each. If the multiplication and the filtering are achieved by means of analogue signal processing, then both components will subsequently be available for A/D conversion in the baseband.

By using conventional analogue technology a reasonably priced demodulator can be manufactured. The disadvantage of this solution is to be found in the two parallel paths through which the in-phase and quadrature components have to pass before sampling as well as in the parallel sampling itself.

The parallel signal paths can be transferred to the digital level if the modulated signal is fed into a single A/D converter in its entirety. In this case the demodulation is carried out by the multiplication with two digital carrier signals. The required sampling rate for the sampling of the QAM signal at the IF level, in accordance with the sampling theorem, will have to be at least twice that of the highest frequency to be found in the signal. For transmission in an 8-MHz channel the resulting minimal sampling frequency would be:

$$f_{\min} = 2\left(f_{IF} + \frac{B}{2}\right) = 2\left(36.15\ \text{MHz} + \frac{8\ \text{MHz}}{2}\right) = 80.3\ \text{MHz}. \qquad (10.14)$$

The high clock rate has various disadvantages when used in consumer receivers (e.g. high cost, high power consumption), so that a totally digital solution must be ruled out at this moment.

A demodulation alternative arises if the QAM signal from the IF range at 36.15 MHz is converted to a second IF range. The centre frequency of the signal should be chosen so as to correspond to the transmitted symbol rate. This technique offers the advantage that the converted QAM signal as a whole can be oversampled by a clock signal of a frequency which is exactly four times the value of the transmitted symbol rate. In the case of a symbol

The "continual pilots" are present in each symbol at the same carrier position (in the case of 2K, for instance, at the 45 positions 0, 48, 54, 87 ... 1323, 1377, 1491, 1683, 1704; in the case of 8K, for instance, at the 177 positions 0, 48, 54, 87 ... 6435, 6489, 6603, 6795, 6816). The distribution along the frequency axis is chosen, so that within one channel no periodicities can occur. Therefore the continual pilots can be used for the coarse adjustment of the frequency of the local oscillator in the receiver. In order to make the synchronising information as robust as possible against transmission errors, the continual pilots have an amplitude which, in comparison to the carriers containing useful information, is increased by the factor 4/3. That is why they are also called boosted pilots.

The "scattered pilots" are scattered over the transmission frame according to a definite plan. This plan can be easily identified in figure 11.5. The aim of the scattering is, firstly, to make a large number of pilots within each symbol for the fine adjustment of the receiver available. Secondly, the scattered pilots can contribute to the temporal synchronisation. Thirdly, the receiver will be able to perform a nearly continuous analysis of the frequency- and the temporal plane, which can be used for the evaluation of the current channel condition ("channel estimation"). The scattered pilots are also transmitted with increased amplitude.

The "transmission-parameter signalling pilots" (TPS pilots) permit a transmission of additional information with which the temporal synchronisation, i.e. the recognition of the beginning of the transmission frame, can be ensured. Moreover, they provide the information about the transmission parameters used. The details of this will be discussed in the following. The TPS pilots, just as the continual pilots, can be found in precisely fixed carrier positions (in the case of 2K, for instance at the 17 positions 34, 50, 209, 346, 413 ... 1262, 1286, 1469, 1594, 1687; in the case of 8K, at the 68 positions 34, 50, 209, 346, 413 ... 6374, 6398, 6581, 6706, 6799). TPS pilots are transmitted with an amplitude, which represents the average amplitude of all carriers transmitting useful information.

The numbers of the various types of pilots named per symbol cannot just be added to determine the channel capacities lost for the transmission of use-ful information, as the possibility that a continual pilot may be at a position intended for a scattered pilot cannot be ignored (see figure 11.5). On closer examination it may be seen that each of the continual pilots is co-located in every fourth symbol with a scattered pilot. This results, on average, in 1512 carriers with useful information per symbol in the 2K case, and in 6048 carriers with useful information in the 8K case, which means that approximately 13% of all carriers have to be utilised for synchronisation, etc.

Attention has already been drawn to the fact that the continual pilots and the scattered pilots are individually modulated so that from an analysis of

this modulation the receiver can, among other things, derive information for the tuning. The modulation is carried out in accordance with the structure of a maximum-length sequence, which is known to the transmitter and to the receiver.

Maximum-length sequences (*m*-sequences) are often referred to as pseudo-random sequences. They have some prominent features. One of these is the ideal, pulse-shaped, periodically recurring auto-correlation function, which is of particular importance in this connection [LÜKE 2].

A maximum-length sequence can be generated by a shift register, in which the positions indicated by the descriptive polynomial are linked by means of EX-OR circuits (see also section 9.3). The polynomial used here has the form

$$g(X) = X^{11} + X^2 + X^0 .$$

X^{11} represents the input of the first cell; X^0 represents the output of the shift register. All sequences commence with the initialisation condition $X^s = 1$, in such a way that the first bit at the output of the shift register coincides with the first carrier of a symbol. Further shifting within the register takes place such that there is a shift step to each carrier, independently of whether it is a pilot or not. When the temporally coincidental carrier happens to be a continual pilot or a scattered pilot, a modulation symbol is allocated to the pilot by the bit at the output of the shift register. When this bit is 0, then the pilot is modulated with the positive real part +4/3, when the bit is 1, then the pilot is modulated with the negative real part -4/3. The imaginary part of the modulation symbol is always zero. If the adjacent carriers in figure 11.5 which form part of a symbol are examined from left to right, i.e. along the frequency axis, a subsampled maximum sequence will be detected at the 176 or 701 positions per symbol at which continual or scattered pilots are to be found. This maximum sequence can now be used for fine-tuning in the receiver.

In every transmission frame the data denoted as TPS are transmitted within each symbol. Basically, they constitute a special data channel, which can carry important information for the duration of every transmission frame. The receiver requires this information for the demodulation of the subsequent transmission frame. The purpose of the TPS data is therefore similar to that of the so-called fast-information channel of the DAB system [ETS 401]. Within each transmission frame there are 68 successive symbols. Each of these symbols contains one bit from a 68-bit TPS word. For the 2K variant 17 carriers per symbol are made available for TPS, and for the 8K variant 68 carriers. In each symbol these TPS carriers all transmit exactly the same individual bits in parallel.

The information prepared by the TPS refers to the modulation procedure (QPSK, 16-QAM, 64-QAM), the constellation model for the case of hierarchical modulation with the possible values $\alpha = 1$ or $\alpha = 2$ or $\alpha = 4$ (see section 11.5), the coderate of the inner error protection (1/2, 2/3, 3/4, 5/6, 7/8), the duration of the guard interval ($\Delta = 1/32$, $\Delta = 1/16$, $\Delta = 1/8$, $\Delta = 1/4$), the OFDM variations (2K and 8K) and the position of the transmission framework within the framework (1,2,3,4). In addition, a cell identifier is also transmitted to identify the network cell from which the received signal is being transmitted [LADEBUSCH].

In view of the importance of an error-free reception of the TPS data, these are transmitted in parallel many times over and are also separately error protected. A shortened BCH code (67, 53) is used. The individual bits are modulated for the TPS carriers with differential 2-PSK (see section 7.2).

A maximum of 68 bits can be used for TPS. 31 bits are required for the word recognition and error protection. 31 bits are used at the moment. The remaining 6 bits are reserved for further use.

11.4 Decoding Technique

The DVB-T standard EN 300 744 only describes the transmitted signal and thus does not specify the receiver side. So various possibilities for the realisation of the units in the decoder are conceivable. The implementation strongly depends on the reception environment. Basically, the processing steps which were carried out at the encoder have to be reversed. In figure 11.6 the fundamental construction of the corresponding receiver is shown

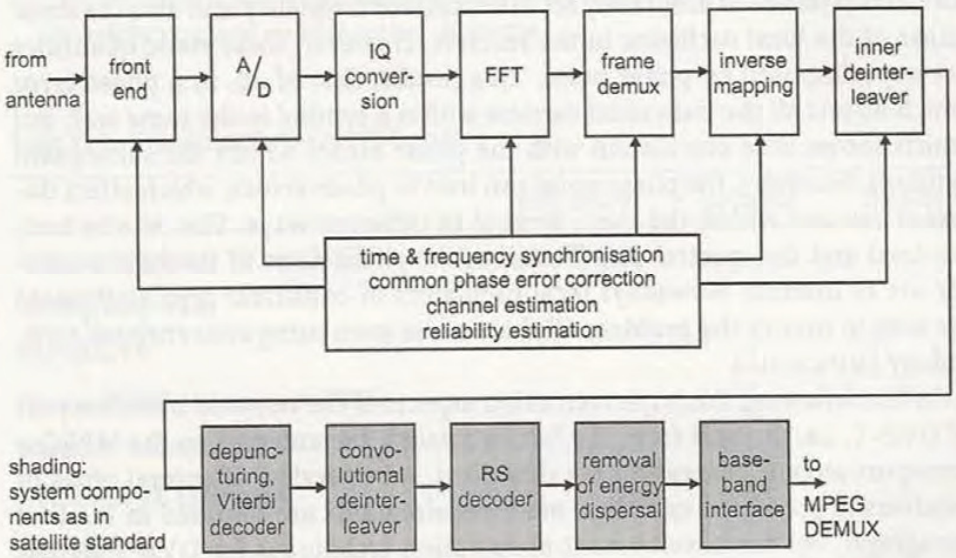


Fig. 11.6. Block diagram of signal processing at the receiving end

[MØLLER]. During the introduction of the first regular DVB-T digital TV service in the UK in November 1998, the first integrated digital receiver chip set was based on 3 chips and only supported the 2K mode. In the meantime single-chip solutions combining A/D conversion, COFDM processing and channel decoding are available and fully standard compliant.

A DVB-T receiver needs to cope with several impairments that occur during terrestrial transmissions (see section 11.1). In addition, the receiver front end will add noise and phase noise to the signal [KLINKEN]. Receiver implementations may differ in the way they handle time and frequency synchronisation and channel estimation. The pilots, which are spread in time and frequency within the OFDM signal, have a known amplitude and phase. Therefore, the measuring of the channel frequency response for attenuation and phase can be carried out on the basis of the continual pilots and on the scattered pilots. Knowing the amplitude and phase of all the individual pilot signals, the receiver is able to equalise each subcarrier. This ideally reverses the effects of the transmission channel. Various so-called channel estimation techniques have an important effect on the overall performance of the receiver [STRUBENH].

The stability of the oscillators required in the receiver is of great importance for the overall performance. On the one hand, the single carriers, which are approx. 1.1 kHz or 4.4 kHz apart, can only be separated free of crosstalk if it can be guaranteed that the sampling is carried out exactly at the zero crossings of all sin(x)/x functions not belonging to the desired carrier (see section 7.6). On the other hand, it must remain possible for the phase information, which is integrated into the QPSK- or QAM-modulated individual carriers, to be recovered. With the aid of the pilots described before, it is possible to accurately set the oscillator frequency and also the static phase of the local oscillator in the receiver. However, these static quantities are superimposed by phase noise. This results, first of all, in a phase error which affects all the individual carriers within a symbol in the same way, but which shows little correlation with the phase errors within the subsequent symbols. Secondly, the phase noise can lead to phase errors, which affect different carriers within the same symbol in different ways. This is why both the level and the spectral distribution of the phase noise in the local oscillator are of interest. Nowadays local oscillators of consumer type equipment are able to master the problem of phase noise even using conventional technology [MUSCHALL].

In the following the implementation aspects of the network interface part of DVB-T, i.e. the part from the "air interface", the antenna, to the MPEG-2 transport stream generation are described. An overview of several types of receivers is presented and their main requirements are outlined in the first paragraph. For the development of reception techniques for DVB-T signals

extensive experiences of the analogue TV reception can be used. The required components and their specific requirements for DVB-T signals are explained in the next section, followed by some new technologies which evolved with the development of digital television.

11.4.1 Receiver Classes

With the focus on implementation aspects it is most important to first determine in which reception environment, namely stationary, portable, or mobile, the receiver device will be operated. While the option "stationary" is mostly associated with reception by a rooftop outdoor antenna and a device which is not very often moved from one place to another, "portable" means that the device can easily be carried or taken from one point to another. It will contain a built-in omnidirectional antenna and will mostly be operated in a nomadic mode; i.e. it will not be operated while moving fast. "Mobile" means reception while moving at high speeds in automobiles, buses, trains, and so on.

In table 11.2 various DVB-T receivers and their main operational environment are outlined. For each of these devices a different reception concept is required. Some characteristic key points related to these devices are:

- A high-end IDTV set will need a high-end reception system which gives optimum reception under difficult (but stationary, sometimes indoor) receiving conditions. It may contain one antenna within the housing of the whole IDTV but can also use an external indoor antenna as well as an outdoor rooftop antenna.
- Set-top boxes are quite similar, maybe with less performance. They will possibly contain an integrated antenna.

Table 11.2. General classification of DVB-T receivers

	stationary	portable	mobile
Integrated Digital TV set (IDTV)	X		
Set-top Box (STB)	X		
Portable TV		X	
Personal Digital Assistant (PDA)		X	X
Home-PC extension	X		
Notebook-PC extension		X	X
Car receiver			X

- The emphasis of handhelds and PDAs is on a lowest possible power consumption combined with smallest packaging. Nevertheless they will be used under quasi-mobile receiving conditions. Also these receivers often have to be "world receivers", allowing reception in all possible environments (frequency range, channel arrangement, bandwidth) and they should be able to handle all possible DVB-T parameter combinations. These devices have to work with simple rod antennas or antennas integrated into the housing. Sensitivity and dynamic range of their tuners will become a classification and quality mark.
- PC-Extensions (like PCI-cards) or USB-adapters will suffer from the highest price pressure. Often manufacturers of these devices have a limited know-how of RF and IF design techniques and technologies, so they have to buy ready developed modules (so-called NIM, see below). One design aspect will be the interference of the PC environment emitting into the DVB-T receiver device.
- Car receivers have to cope with the most difficult receiving conditions, described by the mobile channel. They will use advanced technologies, for instance antenna diversity. Technically they undoubtedly will be the most sophisticated of all types of receivers. The advantage of a car receiver is that it can be adapted to the (most of the time) window-integrated antenna and pre-amplifier system to get the best performance out of DVB-T. This receiver also has to be a "world receiver" (see above), sometimes a receiver which also features other reception standards, like analogue TV, ATSC or ISDB-T. Due to the requirement to integrate the receiver into the infrastructure of an automobile, most of these devices will be OEM devices. Aftermarket devices will probably only play a small role.

Going deeper into technical aspects of the different devices a further classification is possible. Important factors may be dynamic range, input sensitivity, channel adaptation speed, power requirements and EMC immunity (see table 11.3).

11.4.2 Straight Forward Technology – the Classical Approach

For a first rough overview of a DVB-T reception system one can start with a very "classical" approach of a receiver design. It contains a tuner for down-conversion of the incoming RF signal to the first IF, some IF processing like filtering of the downconverted spectrum, maybe a further down-conversion to a second IF, and finally the DVB-T decoder for demodulating and decoding the baseband signal to MPEG-2 data. Figure 11.7 summarises this approach. It is generally valid for most receivers.

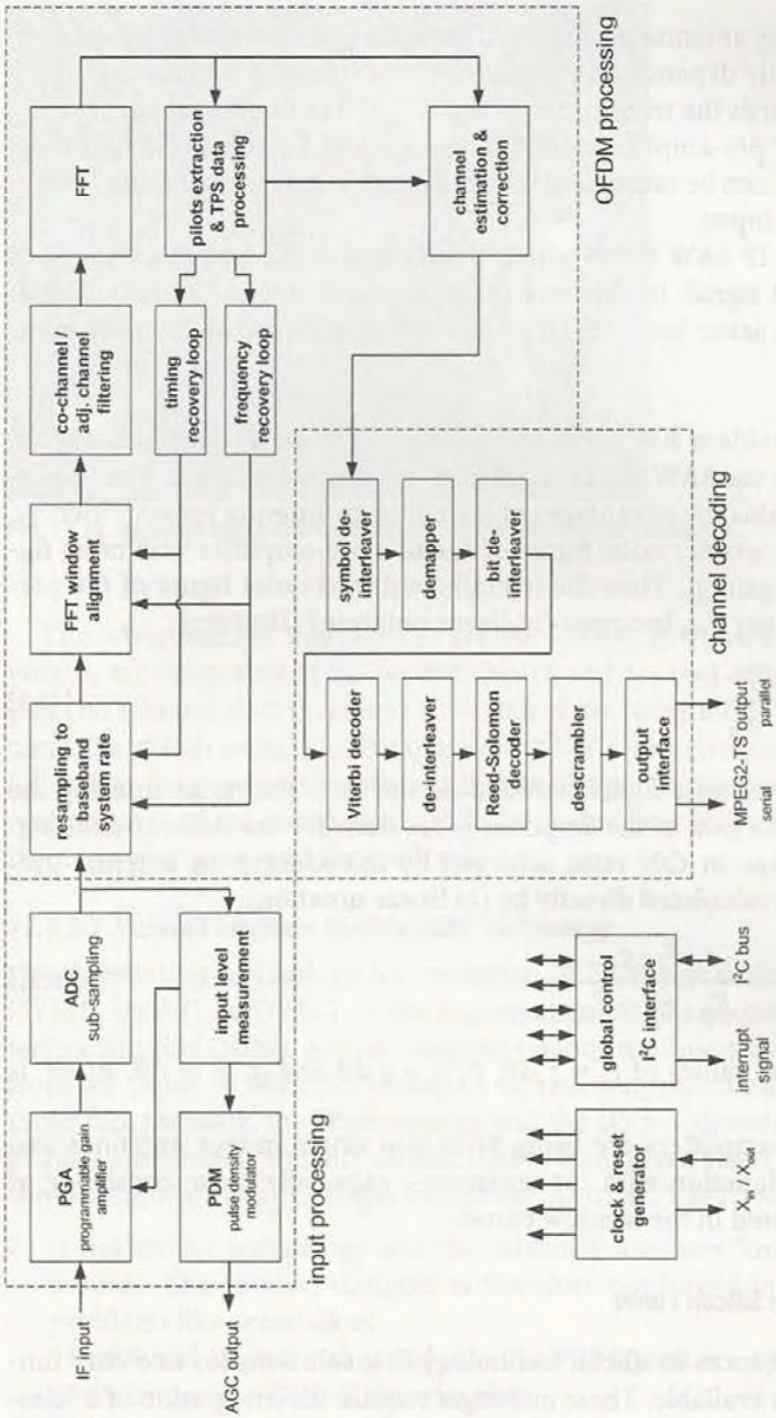


Fig. 11.12. Block diagram of a typical DVB-T decoder chip